ONCOGENIC MYC DISRUPTS THE MOLECULAR CLOCK

AND

METABOLISM IN CANCER CELLS AND DROSOPHILA

by
Annie Lee Hsieh

A dissertation submitted to Johns Hopkins University in conformity with the requirement for the degree of Doctor of Philosophy

Baltimore, Maryland

March 2016

Abstract

Circadian rhythm is a biological rhythm with a period about 24 hours, which coordinates the organismal biological processes with environmental day and night cycle. This 24-hour rhythm is exhibited in every cell in the organism and is generated by the molecular clock circuitry that comprises transcriptional and translational feedback loops. While loss of circadian rhythm or alteration of clock gene expression is broadly observed in human cancers, the molecular basis underlying these perturbations and their functional implications are poorly understood. *MYC* oncogene is amplified in more than half of the human cancers. Its encoded protein, MYC, is a transcription factor that binds to the E-box sequence (5'-CACGTG-3'), which is the identical binding site of the master circadian transcription factor CLOCK::BMAL1. Thereby we hypothesized that deregulated circadian rhythm in cancer cells is a consequence of perturbation of E-box-containing clock genes by ectopically overexpressed MYC.

In this thesis, we provide evidence that MYC or N-MYC activation alters expression of E-box-containing clock genes including *PER1*, *PER2*, *REV-ERBα*, *REV-ERBβ* and *CRY1* in cell lines derived from human Burkitts lymphoma, human osteosarcoma, mouse hepatocellular carcinoma and human neuroblastoma. MYC activation also significantly suppress the expression and oscillation of the circadian transcription factor *BMAL1*. Although public available MYC ChIP-seq data suggest that MYC directly binds to the promoter of *PER1*, *PER2*, *REV-ERBα*, *REV-ERBβ* and *CRY1* in U2OS cells, only silencing of *REV-ERBα* and *REV-ERBβ* is able to rescue *BMAL1* suppression by MYC. Strikingly, in two independent patient cohorts, high *REV-ERBα*

and low *BMAL1* expression are associated with more aggressive tumor and poorer clinical outcome of patients with neuroblastoma. Moreover, overexpressing BMAL1 suppresses colony formation of neuroblastoma cells. Finally, activation of MYC also greatly perturbs glucose metabolism and phospho-AMPK oscillation in U2OS cells.

To further analyze MYC effects on circadian clock *in vivo*, we manipulated *Drosophila* Myc (dMyc) level using genetic models and assess their circadian locomotor behavior. Here, we have demonstrated that overexpressed dMyc in specific clock cell type resulted in reduction of rhythmicity. dMyc activation is able to induce several clock-controlled genes, including *per*, *tim*, *cry* and *cwo*. However, no suppression of *clk*, *Drosophila* homolog of mammalian *BMAL1* is observed. Reduction of the clock synchronizing peptide PDF in the fly brain observed by immunohistochemistry and reduction of valine and leucine in the fly heads measured by GC-MS suggested that dMyc-associated arrhythmicity can be resulted from perturbation of PDF level or branch-chain amino acid metabolism. To explore how endogenous dMyc affect circadian behavior of flies, we also examine the circadian behavior in dMyc hypomorph mutant flies. Surprisingly, loss of dMyc leads to bimodal distribution of rhythmicity, which can be rescued by mutation of dMnt, a known suppressor of dMyc activity. Immunohistochemistry revealed Per staining is dramatically diminished in arrhythmic dMyc mutant flies but not in rhythmic dMyc mutant flies and can be rescued by dMnt mutation, suggesting endogenous dMyc is essential for Per expression. Our results demonstrate a novel role of dMyc in maintaining the integrity of *Drosophila* circadian locomotor behavior. Together, our data showed that a novel role of MYC and dMyc in modulating the molecular clock in cancer cells and in *Drosophila*. While MYC induces

E-box gene REV-ERBα to suppress BMAL1 and clock-regulated metabolism in cancer cells, dMyc is required to maintain E-box gene Per expression to ensure adequate circadian behavior. Our findings not only provide therapeutic opportunities between non-oscillatory cancer cells and circadian-regulated normal cells but also create a new avenue for the role of physiological dMyc in *Drosophila* circadian clock regulation.

Advisor: Dr. Chi Van Dang

Readers: Dr. Guang William Wong and Dr. Chi Van Dang

Acknowledgements

I would like to thank my PhD advisor Dr. Chi Van Dang for being a fantastic mentor and role model. Chi continuously inspires me to pursue interesting science and ask big picture questions. I admire his amazing science intuition, great communication skills and wonderful personality. I also greatly appreciate his supports on my fly project in collaboration with Amita Sehgal. I thank all the past and current members of the Dang Lab for their support, intellectual inputs and friendship: Zandra Walton, Yan Xiang, Brian Altman, Zachary Stine, Arvin Gouw, Jingsong Xia, Steve Lu, Karen Zeller, Jay Kim, Ping Gao and Anne Le. They are wonderful people to work with and they have made my PhD life unforgettably nice. In particular, I would like to think Brian Altman, who guides me through the early stage of my PhD career and generously shares his knowledge and techniques. It was extremely enjoyable to work with Brian and finally publish our paper together. In addition, Brian generously shares some of his data in my dissertation. I would like to give special thanks to Zandra Walton and Yan Xiang, who have been extremely supportive not only in science but also during the stressful times during my residency application. Their positive energy helps me go through the difficult times. Many thanks to my thesis committee members including Will Wong, John Isaacs, Jonathan Powell and Anirban Maitra, for their great scientific suggestions for my project. Particularly, I thank Will Wong for thoroughly reading my dissertation.

Many people from both Hopkins and Penn help me tremendously through my PhD career and contribute to the completion of my thesis project. I thank Anirban Maitra for sharing cell lines. I would like to acknowledge Celeste Simon at Penn for generous

sharing the equipment and actively recruiting us to the scientific community at Penn. I thank Dorothy Hunter for taking care of the facility at Penn. I also thank our collaborators Amita Sehgal, Xiangzhong Zheng, John Hogenesch, John Maris at Penn for sharing their data and inputs on our project. In particular, this thesis on *Drosophila* would not be possible to complete without the intellectual and technique support from Xiangzhong Zheng and Amita Sehgal.

I think the Pathobiology program for giving me the opportunity be part of it. I would like to thank Noel Rose, Edward Gabrielson for leading the graduate program. Warm appreciation goes to my mentors during rotations Philip Wong and Lee Martin for their continuous supports and encouragements. I truly appreciate Tracey McElroy, Stacey Morgan, Nancy Nath and Wilhelmena Braswell for their help during my PhD career. Thanks to my classmates in Pathobiology program, it was extremely fun and helpful to have you all during the stressful first year. I also want to thank my wonderful friends from high school, college and Penn. They have made my life so much fuller.

I would like to thank my wonderful family, my father Shu Hsieh, my mother Sumei Lee and my fun younger sister Shini Hsieh. They are extremely supportive with my decision about coming to the United States. My father and mother both gave me great advice on how to enjoy my time as a PhD student. Thanks for their love and wisdom.

Finally, I would like to give special thank to my fiancé, Edward Shin, for his love, career advice and friendship. I felt extremely lucky to be able to meet him at Penn, someone that I can not wait to spend the rest of my life with.

Table of Contents

Abstract	ii
Acknowledgements	v
Table of Contents	vii
List of Tables	viii
List of Figures	ix
Chapter 1: Introduction	1
Chapter 2: Characterize the molecular clock in MYC-driven cell lines	18
Chapter 3: Investigation of *REV-ERBα* as a direct MYC target gene for disruption of the molecular clock	55
Chapter 4: The role of BMAL1 and REV-ERBα in human neuroblastoma	77
Chapter 5: Metabolic alteration of MYC-disrupted molecular clock in U2OS cells	97
Chapter 6: Investigation of *Drosophila* Myc in fly circadian behavior	113
References	149
Curriculum vitae	161

List of Tables

Table 1. Potential shared target genes of Bmal1 and Myc 12

Table 2. Primers for quantitative real-time PCR on mammalian cell lines. 24

Table 3. Summary of circadian locomotor rhythmicity in dMyc-overexpressing flies 122

List of Figures

Figure 1. Expression of metabolic genes bound by both BMAL1 and MYC in different stages of MYC-driven liver tumor in mice. 13

Figure 2. Hypothesis of MYC-disrupted circadian homeostasis. 15

Figure 3. Myc-dependent growth in human P493 cells. 27

Figure 4. Quantitative RT-PCR of core clock genes and clock-controlled genes in synchronized P493 cells with HIGH MYC versus LOW MYC. 28

Figure 5. Quantitative RT-PCR of core clock genes and clock-controlled genes in synchronized P493 cells with HIGH MYC versus INTERMEDIATE MYC. 29

Figure 6. High BMAL2 expression in INTERMEDIATE MYC cells. 32

Figure 7. Growth curve of mouse hepatocellular carcinoma cell lines. 33

Figure 8. Tet-Off human MYC induces MYC target genes in mHCC cells. 35

Figure 9. MYC upregulates circadian repressor genes in mHCC 3-4 cells. 37

Figure 10. MYC upregulates circadian repressor genes in mHCC EC4 cells. 38

Figure 11. MYC disrupts circadian oscillations in mHCC 3-4 cells. 39

Figure 12. MYC disrupts circadian oscillations in mHCC EC4 cells. 40

Figure 13. MYC disrupts BMAL1 oscillation in mHCC 3-4 single clones. 43

Figure 14. MYC disrupts circadian oscillations in mHCC 3-4 C12 cells 44

Figure 15. U2OS BMAL::Luc MYC-ER cells. 46

Figure 16. MYC upregulates circadian repressor genes in U2OS MYC-ER cells. 48

Figure 17. MYC upregulates circadian repressor genes in U2OS MYC-ER cells. 49

Figure 18. MYC disrupts BMAL1 oscillation and expression in U2OS MYC-ER cells. 50

Figure 19. MYC disrupts circadian oscillations in U2OS MYC-ER cells. 51

Figure 20. Hypothetical mechanism of Myc-mediated circadian disruption. 63

Figure 21. Circadian repressor genes are direct MYC targets. 64

Figure 22. MYC directly engages the E-box promoter elements of circadian rhythm genes. 65

Figure 23. MYC directly engages the E-box promoter elements of REV-ERBα. 66

Figure 24. *PER2* and *CRY1* are not necessary for MYC disruption of BMAL1 promoter oscillation. 68

Figure 25. REV-ERBα and β are necessary for MYC disruption of BMAL1 expression 69

Figure 26. REV-ERBα and β are necessary for MYC disruption of BMAL1 promoter oscillation. 70

Figure 27. *REV-ERBα* is a direct MYC target gene in U2OS MYC-ER cells 71

Figure 28. MYC directly upregulates *REV-ERBα* to suppress *BMAL1* in mHCC-3-4 cells. 72

Figure 29. REV-ERBα and β are necessary for MYC suppression of BMAL1 promoter activity in mHCC 3-4 C12 cells 73

Figure 30. Model of Circadian Rhythm Disruption by MYC 75

Figure 31. Domain structures of MYC family members. 79

Figure 32. Oncogenic *MYC* correlates with elevated *REV-ERBα* in human T-acute lymphoblastic leukemia (T-ALL) 80

Figure 33. N-MYC Directly Upregulates REV- ERB*α* 88

Figure 34. Oncogenic N-MYC upregulates canonical MYC targets and circadian genes 89

Figure 35. Oncogenic N-MYC disrupts circadian oscillation. 90

Figure 36. N-MYC expression correlates with high REV-ERBα expression and disrupted BMAL1 oscillation 91

Figure 37. High-risk neuroblastoma exhibits increased REV- ERBα and decreased BMAL1 and these features correlate with poor prognosis. 93

Figure 38. Overexpression of BMAL1 suppress colony formation in N-MYC- 95

amplified neuroblastoma cell lines.

Figure 39. Principal component analysis of metabolites from U2OS MYC-ER cells 105

Figure 40. MYC Suppresses circadian oscillation of glucose metabolism and alters glutamine metabolism in U2OS Cells 107

Figure 41. MYC Suppresses Circadian Oscillation of cellular energetics. 109

Figure 42. MYC disrupts NAMPT oscillation and induces NAD^+ spikes. 111

Figure 43. Molecular clock circuitry in mammals versus *Drosophila* 115

Figure 44. Circadian locomotor rhythmicity in dMyc-overexpressing flies. 123

Figure 45. *Drosophila* Myc overexpression using Tim-Gal4 driver. 125

Figure 46. Circadian locomotor rhythmicity in dMyc-overexpressing flies. 126

Figure 47. dMyc overexpression alters circadian genes expression using Tim-Gal4 driver. 128

Figure 48. dMyc overexpression alters circadian genes expression using Cry24Pdf-Gal4 driver. 129

Figure 49. dMyc overexpression does not affect dE75 expression using Cry24Pdf-Gal4 driver 130

Figure 50. dMyc overexpression decreases PDF immunostaining of the s-LNv dorsal projections. 132

Figure 51. dMyc overexpression does not alter neuronal processes from the s-LNvs. 134

Figure 52. dMyc overexpression leads to decreased branch-chain amino acids and increased urea. 135

Figure 53. Hypomorphic dMyc flies exhibit dichotomous rhythmicity. 137

Figure 54. Endogenous *Drosophila* Myc level in Myc hypomorph flies. 140

Figure 55. Hypomorphic dMyc flies exhibit dichotomous rhythmicity and can be rescued by dMnt mutation. 141

Figure 56. Loss of dMyc minimally alter circadian genes expression. 142

Figure 57. Loss of dMyc does not alter Per protein level from fly heads. 144

Figure 58. Loss of dMyc leads to reduced Per staining in sLNvs 145

Chapter 1

Introduction

The MYC proto-oncogene is frequently deregulated in human cancers, activating genetic 144programs that orchestrate biological processes to promote growth and proliferation (Da145ng, 2012). Altered metabolism characterized by heightened nutrients uptake, enhanced glycolysis and glutaminolysis and elevated fatty acid and nucleotide synthesis is the hallmark of MYC-driven cancer (Dang, 2013; Hsieh et al., 2015). Recent evidence strongly suggests that MYC- dependent metabolic reprogramming is critical for tumorigenesis, which could be attenuated by targeting specific metabolic pathways using small drug-like molecules. In contrast, metabolic pathways in non-proliferating cells are largely regulated by circadian clock (Bass, 2012). However, how MYC unleashes growth-promoting metabolic processes from circadian constraints is unknown. This thesis uses both *in vitro* and *in vivo* models to define the role of ectopic MYC and endogenous dMyc in circadian clock regulation.

MYC is an E-Box transcription factor

MYC was first discovered as a cellular homolog of *v-myc*, a retroviral gene that was found to induce tumorigenesis in birds (Duesberg and Vogt, 1979; Vennstrom et al., 1982). Its role in human cancer was first recognized through observations of the pathognomonic chromosomal translocations, which juxtaposed the *MYC* gene next to constitutively active immunoglobulin enhancers, in human Burkitt's lymphoma (Dalla-Favera et al., 1982; Taub et al., 1982).

The *MYC* proto-oncogene is aberrantly overexpressed in over half of human cancers (Dang, 2012). It is one of the most frequently amplified oncogene in human cancers and a member of the larger *MYC* family, which includes *MYCN* and *MYCL* (Brodeur et al.,

1984; Nau et al., 1985). Dysregulations of *MYC*, such as amplification, chromosome translocation or loss of upstream repressors, have been found in many human cancers (Beroukhim et al., 2010; He et al., 1998).

MYC encodes the MYC transcription factor, which dimerizes with MAX – another helix–loop–helix leucine zipper protein – to bind DNA and alter gene expression. MYC belongs to the extended MYC transcriptional factor network that includes MAX, MXD proteins, MGA, MNT, MXL, MXLIP, and the carbohydrate response element binding protein (ChREBP) (Carroll et al., 2015). MYC, as a transcriptional factor, activates many genes that are involved in cellular processes, including transcription, translation, chromatin modification and protein degradation.

MYC is downstream of a number of growth-promoting signaling pathways, including those initiated by growth factor-stimulated receptor tyrosine kinases, T cell receptors and WNT signaling (Dang, 2012). In non-transformed cells, cell cycle checkpoints protect against aberrant MYC activity. For example, p53-dependent apoptosis is induced upon acute MYC overexpression in primary mouse embryo fibroblasts (Eischen et al., 1999). MYC also induces expression of ARF, which directly inhibits MYC-mediated transcription and tumorigenesis in a p53- independent manner (Qi et al., 2004). In transformed cells, however, MYC activation selects for surviving cells that have mutation or deletion of p53 or ARF to prevent apoptosis (Eischen et al., 1999).

The indispensable role of MYC in cancer has been observed in both human cell lines and murine models. In human Burkitt's lymphoma cell line, loss of MYC was found to hinder cell proliferation (Yustein et al., 2010). In a mouse model with liver specific, doxycycline

(DOX)- suppressed *MYC* transgene, *MYC* activation by withdrawal of DOX gives rise to aggressive liver tumors that resemble human hepatocellular carcinoma (Shachaf et al., 2004). Intriguingly, these invasive tumors regress when the tumor-bearing animals are re-exposed to DOX to inactivate *MYC* (Shachaf et al., 2004). These findings suggest that MYC is not only essential for tumor initiation, but also critical for maintenance of established tumors, revealing these tumors' addiction to MYC signaling.

It is generally thought that MYC activity is largely through its regulation of transcription. The key mechanism allowing MYC to globally enhance transcription is through augmenting P-TEFb- dependent phosphorylation of RNA polymerase II to release it from the paused state to the elongation state (Rahl et al., 2010). Studies further demonstrate the presence of MYC at nearly all the open chromatin regions in the genome, eliciting a model that MYC is a universal amplifier and the level of amplification purely depend on the patterns of open chromatin within the genes (Chen et al., 2008; Lin et al., 2012; Nie et al., 2012). These observations suggest that MYC simply amplifies the existing transcriptional program within the cell but it is not clear how MYC modulates the ratio between growth-promoting genes versus growth-arresting genes to promote growth and proliferation. Follow-up studies have revealed that MYC is able to selectively activate expression of certain gene sets while globally enhance transcription (Sabo et al., 2014). For instance, overexpressed MYC was found to "invade" enhancers and low affinity core promoters that normally bind little MYC at physiological level as it saturates the high affinity promoters, suggesting supraphysiological level of MYC preferentially activate expression of the genes harboring low affinity promoters or enhancers (Lin et al., 2012; Walz et al., 2014; Wolf et al., 2014). Furthermore, high level of MYC recruits MIZ1

through protein–protein interaction and enhances MIZ1-dependent repression (Walz et al., 2014). Together, these findings indicate that while MYC generally augments RNA elongation throughout the genome, it does so in cooperation with other transcription factors that provide for selective gene expression amplification to coordinate metabolism and cell growth (Dang, 2014; Wolf et al., 2014).

MYC regulation of glucose and glutamine metabolism

Yeast cells sense glucose and glutamine in the environment and activate expression of Ribi genes to initiate ribosome biogenesis (Lippman and Broach, 2009). In *Drosophila*, glucose activates insulin signaling, which acts through PI3K/Akt pathway to activate TOR and repress FOXO (Wullschleger et al., 2006). *Drosophila* Myc (dMyc) is identified as a convergent node downstream of TOR and FOXO signaling in response to nutrients (Teleman et al., 2008). When glucose is abundant, activated TOR rapidly increases dMyc protein to drive ribosome biogenesis. Conversely, when fruit flies are under fasting, FOXO is derepressed from Akt and directly inhibits dMyc expression (Teleman et al., 2008). In mammals, MYC level was also observed to correlate with nutrient level. For example, in rat liver, *MYC* expression dramatically decreases under glucose deprivation (Corcos et al., 1987). Moreover, FOXO3a was found to inhibit MYC activity through induction of MYC antagonist MXI1 proteins in colon cancer cells (Delpuech et al., 2007). Taken together, the physiological role of MYC as a "nutrient sensor" seems to be well conserved during evolution, suggesting that MYC is critical in the process of utilizing extracellular glucose and glutamine for macromolecule synthesis. The importance of MYC in glucose and glutamine metabolism is further corroborated by

heightened glucose and glutamine uptake that observed in neoplastic cells, where unleashed MYC is continuously activated.

Glucose is one of the major nutrients that mammalian cells utilize to synthesize new membranes and organelles as well as to generate high energy molecules, such as ATP, NADH/NADPH and FADH. Glucose is taken up through glucose transporters (GLUTs) and phosphorylated by hexokinase. Glucose-6-phosphate then undergoes a series of reversible and irreversible reactions before conversion to two molecules of pyruvates by pyruvate kinase with a net production of 2 ATPs and 2 NADHs. Pyruvate can be converted to lactate by lactate dehydrogenase (LDH) or to citrate by pyruvate dehydrogenase to enter tricarboxylic acid cycle (TCA cycle).

Many genes involved in glucose metabolism have been documented to be MYC target genes. For example, MYC upregulates genes encoding glucose transporters and hexokinase to increase glucose import (Osthus et al., 2000). MYC also induces expression of glycolytic genes including phosphoglucose isomerase, phosphofructokinase, glyceraldehyde-3-phosphate dehydrogenase, phosphoglycerate kinase, and enolase (Osthus et al., 2000). Furthermore, use of ^{13}C-labeled glucose has revealed increased levels of glycolytic intermediates and lactate in MYC-driven Burkitt's lymphoma cells, suggesting MYC overexpression increases overall glycolytic flux (Le et al., 2010). This observation harkens back to findings by Dr. Otto Warburg back in the 1920s indicating high rates of glycolysis and lactate production in cancer cells even in the presence of oxygen (Warburg et al., 1927). Increased glycolytic flux gives rise to abundant glycolytic intermediates that can be used to generate macromolecules such as nucleotides, amino acids and fatty acids. To maintain high flux of glycolysis, MYC was observed to

upregulate lactate dehydrogenase A (LDHA) to generate NAD^+, which is a co-factor required for the glycolysis particularly by GAPDH (Le et al., 2010). The role of LDHA in MYC-driven cancer cells is underscored by the ability of a specific LDHA inhibitor FX11 to cause cell death [54]. MYC has also been shown to regulate alternative splicing of the rate-limiting enzyme pyruvate kinase by upregulating heterogeneous nuclear ribonucleoproteins (hnRNP) (David et al., 2010). Pyruvate kinase has two distinct isoforms: PKM1 and PKM2. While the embryonic pyruvate kinase isoform, PKM2, promotes aerobic glycolysis, PKM1 favors oxidative phosphorylation. By upregulating hnRNPA1 and hnRNPA2, MYC maintains high ratio of PKM2/PKM1 to ensure high flux of glycolysis in the presence of oxygen (David et al., 2010).

Glutamine is another major nutrient for tumor cells, as it fuels the TCA cycle and also provides sources of nitrogen. Glutamine is imported into the cells through glutamine transporter ASCT2 and is then converted to glutamate by glutaminase (GLS). Several enzymes can further metabolize glutamate to α-ketoglutarate (α-KG) to further enter TCA cycle including glutamine dehydrogenase (GDH), glutamine pyruvate transaminase (GPT) or glutamine oxaloacetate transaminase (GOT).

Unlike most non-transformed cells that use glucose, MYC-driven cancer cells depend on glutamine metabolism (Reitzer et al., 1979). MYC promotes glutamine import by directly inducing the expression of glutamine transporter ASCT2 (Wise et al., 2008). In addition, MYC increases the conversion of glutamine to glutamate for subsequent oxidation in the TCA cycle by upregulating GLS both transcriptionally and post-transcriptionally (Gao et al., 2009; Wise et al., 2008). The reliance on glutamine metabolism of MYC-driven cancers appears especially true under stress conditions, particularly glucose and oxygen

deprivation (Le et al., 2012). Specifically, flux analysis using ^{13}C-labeled glutamine in MYC-overexpressing cells has revealed an enrichment of TCA cycle isotopologues under glucose-deprivation, suggesting while these cells favor glucose as the carbon sources for the TCA cycle, glutamine is an alternative carbon source in the absence of glucose (Le et al., 2012). Moreover, MYC overexpression has been shown sufficient to induce glutamine addiction. For example, high levels of MYC can convert fibroblasts to become addicted to glutamine as evidenced by apoptosis after glutamine withdrawal (Yuneva et al., 2007). Intriguingly, TCA cycle intermediates oxaloacetate and pyruvate can rescue cell death, suggesting glutamine is the major carbon source for the TCA cycle in these MYC- overexpressing cells (Yuneva et al., 2007). Furthermore, knockdown MYC in glioma cells can release cells from a glutamine-addicted state (Wise et al., 2008). Given the fact that MYC-driven tumor is highly dependent on glutamine, it can be anticipated that MYC-driven tumor might be sensitive to inhibitors targeting glutamine metabolism. Indeed, decreased cell growth is observed in MYC-overexpressing cancer cells that treated with glutaminase inhibitors (Le et al., 2012; Wang et al., 2010). It further appears that, when glucose is abundant, the requirement for glutamine may stem from a need for glutamate to synthesize glutathione to protect cells against reactive oxygen species (Le et al., 2012). Moreover, it was observed that glutamine-derived glutamate contributes to MYC-dependent proline synthesis (Liu et al., 2012).

Cellular homeostasis and growth

The activation of metabolic pathways is very dynamic and highly dependent on the state of cell and the external cues, such as growth signals and nutrients. Mammalian cells exhibit two major states in their life: resting state or dividing state. The majority of cells

in our body are differentiated and in the resting state, using energy to maintain basal metabolism. In contrast, a small population of cells in our body exists in the dividing state, including intestinal mucosal cells and hematopoietic cells. These cells have higher energy demands for growth and proliferation.

In resting cells, homeostasis is accomplished by generating sufficient energy from extracellular nutrients to sustain protein synthesis, maintain cellular membrane potentials, turn over or repair damaged organelles and macromolecules. To maintain a constant level of ATP, the major high-energy molecule in the cells, several key factors tightly regulate metabolic pathways in response to external nutrient availability. For example, in the nutrient-replete state, abundant amino acids activate mTOR complex, which stimulates anabolic pathways including protein synthesis, lipid synthesis and ribosomal biogenesis (Efeyan et al., 2012). Conversely, under the nutrient-depleted state, low energy induces AMP-activated protein kinase (AMPK), which phosphorylates and inhibits the majority of anabolic pathways while turning on catabolic, energy-producing pathways including glycolysis, oxidative phosphorylation and fatty acid oxidation (Hardie and Alessi, 2013). Notably, inactivated mTOR and activated AMPK in response to fasting collectively induce autophagy (self-eating), allowing cells to digest their own organelles to produce energy and recycle cellular building blocks (Efeyan et al., 2012; Hardie and Alessi, 2013).

Because food availability and demands for energy-consuming organismal activity are not constant, many organisms have evolved systems to anticipate predictable changes and thereby optimize metabolic efficiency and enhance evolutionary fitness. One such example is circadian rhythm, an autonomous oscillation of biological processes with approximately 24-h period, coordinates feeding and sleeping in both unicellular and

multicellular organisms. In humans and mice, autonomous cellular metabolic oscillation is synchronized with the day–night cycle through a central clock residing in the suprachiasmatic nucleus in hypothalamus (Green et al., 2008). The central clock synchronizes with light via signals from the retina and in turn sends neuronal and hormonal signals to synchronize clocks found in peripheral tissues and cells (Green et al., 2008). Virtually all cells possess a molecular clock circuity with interlocking feedback loops that is comprised of transcriptional activators, such as CLOCK and BMAL1, and the transcriptional repressors, PERs, CRYs and REV-ERBs. CLOCK and BMAL1 form a complex CLOCK::BMAL1 that binds to the canonical DNA sequence 5'-CACGTG-3' (E-Box) to activate several circadian regulators including PERs, CRYs and REV-ERBs. PERs and CRYs form a complex in the cytoplasm and translocate into the nucleus to repress CLOCK::BMAL1 transcriptional activity, whereas REV-ERBs directly repress *BMAL1* expression at retinoic acid receptor-related orphan receptor elements (ROREs). These two feedback loops give rise to the observed 24-h oscillation (Green et al., 2008). CLOCK::BMAL1 diurnally drives a number of biological pathways, particularly metabolic pathways, to coordinate with feeding and sleeping (Bass, 2012).

Intriguingly, the "E-box" motif used by the CLOCK proteins could also be bound by other transcription factors that are involved in metabolism and growth. The carbohydrate-responsive element-binding protein (ChREBP), sterol regulatory element- binding protein (SREBP), microphthalmia-associated transcription factor (MITF), transcription factor EB (TFEB), transcription factor E3 (TFE3), and oncoprotein MYC (Dang, 2012; Giangrande et al., 2003; Sardiello et al., 2009; Yasumoto et al., 1994) are helix–loop–helix proteins

that have canonical E-box binding activities, suggesting the possible interplay between these transcription factors in regulating metabolism, cell homeostasis and growth.

We surmise that the E-box motif, which is highly enriched in regulatory sequences of the human genome provides a means for transcriptional orchestration of anabolic and catabolic metabolism with cell growth and homeostasis (Fernandez et al., 2003). Circadian chromatin Immunoprecipitation Sequencing (ChIP-seq) and gene expression studies in the mouse liver have found oscillation of genes involved in glycolysis, oxidative phosphorylation, lipid synthesis and autophagy, regulated by diurnal BMAL1 E-box binding (Table 1) (Koike et al., 2012). These BMAL1-regulated metabolic genes have also been documented as MYC target genes (Table 1) that exhibit increased expression in the MYC-driven murine liver cancer (Fig. 1) (Hu et al., 2011; Lin et al., 2012). Together these observations suggest that, while BMAL1 diurnally regulates metabolism to maintain homeostasis, MYC may substitute for BMALl1 during proliferation to activate metabolic genes in a sustained and enhanced manner that supports cell growth and division (Dang, 2012) (Fig. 2). Notably, several of these genes encode rate-limiting enzymes in the metabolic pathways, such as phosphofructokinase (PFK) in glycolysis, HMG-CoA reductase (HMGCR) in cholesterol synthesis pathway and NAMPT in NAD^+ salvage pathways; thus by controlling the magnitude and temporal expression of these genes, MYC can effectively reprogram metabolism. Given these observations, we surmise that the ChREBP, SREBP, and MITF/TFE transcription factors are also likely to have inter-related activities to control carbohydrate and lipid metabolism and autophagy, respectively. These factors along with CLOCK::BMAL1 and

Table 1
Potential shared target genes of Bmal1 and Myc.

Cellular processes or metabolic pathways	Genes bound by both Bmal1 [19] and Myc [20]
Glycolysis	Pfkfb3
	Pdk1
	Pdhb
Oxidative phosphorylation	Ndufa4
Ribosome biogenesis	Rplp2
Fatty acids and cholesterol synthesis	Srebf1
	Insig1
	Hmgcr
NAD^+ salvage pathway	NAMPT
Autophagy	Bnip3

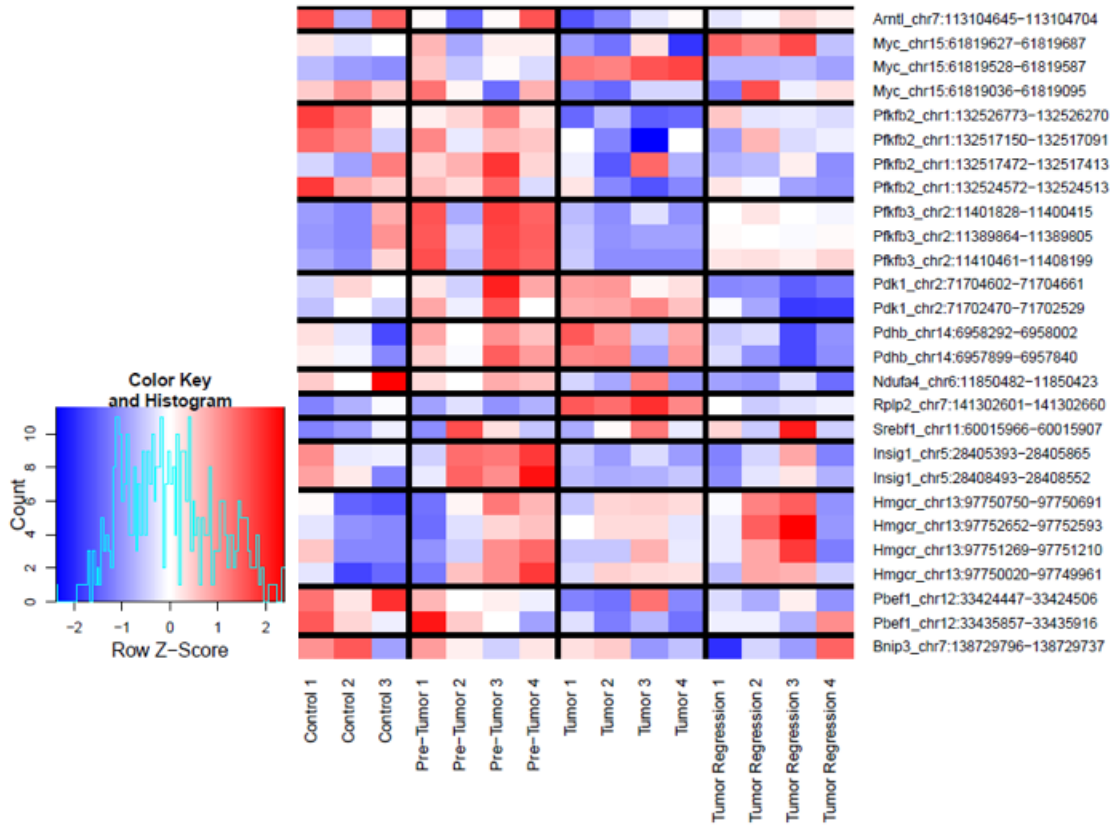

Figure 1. Expression of metabolic genes bound by both BMAL1 and MYC in different stages of MYC-driven liver tumor in mice.

Gene set enrichment analysis of a subset of metabolic genes bound by both BMAL1 and MYC (shown in Table 1) in four stages of liver tumors in liver specific, doxycycline-suppressed, MYC transgenic mice: control (+DOX), pre-tumor (−DOX), tumor (−DOX), tumor regression (+DOX). DOX, doxycycline; red, upregulation; blue, downregulation.

the extended MYC transcription factor family form a tapestry of transcription factors that orchestrate metabolism and cell growth (Fig. 2).

Circadian clock and cancer

Mutations of circadian genes occur in many cancers, but their functional consequences are not well understood (Savvidis and Koutsilieris, 2012). Two key circadian genes, PER1 and PER2, have been identified as putative tumor suppressors in salivary gland, gastro-intestinal system, breast tissue, and the immune compartment (Savvidis and Koutsilieris, 2012; Zhao et al., 2014). Loss of PER2 function predisposed genetically engineered mice to spontaneous lymphomagenesis, but mouse strain specificity was not documented (Fu et al., 2002). Hematologic malignancies such as diffuse large B cell lymphoma, chronic lymphocytic leukemia, and acute myeloid leukemia show strong downregulation of the central circadian regulator BMAL1 (Taniguchi et al., 2009). Indeed, recent studies identify BMAL1 as a putative tumor suppressor (Savvidis and Koutsilieris, 2012; Yeh et al., 2014). Ovarian cancers have altered circadian gene expression and oscillation compared to normal tissue, but the functional significance and mechanism for these alterations were not established (Tokunaga et al., 2008). Still other studies found circadian gene expression alterations in cancers such as pancreatic, prostate, and glioma (Savvidis and Koutsilieris, 2012). Importantly, altered circadian rhythm may affect cancer treatment outcomes, as studies in mice and humans have identified circadian-dependent toxicity in more than 40 anticancer agents, including antimetabolites, mitosis inhibitors, alkylating agents, and cytokines (Levi et al., 2010). Thus, altered

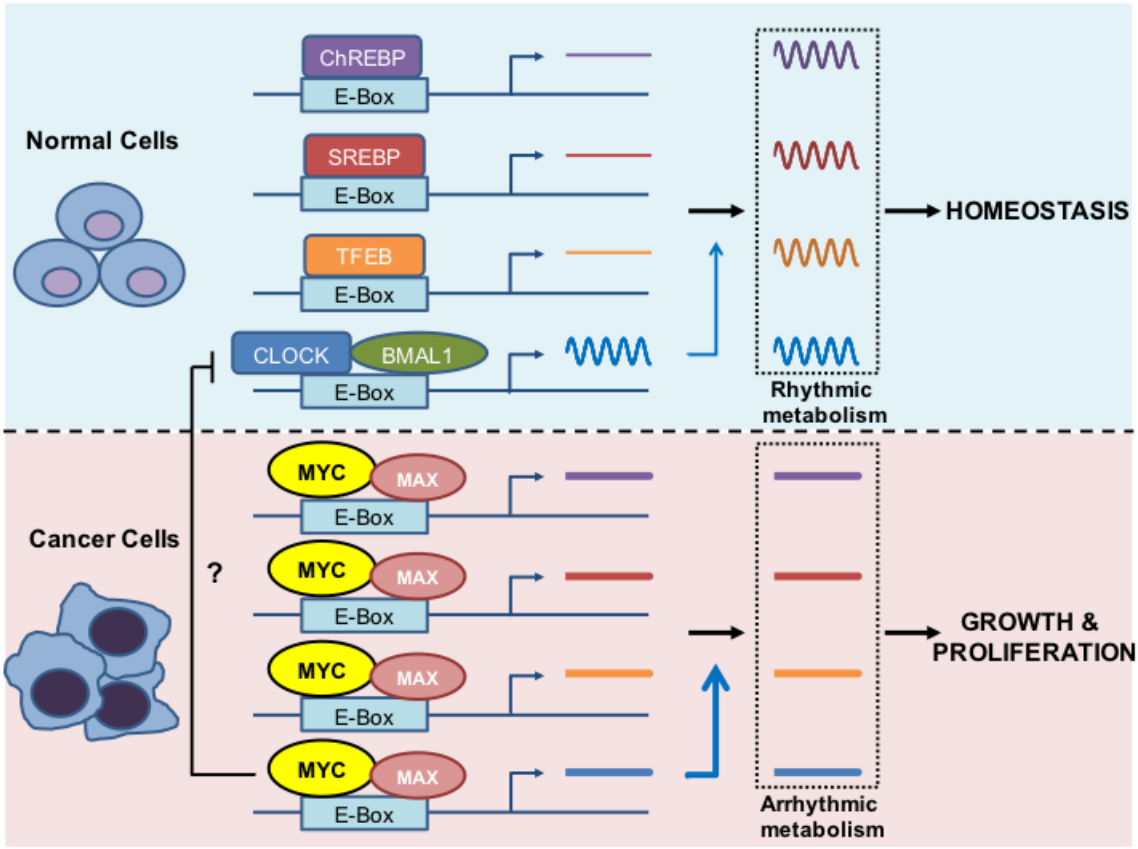

Figure 2. Hypothesis of MYC-disrupted circadian homeostasis.
A schematic representation of rhythmic control of "E-box" containing metabolic genes in normal cells and MYC-dependent, sustained control of "E-box" containing metabolic genes in cancer cells.

circadian gene expression occurs broadly in cancer; however, it is not known whether MYC could contribute to disruption of circadian gene expression.

Myc and circadian rhythm

Remarkable progress has been made in characterizing genomic regulation of MYC and identifying its target genes regulating growth, metabolism, proliferation and apoptosis. However, it is unclear how MYC hijacks clock-controlled metabolic pathways in resting cells and activates genes that normally oscillating to constitutive expression.

In Chapter 2 of this thesis, we found that several E-box-containing clock genes were induced by MYC in human Burkitts lymphoma, human osteosarcoma and murine hepatocellular carcinoma cell lines. Additionally, MYC activation suppresses master clock regulator *BMAL1* expression and oscillation.

In Chapter 3, we first demonstrate that MYC directly regulates E-box containing clock genes, including PER1, PER2, CRY1, REV-ERBα and REV-ERBβ. We then provide evidence that abrogation of *REV-ERBα* and *REV-ERBβ* expression using siRNAs restores MYC-mediated *BMAL1* suppression.

In Chapter 4, using N-MYC inducible neuroblastoma cell lines, we showed that N-MYC similarly represses *BMAL1* expression and oscillation through *REV-ERBα* upregulation. Primary neuroblastoma tumor samples from two patient cohorts revealed that elevated *REV-ERBα* and reduced *BMAL1* expression predict worse clinical outcome. Finally, overexpression of *BMAL1* reduced clonogenicity of two neuroblastoma cell lines.

In Chapter 5, metabolomic experiments are done to explore the metabolic impacts from MYC-mediated *BMAL1* suppression. Interesting, MYC activation abrogates oscillatory glucose metabolism and alters glutamine metabolism. In summary, our observations describe a previously unrecognized role of MYC in suppression clock and clock-regulated metabolism to promote cell proliferation in human cancer.

In Chapter 6, we explored the effect of *Drosophila* Myc (dMyc) on fly circadian locomotor behavior. Interestingly, both gain-of-function and loss-of-function of dMyc result in increased arrhythmicity. Overexpression of dMyc in selected clock neurons induces clock genes, diminishes circadian synchronizing peptide PDF staining and reduces branch chain amino acids in heads of these flies. Loss of dMyc results bimodal distribution of rhythmicity and those arrhythmic flies exhibit diminished Per staining in central clock neurons. The arrhythmicity and loss of Per can be rescued by additional mutation of dMyc repressor dMnt, suggesting dMyc activity is crucial in maintaining rhythmicity in flies.

Chapter 2

Characterize the molecular clock in MYC-driven cell lines

It is very clear now that MYC regulates growth and proliferation through activation of translation machinery, metabolic pathways and cell cycle progression (Dang, 2012; Hsieh et al., 2015; Stine et al., 2015). However, many of these network and pathways are also tightly regulated by circadian clock, particularly metabolism (Bass, 2012). Circadian clock regulates these pathways to maintain homeostasis, however, when MYC level rises, cells are ready to proliferate, it remains unclear how MYC efficiently hijacks the homeostatic regulation and turns metabolism into a high speed factory to support cell growth and proliferation. As transcription factors, MYC and CLOCK::BMAL1 both regulate their target genes through E-box binding. Therefore, we hypothesize that in MYC-driven cancer cells, elevated MYC will compete with CLOCK::BMAL1 at the promoter of its target genes. As a result, growth and metabolic program that are under circadian control by CLOCK::BMAL1 would be activated by MYC constitutively.

There are a number of inducible MYC model systems that we could utilize to address this question. In this chapter, we first examined how ectopic MYC affects clock gene expression and oscillation in human P493-6 lymphocytes. In collaboration with Dr. Dean Felsher's laboratory, we engineered and subcloned mouse hepatocellular carcinoma cell line to demonstrate that MYC suppresses the expression and oscillation of *Bmal1* and the suppression could be restored by removing MYC. Finally, in collaboration with Dr. John Hogenesch, we found that loss of robust *BMAL1* oscillation in osteosarcoma U2OS cells upon MYC induction.

Materials and Methods

Plasmids

c-MYC-ER™ wt and Δ106-143, which are responsive to tamoxifen and 4-hydroxytamoxifen but not to estrogen, were received in the pBabe-puro vector courtesy of Dr, Linda Penn, Ontario Cancer Institute, University Health Network, University of Toronto, Canada) and were described previously (Littlewood et al., 1995). c-MYC-ER™ wt and Δ106-143 were subcloned into pBabe-Zeo (Morgenstern and Land, 1990) (courtesy of Dr. Robert Weinberg, Whitehead Institute for Biomedical Research, Cambridge, MA, USA, Addgene plasmid 1766). Retrovirus was generated in 293T cells using the pCMV-VSVG and pUMVC vectors (Stewart et al., 2003) (courtesy of Dr. Robert Weinberg, Addgene plasmids 8449 and 8454).

Cell culture

P493-6 cells were kindly shared by Dr. Dirk Eick (Munich, Germany). Murine hepatocellular carcinoma cell lines (mHCCs) are primary culture tumor cell line, which were derived by ring cloning from a liver tumor of the LAP-tTA/tet-OFF cMYC conditional transgenic mouse model (Shachaf et al., 2004; Xiang et al., 2015). U2OS cells with BMAL1::luciferase vector were kindly shared by Dr. John Hogenesch (Baggs et al., 2009). P493-6 was cultured in Roswell Park Memorial Institute Medium (RPMI 1640, Mediatech, Manassas, VA, USA). U2OS cells and mHCC cells were cultivated in Dulbecco's modified Eagle's medium (DMEM, Mediatech, starting glucose concentration of 25 mM and starting glutamine concentration of 4 mM). Media was supplemented with 10% fetal bovine serum (FBS, HyClone, Logan, UT, USA or Life Technologies, Grand Island, NY, USA) and 1X Penicillin/Streptomycin (Mediatech) for

all cells. mHCC cell media was additionally supplemented with 2 mM L-Glutamine (Mediatech), 1 mM Sodium pyruvate (Mediatech) and 1X MEM non-essential amino acid (Life Technologies). To repress *c-MYC* expression (LOW Myc cells), P493-6 cells were treated with 0.1μg/ml Tetracycline (sigma) for 48 hours. To generate INTERMEDIATE Myc cells, P493-6 cells were treated with both 0.1μg/ml Tetracycline (sigma) and 1 μM beta-estrodiol and let them adapt for about a week. To induce MYC-ER nuclear translocation, U2OS MYC-ER™ cells were treated with 500 nM 4-hydroxytamoxifen (Sigma, St. Louis, MO, USA) for 24 hour or treated with same amount of ethanol as control. To repress *c-MYC* expression, mHCC 3-4 cells were treated with 20ng/ml tetracycline (Sigma) or treated with media as control.

U2OS BMAL1::Luc cells were stably transduced with MYC-ER™, MYC-ER™ Δ106-143, or pBabe-Zeo empty vector retrovirus using the plasmids and methods described above. Infected cells were selected for with 100 μg/ml Zeocin (Life Technologies) for two weeks, then continually cultured in Zeocin except during experiments.

To generate mHCC 3-4 stably expressing luciferase reporter constructs, plasmids (REV-ERBα::Luc described above or BMAL1::Luc in pGL 4.27 [Promega (Baggs et al., 2009)] were linearized by digestion with Not1 (New England Biolabs) and purified by QIAquick PCR purification kit (Qaigen). mHCC 3-4 cells were then transfected with linearized plasmids using Lipofectamine 2000 (Life Technologies) and selected with Hygromycin (Mediatech) at the following concentrations: 0.8 mg / ml for mHCC 3-4.

To create stable single-cell mHCC 3-4 Bmal1::Luc clones, cells were trypsinized and serially-diluted to 100 cells per 96 well plate. Clones were lysed and mixed with

luciferase assay reagent (Promega) and luciferase activity was measured by luminometer. Only the clones with 10000 or above relative light units were selected. Selected clones were cultured with 20ng/ml tetracycline in regular media for mHCC cells (as described above) for 24 hours. The clones were then screened in Lumicycle™ luminometer (details described in Lumicycle section), and those that showed BMAL1::Luciferase oscillation were used.

All cell culture, except that during live-cell luminometer experiments (see Lumicycle section below), was conducted in a 5% CO2 humidified atmosphere.

Real-Time PCR

All RNAs were extracted by RNeasy Plus Mini Kit (Qiagen) according to manufacturer's instruction and reversed to complementary DNA by using TaqMan Reverse Transcription Reagents (Life Technologies). cDNA was used as template to proceed to quantitative real time PCR (RT-PCR) with specific human or mouse primers. RT-PCRs were performed using the StepONE Plus system, 7900HT Real-time PCR System, or ViiA™ 7 Real-time PCR system (Life Technologies). Relative mRNA expression levels were normalized to β2M and analyzed using comparative delta-delta CT method. All RT-PCR primers are listed in Table 2.

Western blot analysis

Cells were lysed in M-PER Mammalian Protein Extraction Reagent (Thermo Fisher Scientific) buffer supplemented with protease inhibitor cocktail (BD Biosciences, San Jose, CA) and phosphatase inhibitors (Sigma). Proteins were separated by SDS-PAGE using Criterion pre-cast gradient gels (Bio-Rad, Hercules, CA, USA). Primary antibodies

used include: rabbit anti-MYC (Abcam) and mouse anti-α-Tubulin (EMD Millipore, Billerica, MA, USA). Secondary antibodies used include: Alexa-Flour 680 goat anti-rabbit IgG (Life Technologies, Grand Island, NY). Immunoblots were imaged with the Odyssey CLx infrared imaging system (Licor) and uniformly contrasted.

Circadian mRNA Experiments

Circadian mRNA experiments for U2OS MYC-ER™, mHCC 3-4 and mHCC EC4 were carried out in the media described above as a 'split timecourse'. 24 hours prior to the start of the experiment, half the cells were cultured in 0.1 μM dexamethasone (dex,

Gene Name	Sequence or Product Number	Source
	Human Primers	
PER1	ACTCCTGCGACCAGGTACTGGCTG, GGCCACCACGGATGCACGA	Primer Blast
PER2	GGATGCCCGCCAGAGTCCAGAT, TGTCCACTTTCGAAGACTGGTCGC	Primer Blast
REV-ERBα (*NR1D1*)	TGGACTCCAACAACAACACAG, GATGGTGGGAAGTAGGTGGG	Primer Bank [4] ID#300116298c1
ODC1	Hs.PT.51.22750281.gs	IDT
REV-ERBβ (*NR1D2*)	Hs.PT.51.14785042	IDT
β2M	GGCCGAGATGTCTCGCTCCG, TGGAGTACGCTGGATAGCCTCC	Primer Blast
BMAL1 (*ARNTL*)	Hs00154147_m1	Taqman Gene Expression Assay
NAMPT	Hs00237184_m1	Taqman Gene Expression Assay
CRY1	Hs01565974_m1	Taqman Gene Expression Assay
CRY2	Hs.PT.53a.3983568	Taqman Gene Expression Assay
	Mouse Primers	
β2M	ACCGGCCTGTATGCTATCCAGAAA, GGTGAATTCAGTGTGAGCCAGGAT	Previously Published [5]
REV-ERBβ (*Nr1d2*)	Mm.PT.51.12747673	IDT
REV-ERBα (*Nr1d1*)	Mm00520708_m1	Taqman Gene Expression Assay
Per2	Mm00478113_m1	Taqman Gene Expression Assay
Nampt	Mm00451938_m1	Taqman Gene Expression Assay
BMAL1 (*Arntl*)	Mm00500226_m1	Taqman Gene Expression Assay
Per1	Mm00501813_m1	Taqman Gene Expression Assay
Cry1	Mm00514392_m1	Taqman Gene Expression Assay
Odc1	Mm.PT.53a.23589427	Taqman Gene Expression Assay

Table 2. Primers for quantitative real-time PCR on mammalian cell lines.

Sigma), and at the start of the experiment, the other half of the cells were cultured in dexamethosone. At each timepoint, two plates were harvested representing 0 and 24 hours +dex, 4 and 28, etc, to arrive at a 52 hour timecourse. mRNA was processed and analyzed as described above.

Lumicycle

Lumicycle analysis of U2OS BMAL1::Luc cells was described previously (Baggs et al., 2009). Briefly, three days prior to analysis, cells were plated in 35 mm dishes at a concentration of 250,000 cells / plate. 24 hours later, cells were transfected with siRNA as described above. 48 hours post transfection, cells were cultured atmospheric conditions, in phenol red-free DMEM (Sigma, St. Louis, MO, USA) containing 5% FBS (Hyclone or Gibco), 25 mM D-glucose (Sigma), 35 mg/L sodium bicarbonate (Gibco), 10 mM HEPES (Gibco), Pen/Strep (Mediatech), 0.1 mM beetle-luciferin (Promega), and 0.1 µuM dexamethasone (Sigma), and dishes were sealed with high vacuum grease (Dow Corning, Midland, MI, USA). Plates were measured for luminescence every 10 minutes for at least 4 days on a Lumicycle™ luminometer (Actimetrics, Wilmette, IL, USA). The experiment for mHCC 3-4 BMAL1::Luc cells was performed in the same way, except that cells were treated with either tetracycline or mHCC media 24 hours before the plates were sealed.

Results

Clock gene expression and oscillation in P493-6 lymphocytes

To address the question whether aberrant c-MYC overexpression would disrupt the molecular clock, we first used MYC-inducible, tetracycline (Tet)-repressive cell line P493-6 that has been used in previous study from the lab (Yustein et al., 2010). P493-6 cells were derived from human Burkitts lymphoma and were engineered with a Tet-repressive ectopic MYC vector and an EBNA2-ER fusion protein. EBNA2-ER fusion protein restricts the expression of endogenous MYC only in the presence of estradiol. Therefore, ectopic MYC is induced in the absence of tetracycline and endogenous MYC can be induced when the cells are exposed to estradiol. P493-6 cells thus have three states: HIGH MYC (-Tet), LOW MYC (+Tet) and INTERMEDIATE MYC (+Tet + estradiol) (Fig. 3) (Yustein et al., 2010). HIGH MYC cells express significant higher level of MYC protein and grow much faster than either INTERMEDIATE MYC or LOW MYC cells (Fig. 3).

We first examine core clock gene expression in HIGH MYC and LOW MYC cells by harvesting RNA every 4 hours for 48 hours after synchronizing cells with 50% of fetal bovine serum (FBS), which has been shown to synchronize cultured cells up to three consecutive days (Balsalobre et al., 1998). As shown in Fig. 4, *PER2*, *REV-ERBα* and *CLOCK* is upregulated by MYC among all time points. Selected genes that are documented under the control of circadian rhythm, such as Nicotinamide phosphoribosyltransferase (*NAMPT)* and *SIRT1* (Fig. 4), are also strongly induced by Myc. Interestingly, central clock gene *BMAL1* is not detectable (Fig 6A) among all time points.

Despite the change in the expression level of several core clock genes upon MYC induction, there is no appreciable oscillation of all the genes we examined even in LOW

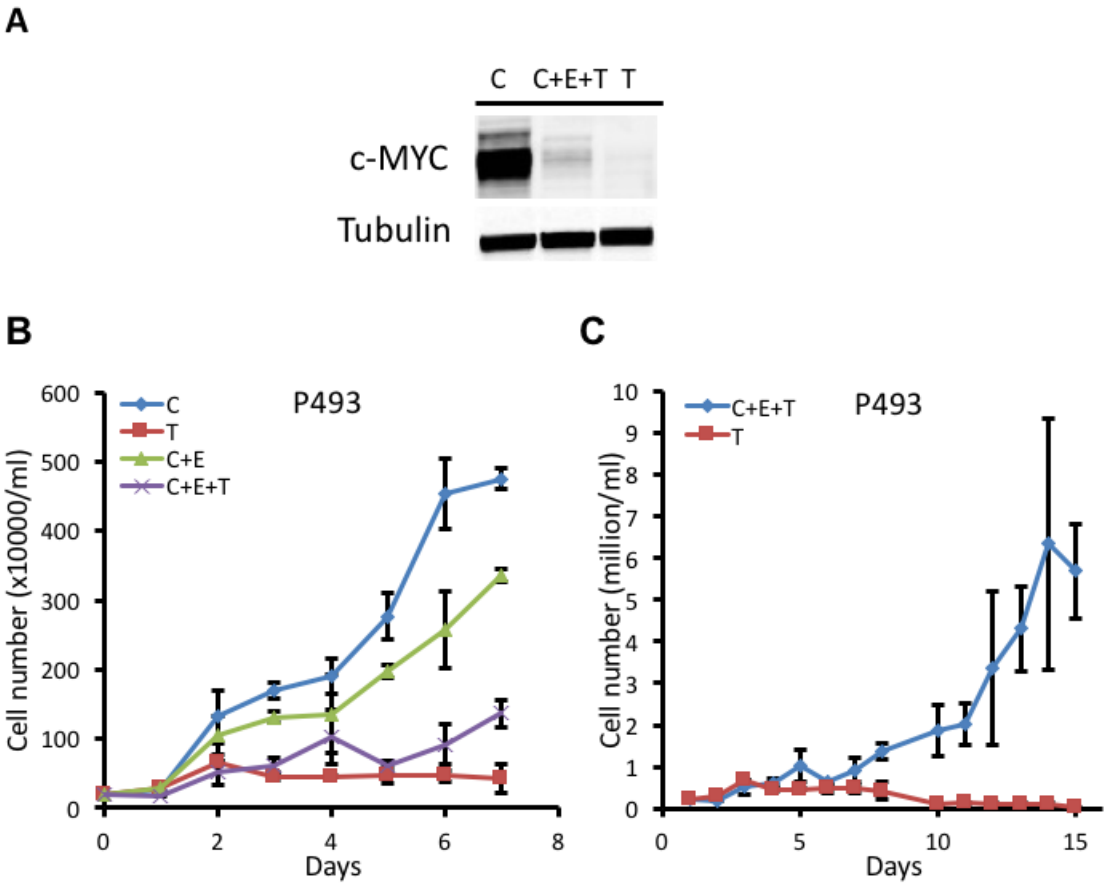

C: P493 cells without any treatment
TE: P493 cells treated with 0.1 ug/ml tetracycline and 1uM estradiol
T: P493 cells treated with 0.1 ug/ml tetracycline

Figure 3. Myc-dependent growth in human P493 cells.
(A) c-MYC protein level determined by immunoblotting (B, C) Growth curve of untreated P493 cells [C], P493 cells with 0.1ug/ml tetracycline and 1uM estradiol [C+E+T], P493 cells with 1uM estradiol [C+E] and P493 cells treated with 0.1 ug/ml tetracycline [T]

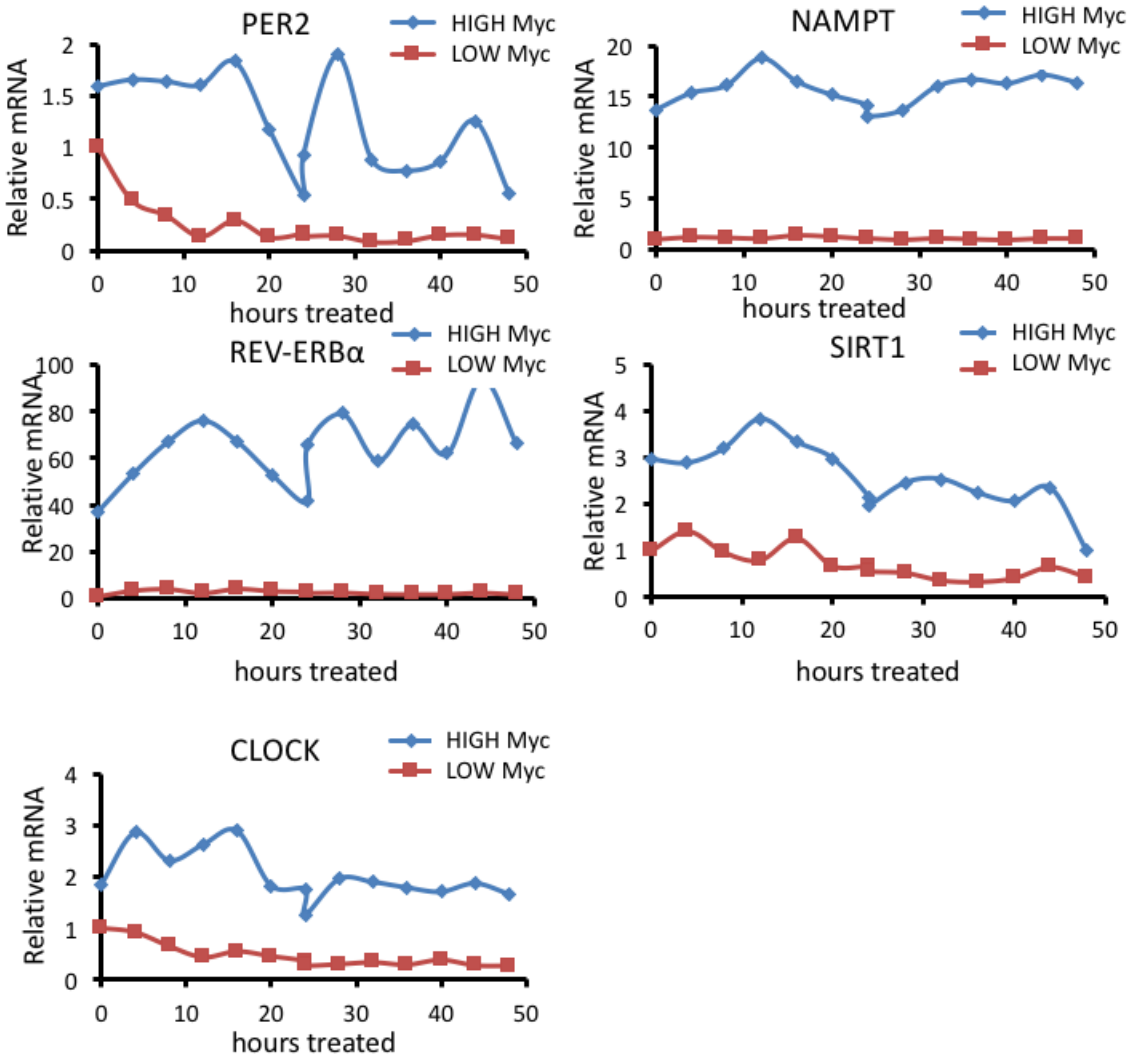

Figure 4. Quantitative RT-PCR of core clock genes and clock-controlled genes in synchronized P493 cells with HIGH MYC versus LOW MYC.
Time series (every 4 hr) expression of *PER2*, *REV-ERBα*, *CLOCK*, *NAMPT*, *SIRT1* mRNA (relative to *β2M*) determined by RT-PCR in synchronized P493 cells with HIGH MYC (-Tet) or LOW MYC (+Tet).

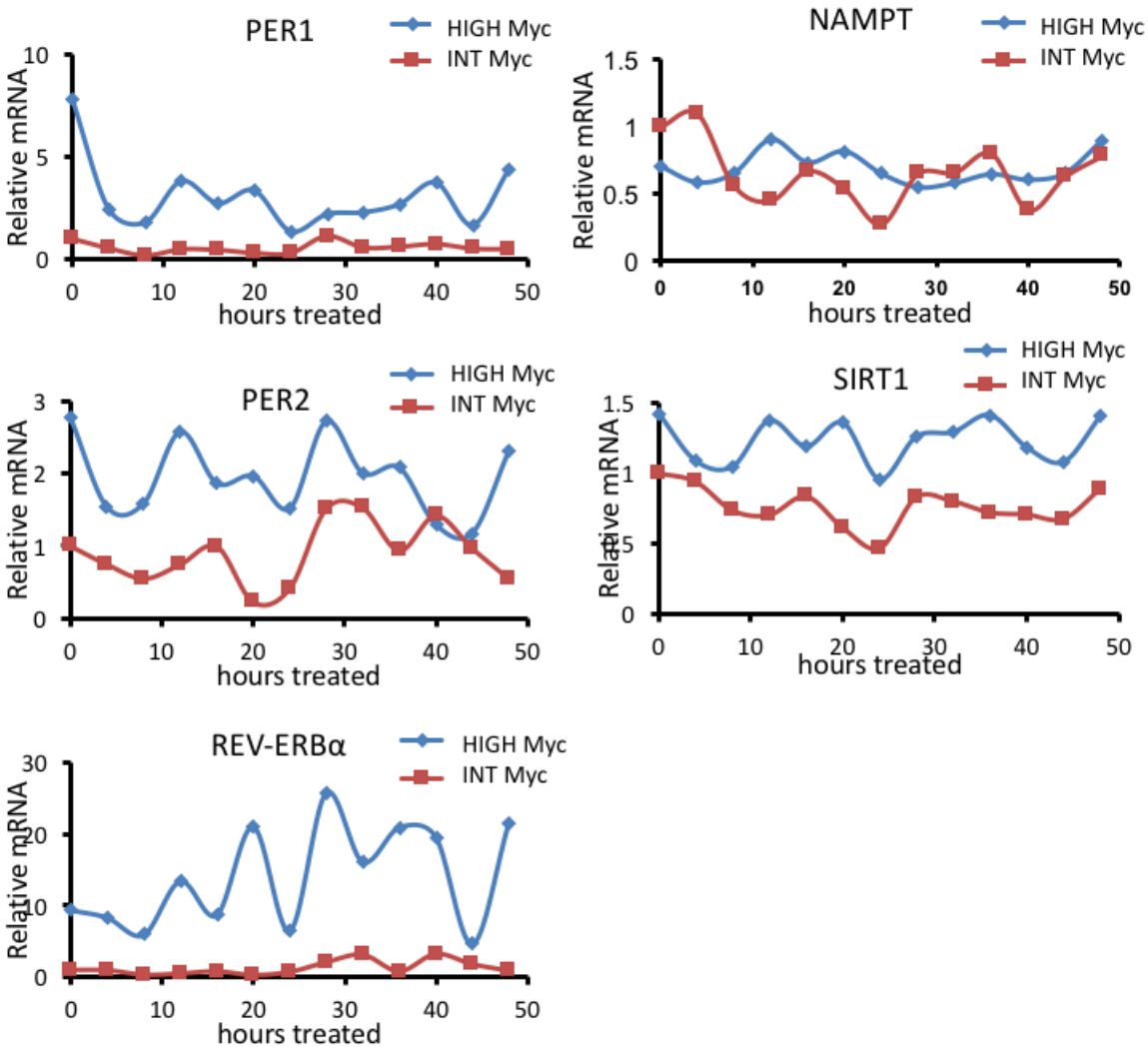

Figure 5. Quantitative RT-PCR of core clock genes and clock-controlled genes in synchronized P493 cells with HIGH MYC versus INTERMEDIATE MYC.

Time series (every 4 hr) expression of PER1, PER2, REV-ERBα, NAMPT, SIRT1 mRNA (relative to *b2M*) determined by RT-PCR in synchronized P493 cells with HIGH MYC (-Tet) or INTERMEDIATE MYC (+Tet+Estradiol). INT: INTERMEDIATE MYC

MYC cells. Lack of circadian oscillation in LOW MYC cells could be explained by two reasons. First, LOW MYC cells are usually sicker and it is possible that loss of rhythm is a manifestation of sick cells. Second, BMAL1 could be silenced at the genetic or epigenetic level in P493 cells. In fact, previous literature has documented that Bmal1 is epigenetically silenced in human hematopoietic cancers (Taniguchi et al., 2009).

Since there is no detectable clock gene oscillation in LOW MYC, we then study mRNA expression in INTERMEDIATE MYC cells. The fact that these endogenous MYC-expressing cells are still able to grow eliminate the concern of these cells being too sick (Fig. 3). Previous literature has demonstrated that endogenous MYC exhibits circadian rhythm and it is also a target of PER2 in mice (Fu et al., 2002). Therefore, we suspected that INTERMEDIATE MYC cells are likely to exhibit circadian rhythm. As shown in Fig 3, INTERMEDIATE MYC cells express minimal MYC protein level compare to HIGH MYC cells. However, in contrast to LOW MYC cells, INTERMEDIATE MYC cells are still able to proliferate with a much slower speed compare to HIGH MYC cells (Fig. 3).

When we examine the clock gene expression in INTERMEDIATE MYC cells for 48 hours, as expected, E-box containing genes such as *PER1*, *PER2* and *REV-ERBα* are upregulated in HIGH MYC cells compare to INTERMEDIATE MYC cells (Fig. 5). The ratio of expression level of these genes between HIGH MYC cells and INTERMEDIATE MYC cells, however, is smaller. Notably, the expression of *NAMPT* is not different in HIGH MYC cells versus INTERMEDIATE MYC cells (Fig. 5). This observation suggests that *NAMPT* induction might already be saturated even with minimal MYC elevation. *BMAL1* remains undetectable in INTERMEDIATE MYC cells. Surprisingly, the expression of *BMAL1* paralog *BMAL2* is dramatically induced in INTERMEDIATE

MYC cells (~500 fold) compare to HIGH MYC cells (Fig. 6B). The mechanism of how *BMAL2* is induced as well as the functional significance of high level of *BMAL2* in INTERMEDIATE MYC cells still requires further investigation. Unfortunately, we are still unable to appreciate circadian oscillation of clock genes in INTERMEDIATE MYC cells (Fig. 5), suggesting perhaps there is an irreversible disruption of the molecular clock in P493-6 cells regardless of MYC expression level.

Clock gene expression and oscillation in mouse hepatocellular carcinoma cell lines

Having observed that *BMAL1* is not expressed in P493-6 cells even in INTERMEDIATE MYC cells, it is hard to assess the effect from MYC on circadian rhythm if a cell line does not have rhythm to begin with. We went on and search for other MYC-inducible models. Previous literature on circadian rhythm often use mouse liver to assess the oscillation of core clock components. *Ex vivo* liver tissue from *Per2-luc* mice that was genetically knock-in a fusion protein of *Per2* and luciferase is able to show endogenous *Per2* oscillation over several days using luminometer recording (Yoo et al., 2004). Recent study also showed a significant portion of metabolic genes that are oscillating and bound by clock components in mouse liver (Koike et al., 2012. Most interestingly, canonical MYC target NAMPT also exhibits a robust cycling in mouse liver, which will be an interesting clock output to evaluate the effect of overexpressed MYC on oscillatory metabolism (Koike et al., 2012).

To study the effect of ectopic MYC on clock gene oscillation in liver, we used a human MYC-inducible, tetracycline-repressive mouse hepatocellular carcinoma (HCC) mouse

A

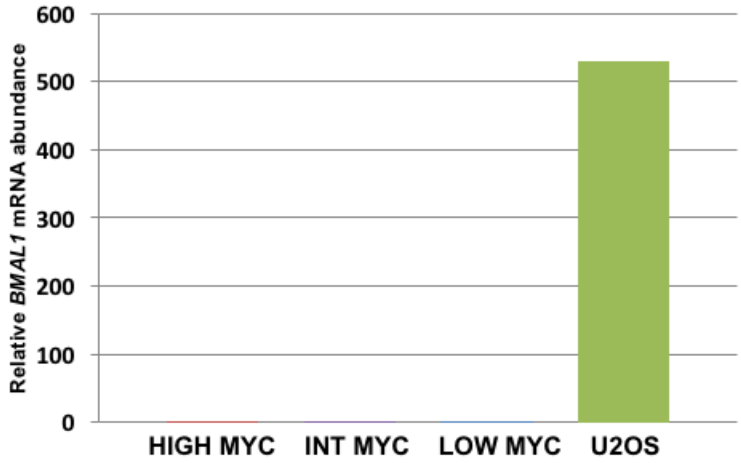

B

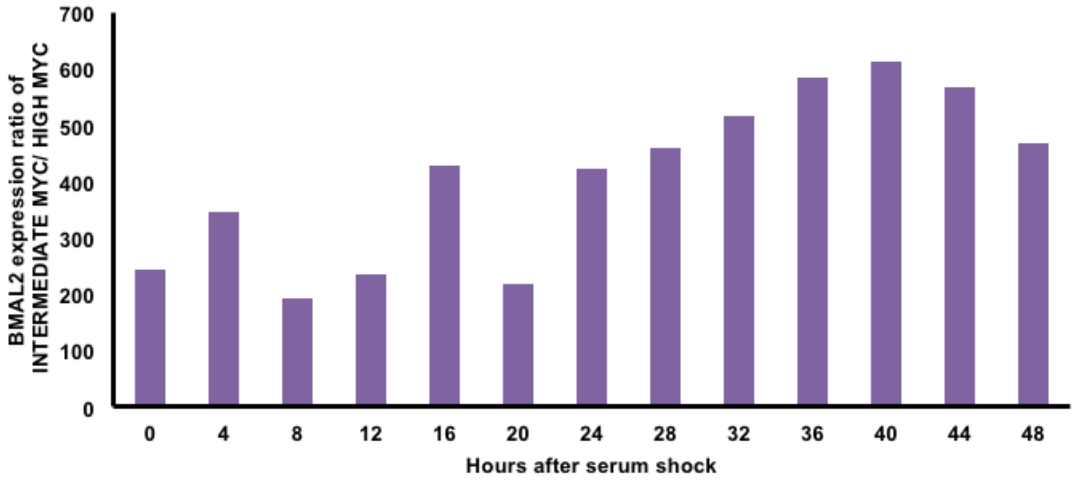

Figure 6. High BMAL2 expression in INTERMEDIATE MYC cells.
(A) BMAL1 mRNA expression (normalized to expression of *β2M*) determined by RT-PCR in HIGH MYC, INTERMEDIATE MYC, LOW MYC and U2OS cells. (B) Ratio of Time series (every 4 hr) BMAL2 expression in synchronized INTERMEDIATE MYC versus HIGH MYC cells.

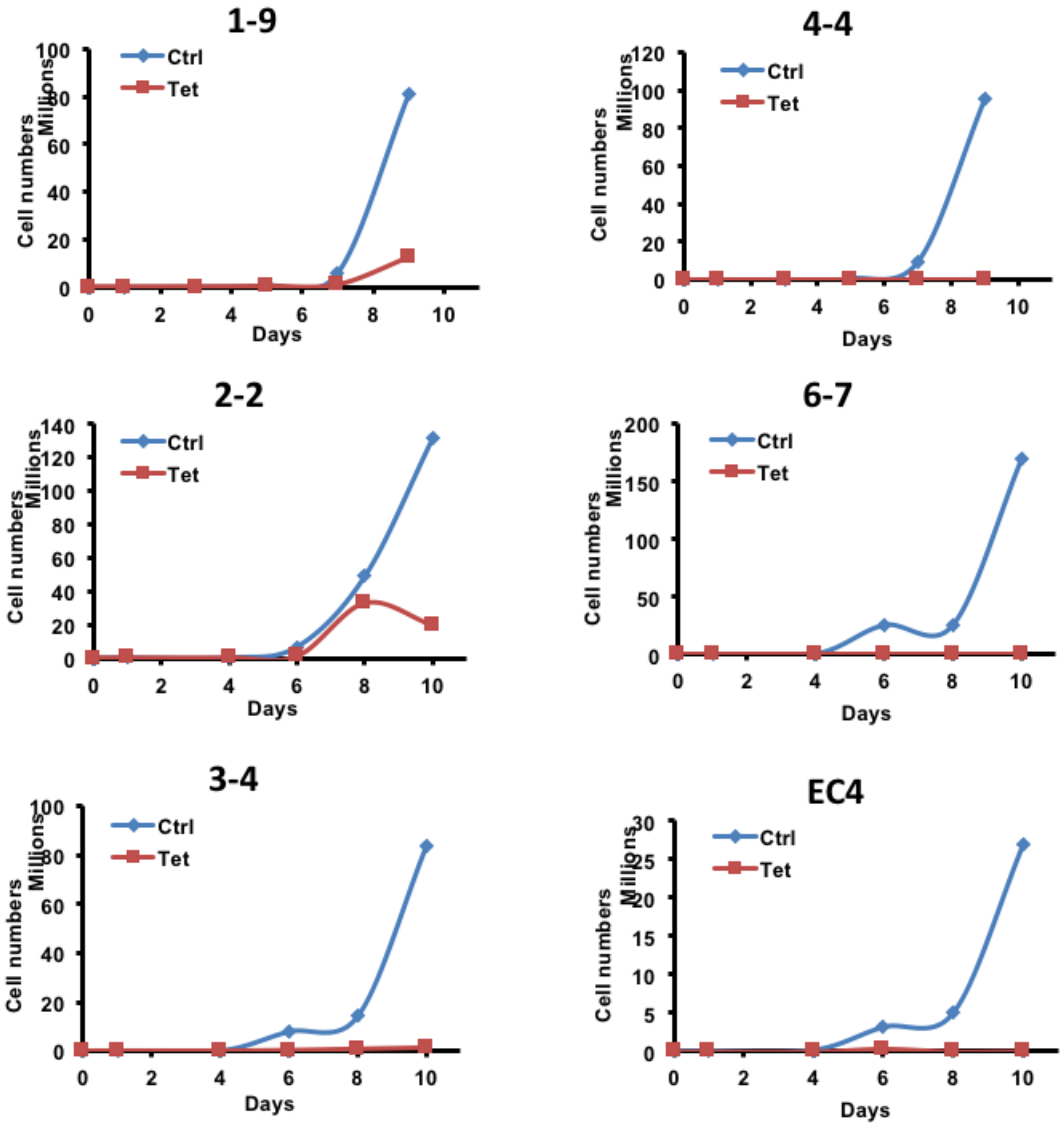

Figure 7. Growth curve of mouse hepatocellular carcinoma cell lines.
Growth curve of mouse hepatocellular carcinoma cell lines (mHCCs) 1-9, 2-2, 3-4, 4-4, 6-7 and EC4 in the absence (Ctrl) and presence (Tet) of tetracycline.

model kindly shared by Dr. Dean Felsher. Human MYC is ectopically expressed in these mice and is sufficient to induce aggressive mouse liver tumor which would regress after giving the mice doxycycline water (Shachaf et al., 2004) (Fig. 8A). This model provides us a great tool to study circadian rhythm because not only we can manipulate MYC level very easily, the effect of MYC on growth and potentially metabolism is reversible. In order to test our hypothesis *in vitro*, we use cell lines that derived from the mouse HCC. First of all, we assess the growth curve in these cell lines in the presence and absence of tetracycline. All six lines that derived from the mouse HCC show dramatic growth advantage in the absence of tetracycline when MYC is induced (Fig. 7). Among those, we choose 3-4 cells because its morphology resembles human hepatocytes. We also further characterize EC4 cells due to its dependency on MYC for proliferation.

Both 3-4 and EC4 cells expressed high level of human c-MYC in the normal culture condition. The expression can be turned off upon treatment of tetracycline as short as 6 hours (Fig. 8B). Twenty-four hours after tetracycline treatment, c-MYC protein is almost undetectable on immunoblot (Fig. 8B). To assess that high level of c-MYC protein is functional, we examine mRNA expression of two canonical MYC targets, *Ornithine Decarboxylase 1(Odc1)* and *Nampt* in the presence and absence of tetracycline. As expected, both ODC1 and NAMPT are strongly induced in the absence of tetracycline, suggesting ectopic human MYC is functionally intact (Fig. 8B).

Next, we assessed mRNA expression of several core clock genes, including positive regulator *BMAL1* and negative regulators in the MYC ON state (-Tet) and MYC OFF state (+Tet) of mHCC 3-4 and EC4 cells. Similar to P493 cells, E-box containing genes *Per1*, *Per2*, *Cry1*, *Rev-erbα* and *Rev-erbβ* are significantly induced in the MYC ON state

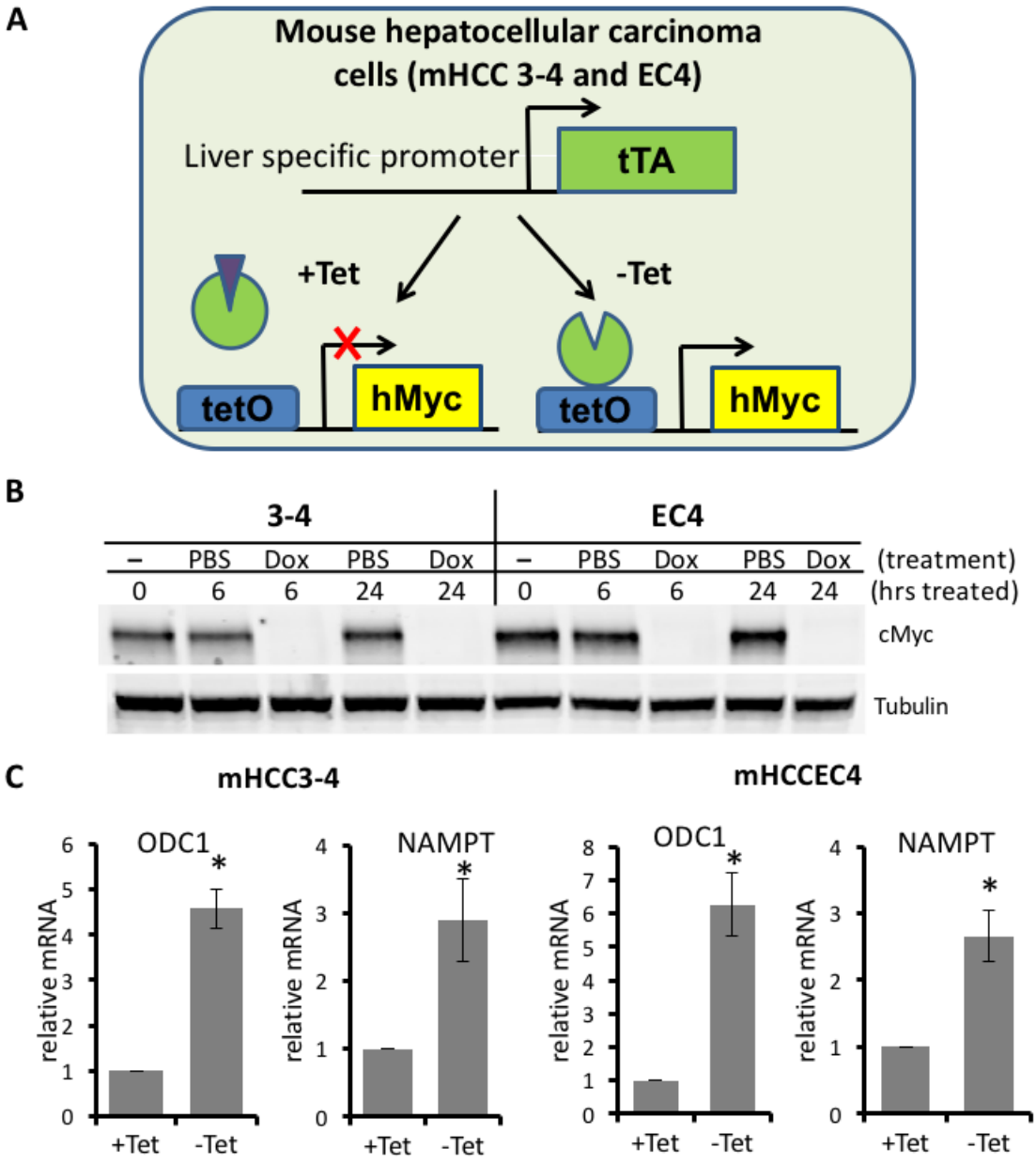

Figure 8. Tet-Off human MYC induces MYC target genes in mHCC cells. (A) Schematic illustrating the strategies used in mouse hepatocellular carcinoma (mHCC) 3-4 (A) to overexpress human MYC. (B) MYC (cMyc) protein level determined by immunoblotting in mHCC 3-4 cells cultured without tetracycline (-), with PBS control (PBS), or 20ng/ml tetracycline (Dox) for 6 or 24 hours . (C) Expression of ODC1 and NAMPT in mHCC 3-4 and EC4 cells as determined by RT-PCR. Data are shown as means ± SD (n = 5).

of mHCC 3-4 (Fig. 9). In contrast, central clock regulator *Bmal1* is suppressed by MYC (Fig. 9). mHCC EC4 cells exhibit similar expression patterns as mHCC 3-4, however, *Per2* and *Rev-erbβ* was not significantly induced by MYC in EC4 cells, and *Bmal1* is actually induced by MYC (Fig. 10).

It appears that expression of the majority of clock genes is altered upon MYC overexpression, so we hypothesized that the oscillation of these clock genes will also be disrupted by overexpressed MYC. To assess of the circadian oscillation of these genes, we synchronized both mHCC 3-4 and EC4 cells with dexamethasone at time zero, which has been shown to synchronize cells and allow cells to oscillate one more day compare with serum shock, then we harvested the cells every four hours and analyzed mRNA expression of these clock genes. We found *Bmal1* mRNA expression is suppressed in the later time points and *Per2* is slightly induced at most time points. Oscillation of *Per2* is minimally perturbed by high MYC. In MYC OFF state, *Rev-erbα* and *Rev-erbβ* showed strong circadian oscillation with peak at 4, 24 hours and trough at 16, 40 hours after dexamethasone treatment. This oscillation is greatly disrupted in MYC ON state (Fig 11). In EC4 cells, *Bmal1* is upregulated at most time points and *Per2* is minimally altered (Fig. 12), which is consistent with *Per2* mRNA expression in unsynchronized cells (Fig 10). *Per1*, *Rev-erbα*, *Nampt* and *Cry1* are greatly induced by MYC at all time points (Fig. 12). Notably, while Rev-erbα oscillation appears to be disrupted in MYC ON state, Rev-erbβ and Cry1 oscillation is largely intact (Fig. 12). Our observation suggested that elevated MYC indeed alters mRNA expression of several components in the molecular clock circuitry and the disruption can be reversed when MYC is removed.

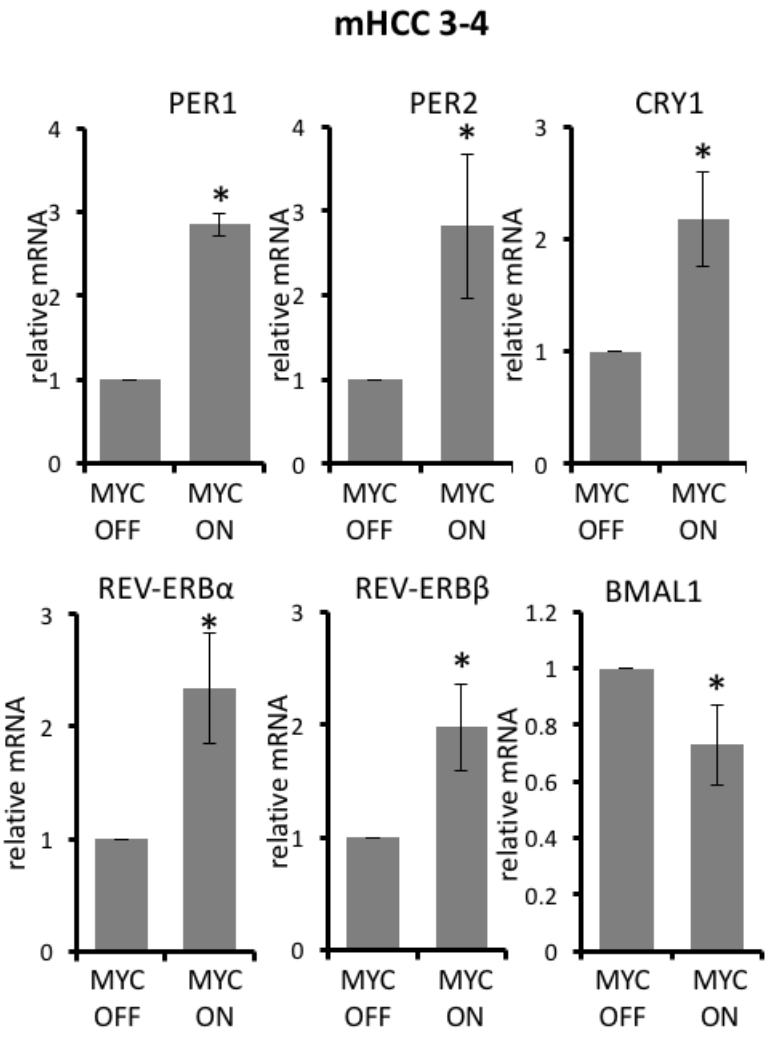

Figure 9. MYC upregulates circadian repressor genes in mHCC 3-4 cells.
(A) Expression of clock factor genes (indicated above each graph) in mHCC 3-4 cells treated with (+Tet, MYC-OFF) or without (-Tet, MYC-ON) tetracycline for 24 hr. mRNA expression determined by RT-PCR was normalized to *β2M* expression. Means and SDs from at least three experiments are shown. *$p < 0.05$ by Student's t test -Tet (MYC-ON) samples relative to +Tet (MYC-OFF) samples.

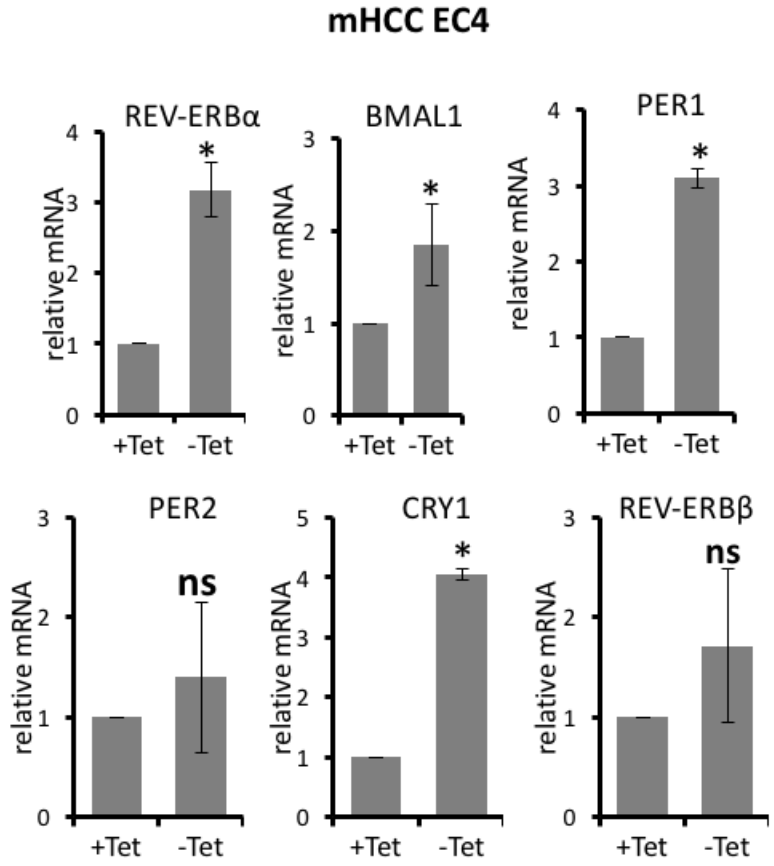

Figure 10. MYC upregulates circadian repressor genes in mHCC EC4 cells. (A) Expression of clock factor genes (indicated above each graph) in mHCC EC4 cells treated with (+Tet, MYC-OFF) or without (-Tet, MYC-ON) tetracycline for 24 hr. mRNA expression determined by RT-PCR was normalized to *β2M* expression. Means and SDs from at least three experiments are shown. *$p < 0.05$ by Student's t test -Tet (MYC-ON) samples relative to +Tet (MYC-OFF) samples, ns = not significant.

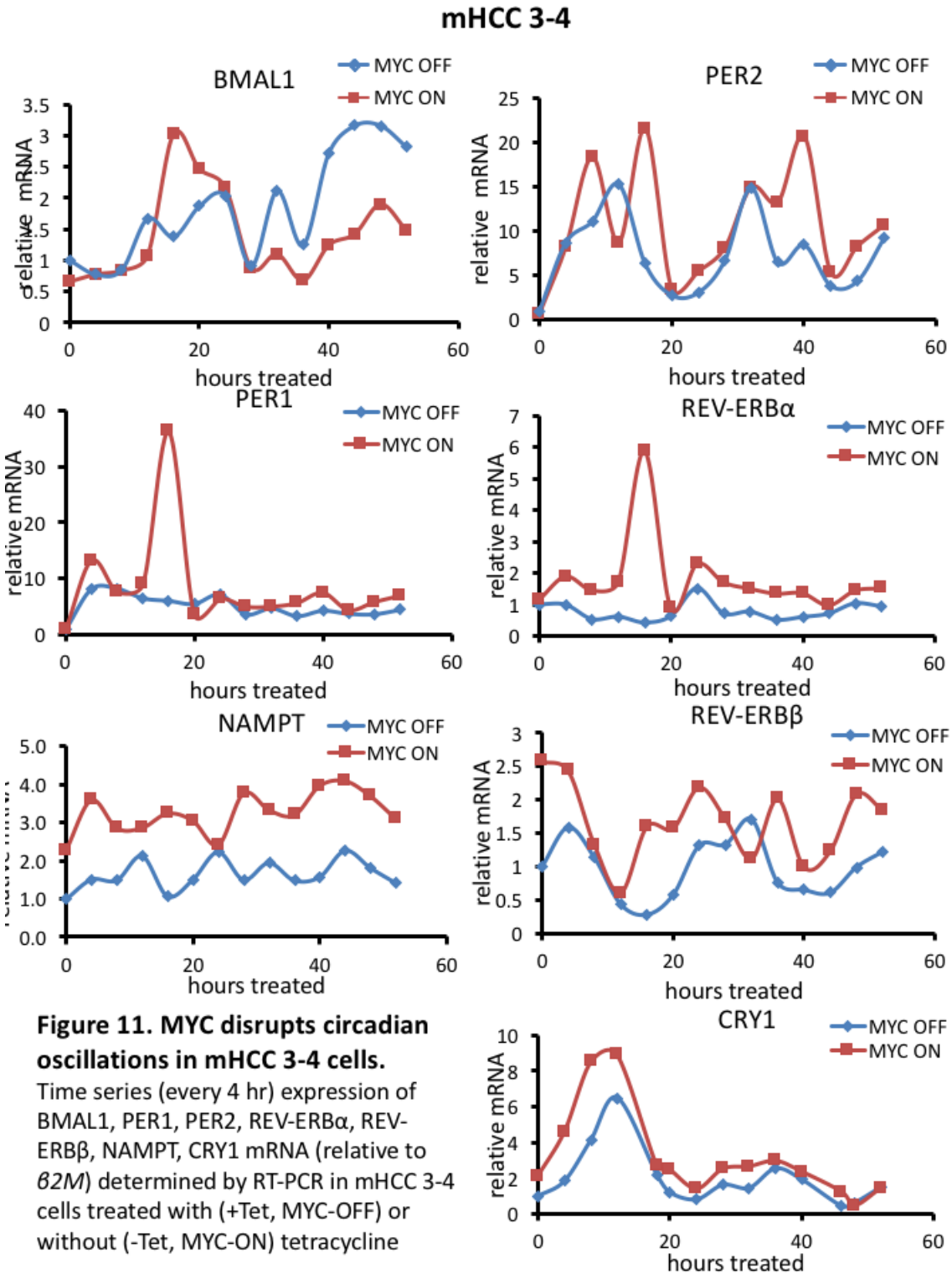

Figure 11. MYC disrupts circadian oscillations in mHCC 3-4 cells.
Time series (every 4 hr) expression of BMAL1, PER1, PER2, REV-ERBα, REV-ERBβ, NAMPT, CRY1 mRNA (relative to *β2M*) determined by RT-PCR in mHCC 3-4 cells treated with (+Tet, MYC-OFF) or without (-Tet, MYC-ON) tetracycline

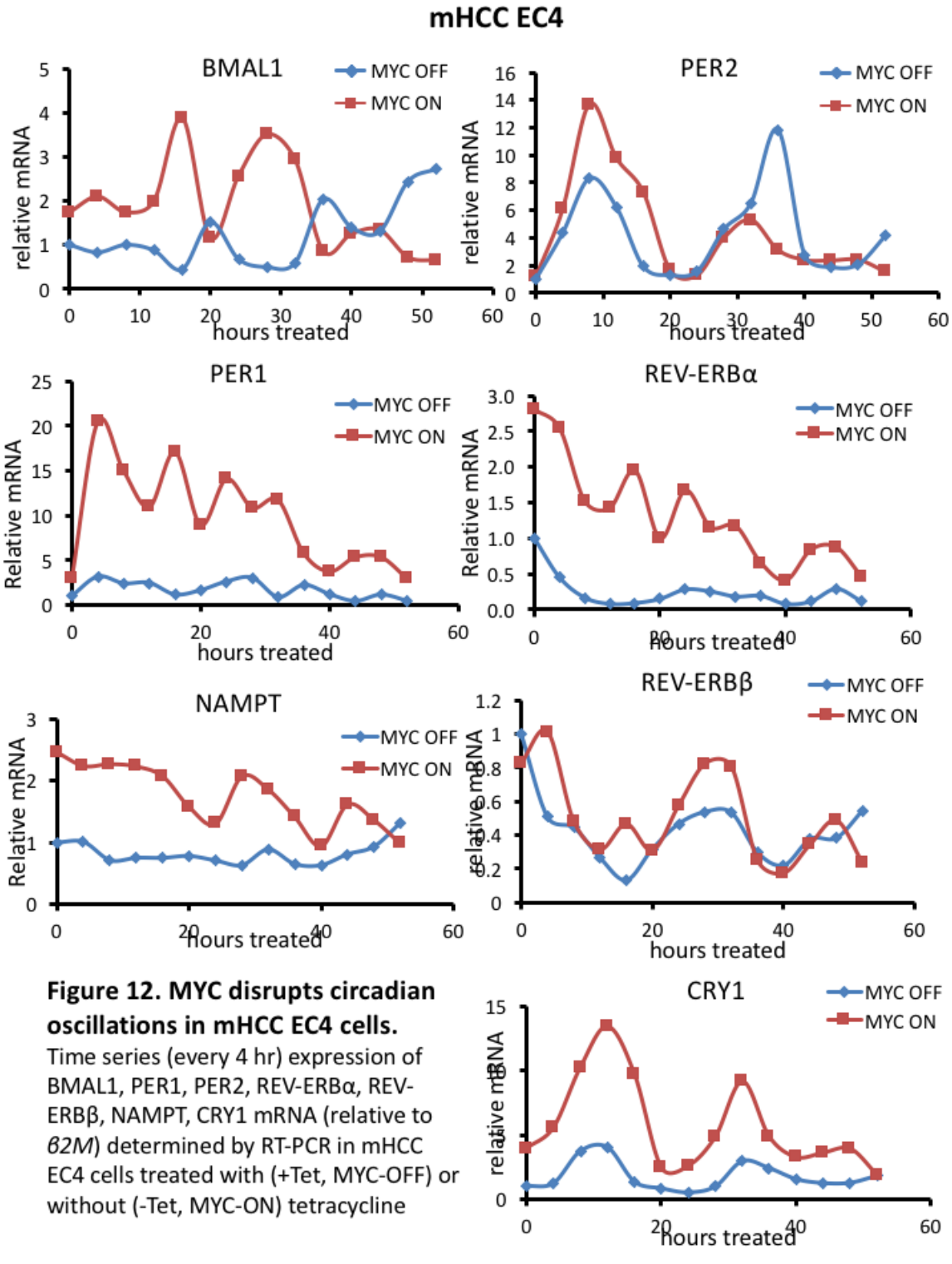

Figure 12. MYC disrupts circadian oscillations in mHCC EC4 cells. Time series (every 4 hr) expression of BMAL1, PER1, PER2, REV-ERBα, REV-ERBβ, NAMPT, CRY1 mRNA (relative to *β2M*) determined by RT-PCR in mHCC EC4 cells treated with (+Tet, MYC-OFF) or without (-Tet, MYC-ON) tetracycline

Generating *BMAL1::Luc* single clones from mHCC 3-4 cell line

Bmal1 oscillation in mHCC cells appears to be altered by MYC overexpression, however, the weak oscillation of *Bmal1* in MYC OFF cells prevent us from observing stronger effect of MYC disruption. The weaker oscillation of *Bmal1* in MYC OFF cells is a possible consequence from a mixed cell population of non-oscillators and strong-oscillators. Therefore, we proceed to subclone the cells and identify strong oscillators within the heterogeneous population to increase the signal to noise ratio.

To screen for strong oscillators, a quick and easy assay to determine which clone is cycling is critical. In collaboration with Dr. John Hogenesch, we transfect mHCC cells with BMAL1::Luc construct, which has a luciferase reporter downstream of the BMAL promoter. By using a real-time luminometer, LumiCycle®, allows us to observe continuous oscillation of BMAL1 promoter activity every 10 minutes over several days.

We started with mHCC 3-4 cells because it exhibits relative stronger circadian oscillation. mHCC 3-4 cells were cultured in the presence of tetracycline (MYC OFF) while we select for strong oscillatory clones. A number of clones, including C12, C4, C8 and C9 were selected based on high luciferase signals and appreciable oscillation in the presence of tetracycline. Strikingly, when tetracycline was withdrawal from these clones (MYC ON), BMAL1 oscillation is blunted (Fig. 13). However, although the *BMAL1-luc* is lower in C12, C4 and C9 in MYC OFF cells, *BMAL1-luc* level is higher in C8 MYC OFF cells (Fig. 13). Based on our observation, MYC suppress *Bmal1* expression in polyclonal and the majority of monoclonal mHCC 3-4 cells, but why some clones still exhibit high level of *BMAL1-luc* under high MYC requires further investigation. These observations

corroborate the fact that elevated MYC is able to blunt the oscillation and levels of *Bmal1* promoter activity, and this disruption can be recovered when MYC is removed.

Next, we are interested to see the expression of other clock components in these single clones. mHCC 3-4 C12 was cultured, synchronized and harvested every 4 hours (Fig. 14). Surprisingly, mRNA expression of *Bmal1* is not consistent with the oscillation with *Bmal1* promoter activity observed through *BMAL1::Luc*. Instead, slight phase shift is observed in the oscillation of *Bmal1* mRNA. This discrepancy between *BMAL1::Luc* promoter oscillation and endogenous *Bmal1* mRNA oscillation is unclear and would need further investigation. *Per2* mRNA oscillates beautifully in MYC OFF cells and only slight phase shift is observed in MYC ON cells. *Per1*, *Rev-erbα* and *Nampt* are upregulated by MYC in a similarly way compare with mHCC 3-4 parental cell lines. Notably, this strong oscillatory clone C12, exhibits beautiful oscillation of *Nampt* mRNA in the presence of tetracycline (MYC OFF). This oscillation, however, is disrupted when MYC is induced.

U2OS clock gene expression and oscillation

There are two approaches to study the effect of oncogenic MYC on the molecular clock circuitry. One way is to turn off MYC in a cell line rely on high levels of MYC to maintain its growth, such as P493-6 and mouse hepatocellular carcinoma cell lines. The other way is overexpressing MYC in a cell line that normally grows without ectopic MYC. U2OS cells are the cell line we used for the second approach.

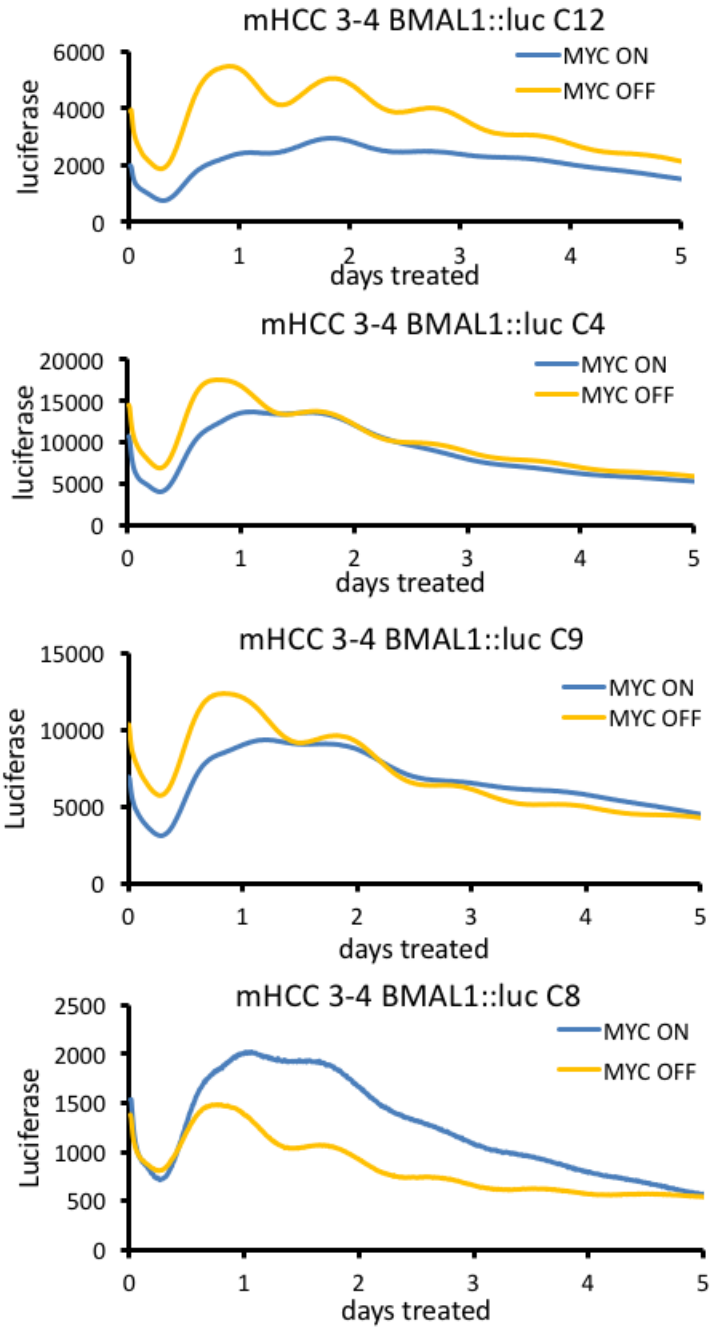

Figure 13. MYC disrupts BMAL1 oscillation in mHCC 3-4 single clones.
Temporal luminescence of mHCC 3-4 BMAL1::Luc cell clone C12 treated with tetracycline (tet, MYC-OFF) or control (tet, MYC-ON) and synchronized with dexamethasone. BMAL1 promoter activity luminescence was continuously measured (every 10 min) in a LumiCycle luminometer. RLU = relative light units.

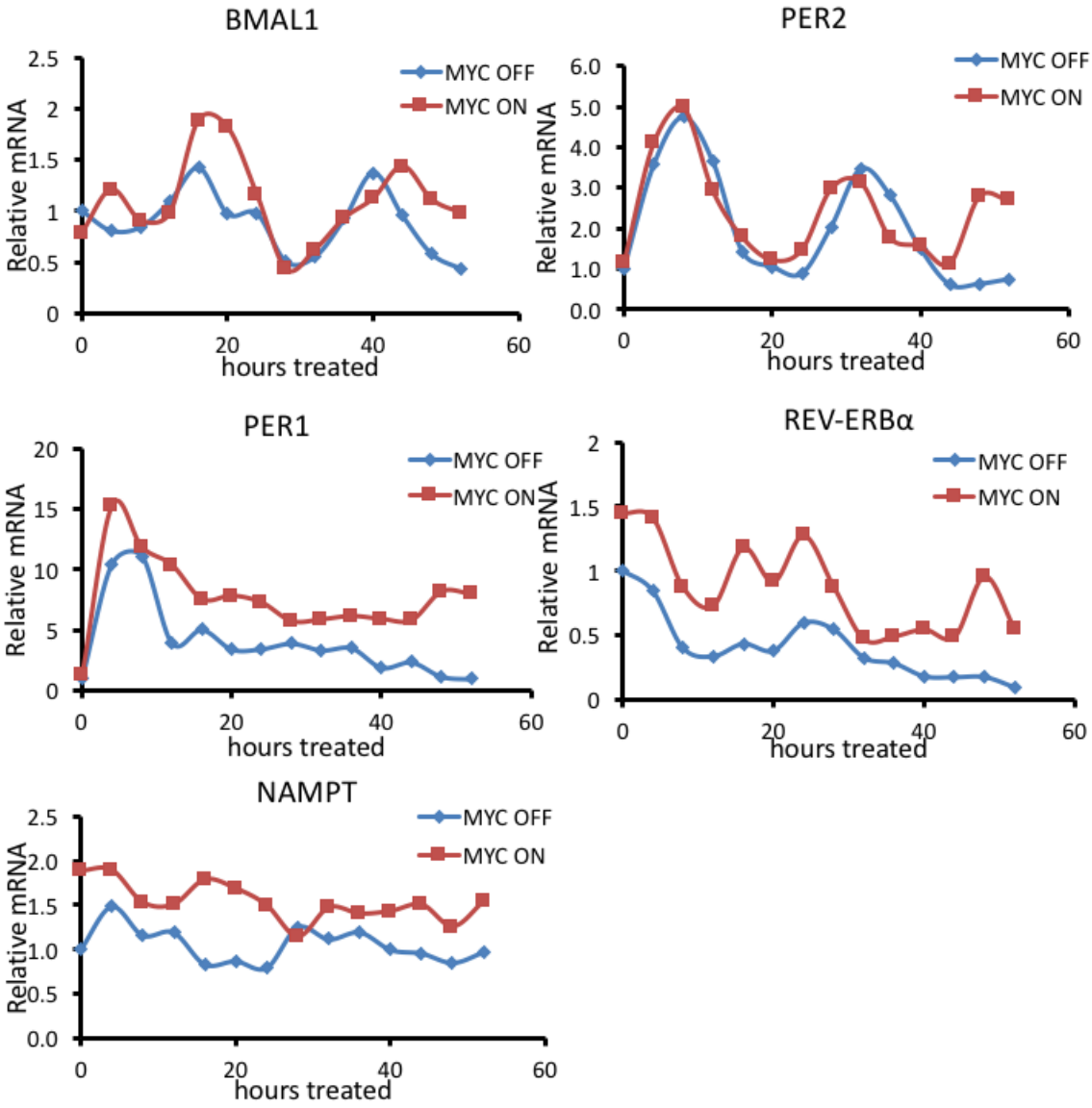

Figure 14. MYC disrupts circadian oscillations in mHCC 3-4 C12 cells
Time series (every 4 hr) expression of BMAL1, PER1, PER2, REV-ERBα, NAMPT mRNA (relative to *β2M*) determined by RT-PCR in synchronized mHCC 3-4 cells C12 cells treated with (+Tet, MYC-OFF) or without (-Tet, MYC-ON) tetracycline

U2OS cell line is derived from human osteosarcoma cells. It normally expresses low level of endogenous MYC (Fig. 15A). The endogenous MYC appears to oscillate and response to dexamethasone treatment (Fig. 15A). The U2OS cell line we use (U2OS *BMAL1::Luc*) was engineered with luciferase reporter downstream of *BMAL1* promoter (Fig. 15B), kindly shared by Dr. John Hogenesch, allowing us to observe *BMAL1* promoter activity continuously using LumiCycle luminometer. In addition, U2OS *BMAL1::Luc* cells, unlike most cancer cell lines, exhibit robust oscillation of *BMAL1* promoter (Fig. 18), serve as a great model system to study circadian rhythm.

We transfected U2OS *BMAL1::Luc* cells with MYC-ER construct which expressing MYC-estrogen receptor (MYC-ER) fusion protein to study the effect of MYC (Fig. 15B). In the presence of estrogen analog 4-hydroxytamoxifen (4OHT), MYC-ER fusion protein will translocate into the nucleus and activate MYC target genes (Fig. 15B). We also introduced mutant MYC-ER construct (MYC-ER Δ106-143) into U2OS *BMAL1::Luc* cells to serve as control. The MYC-ER Δ106-143 construct expresses a fusion protein that is similar to MYC-ER but lacks MYC transactivation domain. Immunoblot showed after 24 hours of 4OHT treatment, there is less MYC-ER protein compare to cells treated with ethanol, suggesting that MYC-ER protein indeed translocated into the nucleus where it was tagged for degradation (Fig. 15C). Similar to other MYC inducible cell lines, canonical MYC targets ODC1 and NAMPT are induced in the cells treated with 4OHT (MYC ON) compare to the cells treated with ethanol (MYC OFF) cells. In contrast, ODC1 was induced in U2OS MYC-ER Δ106-143 cells with much lesser degree and NAMPT is not induced (Fig. 15D).

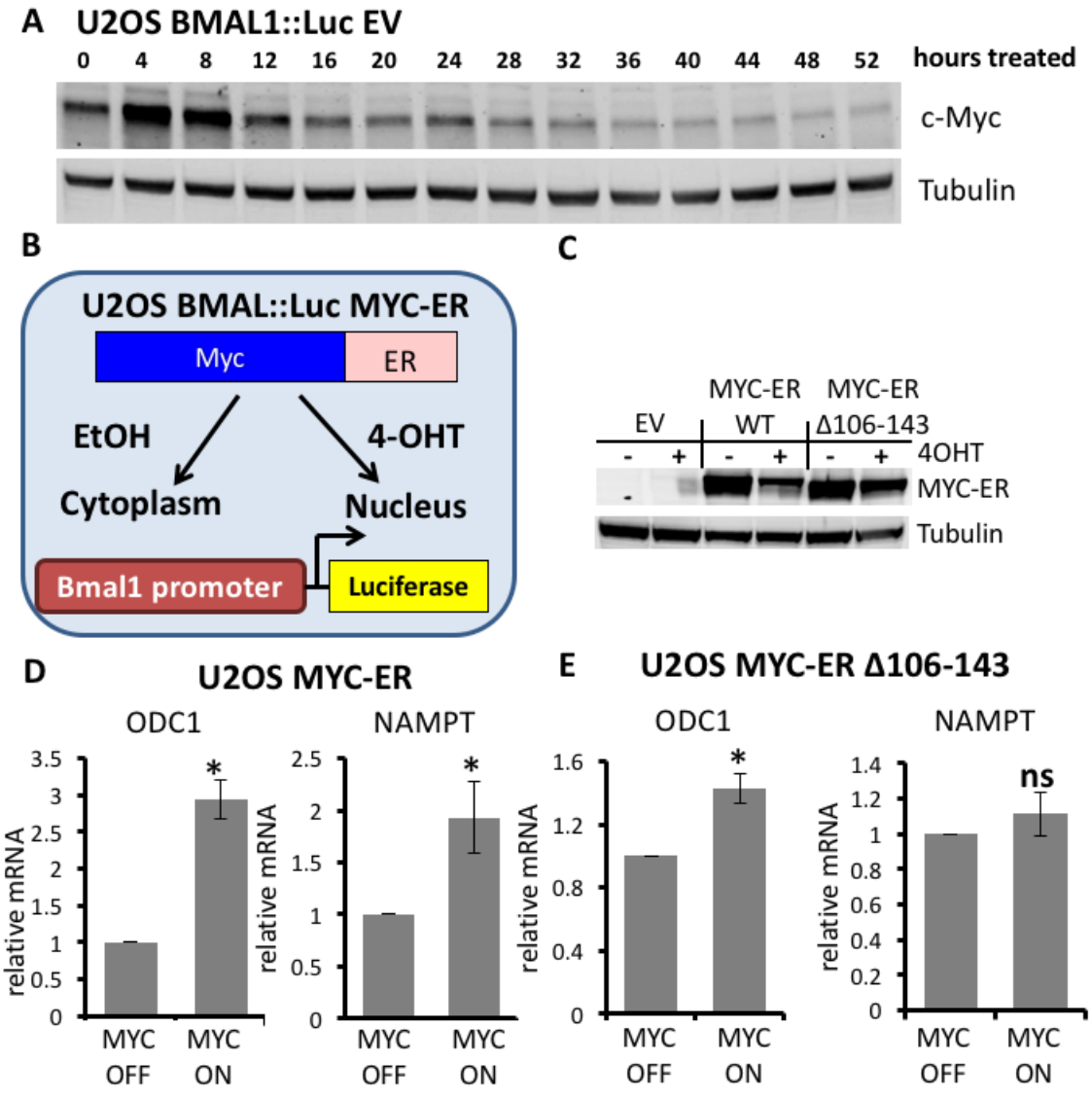

Figure 15. U2OS BMAL::Luc MYC-ER cells.

(A) MYC (cMyc) protein level determined by immunoblotting in synchronized U2OS BMAL1::Luc cells expressing pBabe-Zeo empty vector (EV) (B) Schematic illustrating the strategies used in U2OS BMAL1::Luc MYC-ER cells (C) MYC immunoblot in U2OS BMAL1::Luc cells expressing pBabe-Zeo empty vector (EV), human wild-type MYC-ER™ (WT) or human MYC-ER™ Δ106-143 were treated with 4-hydroxytamoxifen (4OHT, MYC-ON) to activate MYC-ER™ or ethanol (EtOH, MYC-OFF) control (D, E) Expression of ornithine decarboxylase (ODC1) or NAMPT in U2OS MYC-ER™ (D) or MYC-ER™ Δ106-143 cells (E) as determined by RT- PCR, normalized to beta-2-microglobulin. Data are shown as means ± SD (n = 4). ns = not significant.

Next we checked the expression profile of multiple core clock genes. As expected, compare with MYC OFF cells, a number of E-box containing genes in MYC ON cells are significantly upregulated, including *PER2*, *CRY1*, *REV-ERBα* and *REV-ERBβ*. *BMAL1*, consistent with mHCC 3-4, is dramatically suppressed (Fig. 16). Conversely, in U2OS MYC-ER Δ106-143 cells, despite mutant MYC-ER fusion protein translocates to the nucleus (Fig. 15C), lacking transactivation domain of MYC fails to induce the majority of core clock components (Fig. 17).

Given the observation that MYC-ER in U2OS cells induces several core clock genes, we hypothesized that MYC-ER would blunt *BMAL1::Luc* oscillation similarly to mHCC 3-4 C12 (Fig 2-11). As expected, *BMAL1::Luc* oscillates very nicely in MYC-OFF cells but the oscillation was dramatically blunted in MYC-ON cells (Fig. 18A). Interestingly, this phenomenon is not observed in U2OS MYC-ER Δ106-143 cells in the presence of 4OHT (Fig. 18A). Furthermore, *BMAL1::Luc* oscillation was not altered in U2OS BMAL1::Luc parental cells or empty vector transfected cells in the presence of 4OHT (Fig. 18B).

The dramatic disruption of *BMAL1::Luc* in MYC-ON cells suggests that the major clock regulator is profoundly affected in the presence of elevated MYC-ER. We are curious to see whether endogenous *BMAL1* oscillation will be blunted in a similar way as *BMAL1::Luc*. Indeed, endogenous *BMAL1* is suppressed and its oscillation was severely disrupted in MYC-ON cells (Fig. 19). *PER2* and *CRY1* showed nice circadian oscillation in MYC-OFF cells. However, their mRNA oscillation is greatly disrupted in MYC-ON cells. Consistent with what we observe in unsynchronized cells, elevated MYC induces *PER2*, *REV-ERBα*, *CRY1* and *NAMPT* expression across all time points. In addition, the

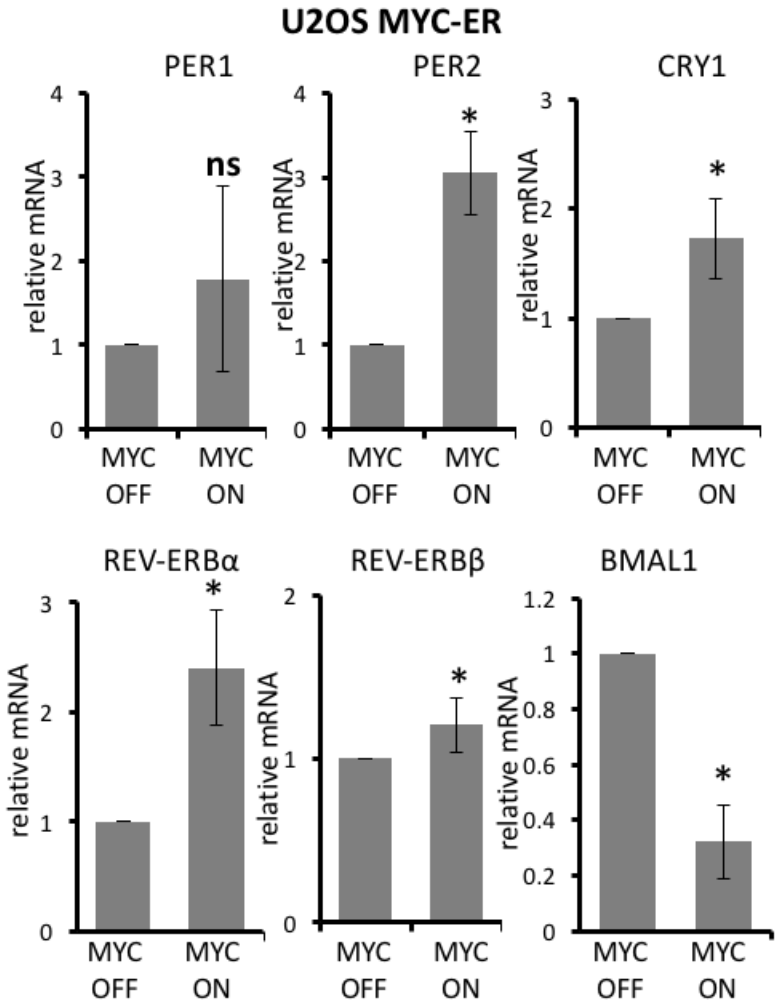

Figure 16. MYC upregulates circadian repressor genes in U2OS MYC-ER cells.

(A) Expression of clock factor genes (indicated above each graph) in U2OS MYC-ER cells treated with either 4OHT (MYC-ON) or EtOH (MYC-OFF) control for 24 hr. mRNA expression determined by RT-PCR was normalized to *β2M* expression. Means and SDs from at least three experiments are shown. *$p < 0.05$ by Student's t test -Tet (MYC-ON) samples relative to +Tet (MYC-OFF) samples, ns = not significant.

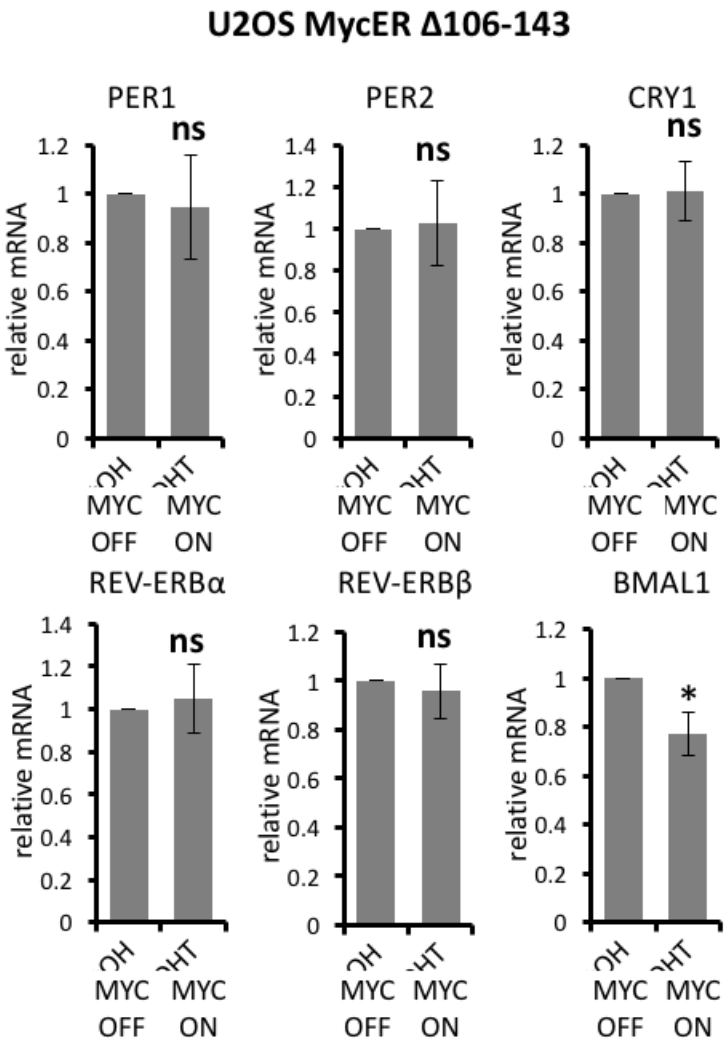

Figure 17. MYC upregulates circadian repressor genes in U2OS MYC-ER cells.

(A) Expression of clock factor genes (indicated above each graph) in U2OS MYC-ER™ Δ106-143 cells treated with either 4OHT (MYC-ON) or EtOH (MYC-OFF) control for 24 hr. mRNA expression determined by RT-PCR was normalized to *β2M* expression. Means and SDs from at least three experiments are shown. *p < 0.05 by Student's t test -Tet (MYC- ON) samples relative to +Tet (MYC-OFF) samples, ns = not significant.

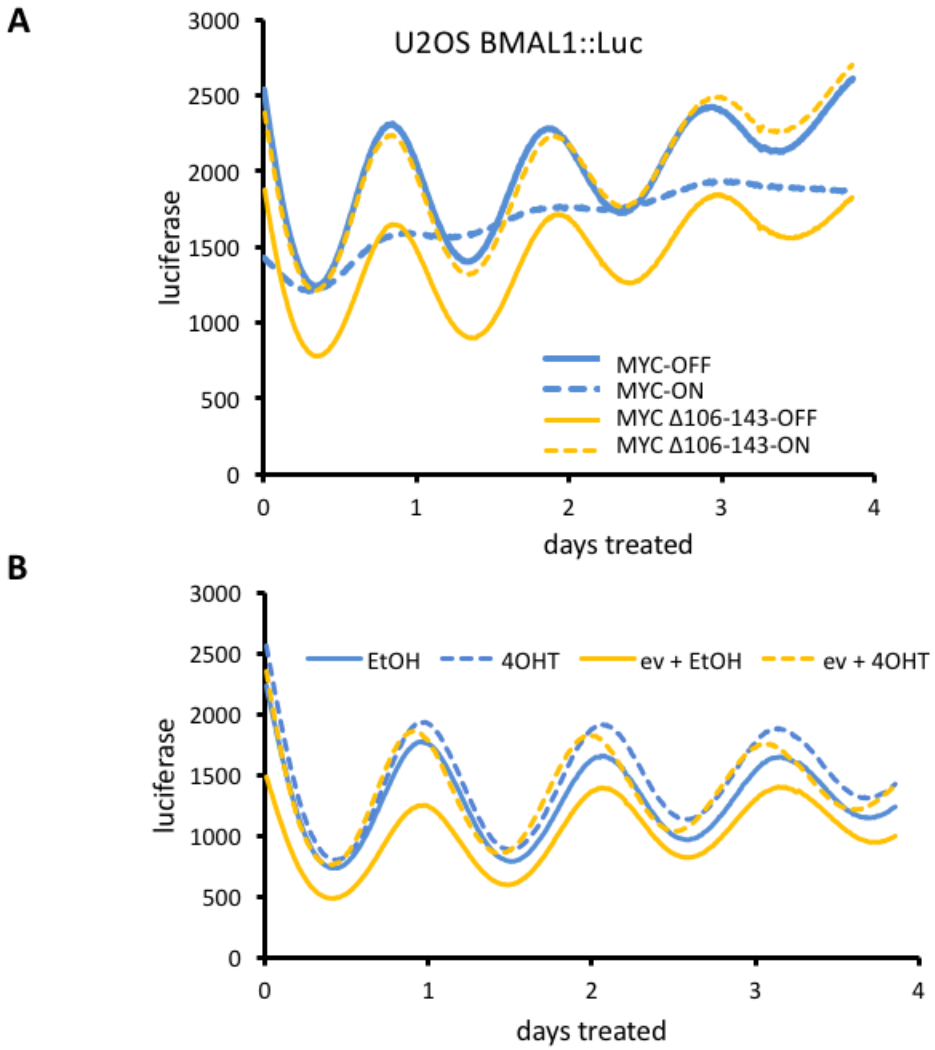

Figure 18. MYC disrupts BMAL1 oscillation and expression in U2OS MYC-ER cells.

(A) U2OS BMAL1::Luc cells stably expressing either human wild-type MYC-ER^{TM} or human MYC-ER^{TM} Δ106-143 were treated with 4-hydroxytamoxifen (4OHT, MYC-ON) to activate MYC-ER^{TM} or ethanol (EtOH, MYC-OFF) control and synchronized with dexamethasone. BMAL1 promoter activity luminescence was continuously measured (every 10 min) in a LumiCycle luminometer. Data are representative of more than three experiments. (B) U2OS BMAL1::Luc cells expressing pBabe-Zeo empty vector (ev) or mock infected were cultured with 4OHT or ethanol, synchronized with dexamethasone, and monitored in LumiCycle luminometer. Data are representative of three or more experiments.

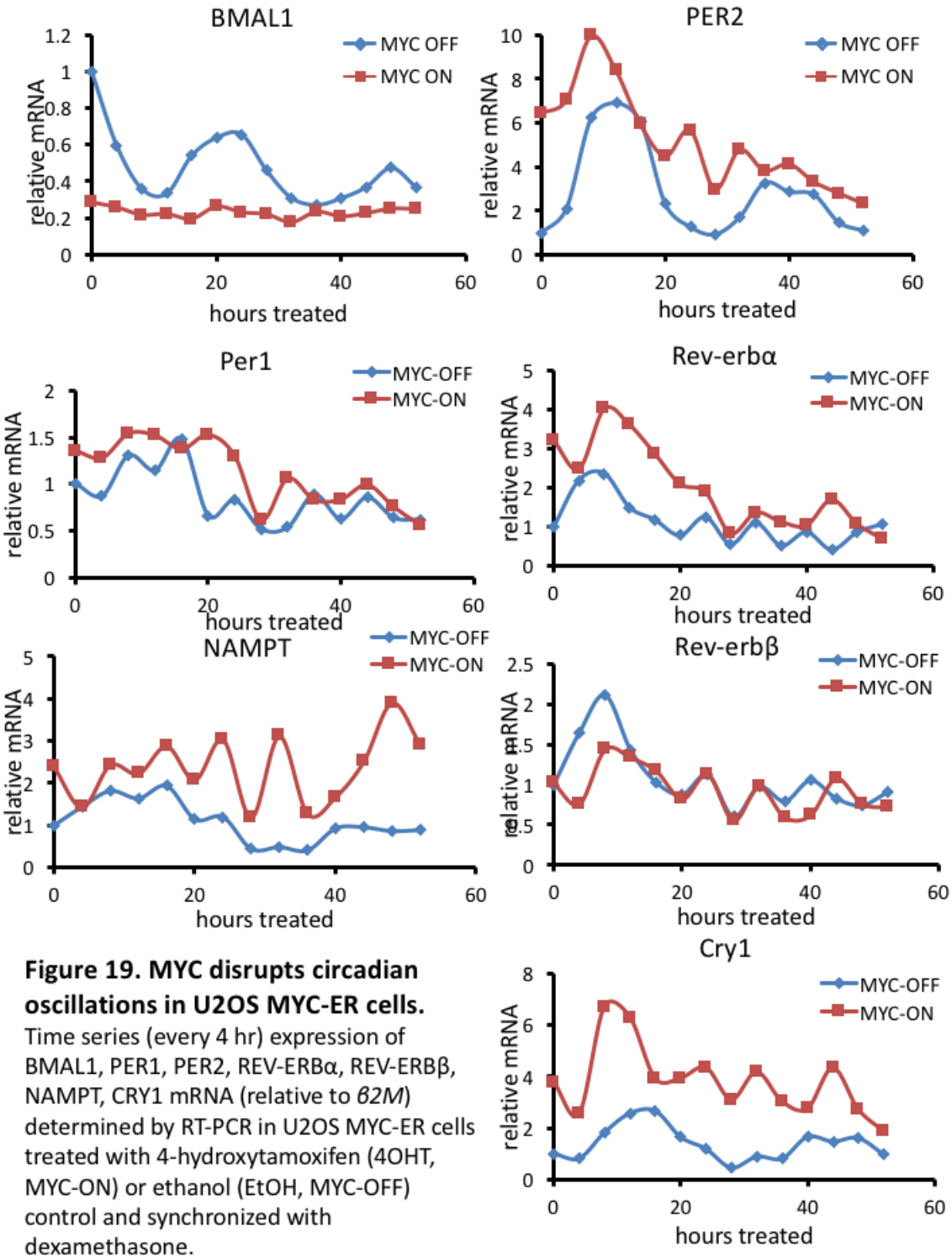

Figure 19. MYC disrupts circadian oscillations in U2OS MYC-ER cells. Time series (every 4 hr) expression of BMAL1, PER1, PER2, REV-ERBα, REV-ERBβ, NAMPT, CRY1 mRNA (relative to *β2M*) determined by RT-PCR in U2OS MYC-ER cells treated with 4-hydroxytamoxifen (4OHT, MYC-ON) or ethanol (EtOH, MYC-OFF) control and synchronized with dexamethasone.

period of mRNA oscillation of these genes in MYC-ON cells also appears to be shorter than MYC-OFF cells.

Discussion

In this chapter, we have demonstrated that overexpressing of oncogenic MYC can suppress and disrupt the oscillation of major clock regulator BMAL1 and induce E-box containing clock genes, including PER1, PER2, REV-ERBα, REV-ERBβ and CRY1 in several different MYC-inducible cell models. The mechanism in which E-box transcription factor MYC replaces CLOCK::BMAL1 to regulate clock genes has been implicated from previous research on other E-box binding transcription factor, such as *Usf1*. *Usf1* has been shown to activate *Per1*, *Per2*, *Cry1* and *Cry2* in Clock mutant ($Clock^{\Delta 19}$) mouse liver and rescue the period lengthening of wheel-running in these mice (Shimomura et al., 2013). Genome-wide ChIP-Seq analysis revealed an increase in the Usf1 binding sites in $Clock^{\Delta 19}$ mice compare to wild type mice, suggesting that Usf1 replace Clock binding sites when $Clock^{\Delta 19}$ binding affinity is low (Shimomura et al., 2013). Consistent with Usf1-induced *Per* expression, our result showed overexpressed MYC, which might have equivalent or higher E-box binding affinity compare to CLOCK::BMAL1, could also induce Per expression likely through direct binding. Furthermore, MYC overexpression during the development of embryonic stem cells has been demonstrated to suppress emergence of *mBmal1* and *PER2* oscillation (Umemura et al., 2014).

Suppression of Bmal1 expression and oscillation in mHCC 3-4 and U2OS MYC-ER cells, however, is probably not due to direct suppression from MYC since there is no E-box at Bmal1 promoter. Interestingly, clock genes that are induced by MYC, including PER1, PER2, REV-ERBα, REV-ERBβ and CRY1, are all negative regulators of BMAL1. Whether suppression of *BMAL1* is due to elevation of these repressors of *BMAL1* either by inhibiting its activity or its expression, additional studies in Chapter 3 will help to elucidate the mechanism. Notably, *Bmal1* is elevated by MYC in mHCC EC4 cells, suggesting there is heterogeneity in rewiring the circadian circuitry in cancer cells. This heterogeneity is well-addressed in recently published article showing that transient transfection of c-MYC in human colorectal cancer cell line HCT116 resulted in reduction of PER1 expression, which is opposite from what we observed in four cell lines we tested here (Repouskou and Prombona, 2016).

Our finding in P493 cells revealed that although *BMAL1* expression is completely not detectable regardless of MYC level, BMAL2 is induced dramatically in INTERMEDIATE MYC cells. BMAL2 has been shown to be a functionally redundant paralog of BMAL1, supported by the observation that constitutively expressing BMAL2 is able to rescue the arrhythmicity and metabolic phenotypes of *Bmal1*-knockout mice (Shi et al., 2010). However, even with high level of BMAL2 expression in INTERMEDIATE Myc cells, the oscillation of *PER1* or *PER2* is still hard to appreciate, suggesting BMAL2 might not be functionally redundant in P493 cells, at least in circadian clock control. Notably, *BMAL2* is amplified in about 10-15% ovarian cancer, testicular cancer and neuroendocrine prostate cancers (Cerami et al., 2012; Gao et al.,

2013), which implicated that the huge surge of *BMAL2* expression in INTERMEDIATE MYC cells could be related to estradiol treatment.

Chapter 3

Investigation of *REV-ERBα* as a direct MYC target gene for disruption of the molecular clock

Circadian rhythm consists of positive regulators and negative regulators. Positive regulator CLOCK and BMAL1, form heterodimer and bind to E-box to drive the expression of its target genes or negative regulators. These negative regulators, including PERs, CRYs and REV-ERBs, form two major feedback loops to suppress CLOCK and BMAL1. The first feedback loop is formed by the protein complex of PER and CRY, which inhibits the activity of CLOCK::BMAL1 heterodimer. The second loop is through the repression of *BMAL1* transcription by REV-ERBs. The time delay from the transcription and translation of the positive regulators and negative regulators is the molecular basis of circadian oscillation.

In Chapter 2, we have used several different *MYC*-inducible models to demonstrate that overexpressed oncogenic MYC is sufficient to suppress *BMAL1* expression. By examine mRNA expression of various core clock components; we have discovered that MYC also induces several clock-controlled genes, particularly PER2, CRY1 and REV-ERBs across different cell lines. Interestingly, these "clock-controlled genes" are all repressors of CLOCK::BMAL. The observation of induction of negative regulators and suppression of Bmal1 suggests a potential mechanism that happening in cancer cells: MYC suppress the molecular clock by upregulating clock repressors. Several clock genes have been associated with cancer. For instance, previous study showed that Per2 as a tumor suppressor and is able to regulate endogenous *MYC* in several cancers. *REV-ERBα* has been documented to be amplified in ERBB2-positive human breast cancer (Kourtidis et al., 2010). CRY1 has been reported to be epigenetic silencing in chronic lymphocytic leukemia (Hanoun et al., 2012). However, there is no evidence so far that suggest which clock repressor is downstream of oncogenic MYC.

In this chapter, we provide evidence from public available dataset that several clock repressors are indeed direct MYC targets and MYC binding sites are well conserved. Among these clock repressors, we are able to demonstrate that only REV-ERBα and REV-ERBβ are responsible for suppressing BMAL1 expression and oscillation upon MYC overexpression. Finally, we showed that knockdown of both REV-ERBα and REV-ERBβ is able to rescue *BMAL::Luc* level and oscillation.

Materials and Methods

Plasmids

c-MYC-ER™ wt and Δ106-143, which are responsive to tamoxifen and 4-hydroxytamoxifen but not to estrogen, were received in the pBabe-puro vector courtesy of Dr, Linda Penn, Ontario Cancer Institute, University Health Network, University of Toronto, Canada) and were described previously (Littlewood et al., 1995). c-MYC-ER™ wt and Δ106-143 were subcloned into pBabe-Zeo (Morgenstern and Land, 1990) (courtesy of Dr. Robert Weinberg, Whitehead Institute for Biomedical Research, Cambridge, MA, USA, Addgene plasmid 1766). Retrovirus was generated in 293T cells using the pCMV-VSVG and pUMVC vectors (Stewart et al., 2003) (courtesy of Dr. Robert Weinberg, Addgene plasmids 8449 and 8454).

The promoter region of human REV-ERNα (NR1D1) corresponding to bases -1156 to +31, where 0 is the ATG start site, or a region exactly 2000 bases upstream of this, were cloned from U2OS BMAL1::Luc genomic DNA harvested by DNEasy Blood and Tissue Kit (Qiagen, Gaithersburg, MD, USA) using the Phusion ™ High-Fidelity DNA Polymerase (New England Biolabs, Ipswitch, MA), and inserted into the pGL4.15

promoterless luciferase construct (Promega, Madison, WI, USA). The inserts in the resulting vector were sequenced by the University of Pennsylvania DNA Sequencing Facility and confirmed to not have mutations.

Cell culture

Murine hepatocellular carcinoma cell lines (mHCCs) are primary culture tumor cell line, which were derived by ring cloning from a liver tumor of the LAP-tTA/tet-OFF cMYC conditional transgenic mouse model (Shachaf et al., 2004; Xiang et al., 2015). U2OS cells with BMAL1::luciferase vector were kindly shared by Dr. John Hogenesch (Baggs et al., 2009). U2OS cells and mHCC cells were cultivated in Dulbecco's modified Eagle's medium (DMEM, Mediatech, starting glucose concentration of 25 mM and starting glutamine concentration of 4 mM). Media was supplemented with 10% fetal bovine serum (FBS, HyClone, Logan, UT, USA or Life Technologies, Grand Island, NY, USA) and 1X Penicillin/Streptomycin (Mediatech) for all cells. mHCC cell media was additionally supplemented with 2 mM L-Glutamine (Mediatech), 1 mM Sodium pyruvate (Mediatech) and 1X MEM non-essential amino acid (Life Technologies. To induce Myc-ER nuclear translocation, U2OS MYC-ER™ cells were treated with 500 nM 4-hydroxytamoxifen (Sigma, St. Louis, MO, USA) for 24 hour or treated with same amount of ethanol as control. To repress *c-MYC* expression, mHCC 3-4 cells were treated with 20ng/ml tetracycline (Sigma) or treated with media as control.

U2OS BMAL1::Luc cells were stably transduced with MYC-ER™, MYC-ER™ Δ106-143, or pBabe-Zeo empty vector retrovirus using the plasmids and methods described

above. Infected cells were selected for with 100 µg/ml Zeocin (Life Technologies) for two weeks, then continually cultured in Zeocin except during experiments.

To generate mHCC 3-4 stably expressing luciferase reporter constructs, plasmids (REV-ERBα::Luc described above or BMAL1::Luc in pGL 4.27 [Promega (Baggs et al., 2009)] were linearized by digestion with Not1 (New England Biolabs) and purified by QIAquick PCR purification kit (Qaigen). mHCC 3-4 cells were then transfected with linearized plasmids using Lipofectamine 2000 (Life Technologies) and selected with Hygromycin (Mediatech) at the following concentrations: 0.8 mg / ml for mHCC 3-4.

To create stable single-cell mHCC 3-4 Bmal1::Luc clones, cells were trypsinized and serially-diluted to 100 cells per 96 well plate. Clones were lysed and mixed with luciferase assay reagent (Promega) and luciferase activity was measured by luminometer. Only the clones with 10000 or above relative light units were selected. Selected clones were cultured with 20ng/ml tetracycline in regular media for mHCC cells (as described above) for 24 hours. The clones were then screened in Lumicycle™ luminometer (details described in Lumicycle section), and those that showed BMAL1::Luciferase oscillation were used.

All cell culture, except that during live-cell luminometer experiments (see Lumicycle section below), was conducted in a 5% CO2 humidified atmosphere.

siRNA

Human or mouse SMARTpool® siRNAs were purchased from Dharmacon (GE Healthcare, Lafayette, CO, USA). Cells were transfected with siRNAs using

Lipofectamine 2000 or RNAiMAX (Life Technologies). Non-targeting siRNAs with same molar amount were used as negative control.

ChIP

Chromatin immunoprecipitation was done by using Imprint® Ultra Chromatin Immunoprecipitation Kit, according to manufacturer's instructions (Sigma). Briefly, cells were washed in PBS, crosslinked in 1% Formaldehyde (Sigma), lysed, sonicated and then immunoprecipitated with rabbit anti-MYC antibody (Abcam, Cambridge, MA, USA). Myc-bound DNA fragments were reverse crosslinked, eluted and then amplified by quantitative RT-PCR. Primer pairs for ChIP assay were: REV-ERBα, 5'-GCTTTGCCAGGCAGAAAGGGTAAA-3' and 5'-GCAACGACAAGACTGTCGGGATTT-3'; REV-ERBα minus 2K, 5'-TGGCTTTCATGTTTCCCAGGCA-3' and 5'- TCCCAGTGCTTCTAGAGAGGGTTT-3'; NPM1, 5'-GCTACATCCGGGACTCACC-3' and 5'-GCTGCCATCACAGTACATGC-3'.

Real-Time PCR

All RNAs were extracted by RNeasy Plus Mini Kit (Qiagen) according to manufacturer's instruction and reversed to complementary DNA by using TaqMan Reverse Transcription Reagents (Life Technologies). cDNA was used as template to proceed to quantitative real time PCR (RT-PCR) with specific human or mouse primers. RT-PCRs were performed using the StepONE Plus system, 7900HT Real-time PCR System, or ViiA™ 7 Real-time PCR system (Life Technologies).

Luciferase

Cells were washed with PBS, lysed with 1X Passive lysis buffer (Promega) and dislodged by cell scraper. Cell lysates were then collected, mixed with luciferase assay reagent (Promega) and luciferase activity was measured by luminometer.

Lumicycle

Lumicycle analysis of U2OS BMAL1::Luc cells was described previously (Baggs et al., 2009). Briefly, three days prior to analysis, cells were plated in 35 mm dishes at a concentration of 250,000 cells / plate. 24 hours later, cells were transfected with siRNA as described above. 48 hours post transfection, cells were cultured atmospheric conditions, in phenol red-free DMEM (Sigma, St. Louis, MO, USA) containing 5% FBS (Hyclone or Gibco), 25 mM D-glucose (Sigma), 35 mg/L sodium bicarbonate (Gibco), 10 mM HEPES (Gibco), Pen/Strep (Mediatech), 0.1 mM beetle-luciferin (Promega), and 0.1 μuM dexamethasone (Sigma), and dishes were sealed with high vacuum grease (Dow Corning, Midland, MI, USA). Plates were measured for luminescence every 10 minutes for at least 4 days on a Lumicycle™ luminometer (Actimetrics, Wilmette, IL, USA). The experiment for mHCC 3-4 BMAL1::Luc cells was performed in the same way, except that cells were treated with either tetracycline or mHCC media 24 hours before the plates were sealed.

Results

Elevated MYC directly upregulates negative regulators of the molecular clock

Given the observation that elevated MYC suppresses BMAL1 in both U2OS cells and mHCC 3-4 cells (Fig. 9, 16) and induces several negative regulators, including PER2, CRY1, REV-ERBα in all cells we tested (Fig 4, 9, 16), we hypothesize that the induction of negative regulators by MYC contributes to clock suppression in cancer cells (Fig. 20).

To delineate whether these clock repressors behave like direct MYC targets, we first examine the public available MYC ChIP-seq data in several cancer cell lines from ENCODE project using UCSC genome browser (Fig. 21) (Kent et al., 2002; Walz et al., 2014). *PER2*, *CRY1*, *REV-ERBα* (*NR1D1*) and *REV-ERBβ* (*NR1D2*) promoter has strong MYC binding in U2OS cells with MYC overexpression (Fig. 21) and human chronic myelogenous leukemia cell line K562 (Fig. 22, 23) However, there is no MYC binding at *BMAL1* (*ARNTL*) promoter in these two cell lines. In addition, phylogenetic analysis of MYC binding site at *PER2* (Fig. 22), *CRY1* (Fig. 22) and *REV-ERBα* (NR1D1) (Fig. 23) showed that MYC-bound E-Box is well conserved down to Wallaby (Siepel et al., 2005). All these data indicate that *PER2*, *CRY1*, *REV-ERBα* and *REV-ERBβ* are direct MYC targets.

REV-ERBα and REV-ERBβ are critical BMAL1 repressor downstream of MYC overexpression

We then sought to identify the key repressor that is responsible for *BMAL1* suppression downstream of MYC. While 90% of *PER2* and *CRY1* expression was knockdown by use of small interfering RNA (siRNA), *BMAL1* transcript level is not rescued (Fig. 24A and B). Similarly, knockdown of either *PER2* or *CRY1* fail to rescue the dampened

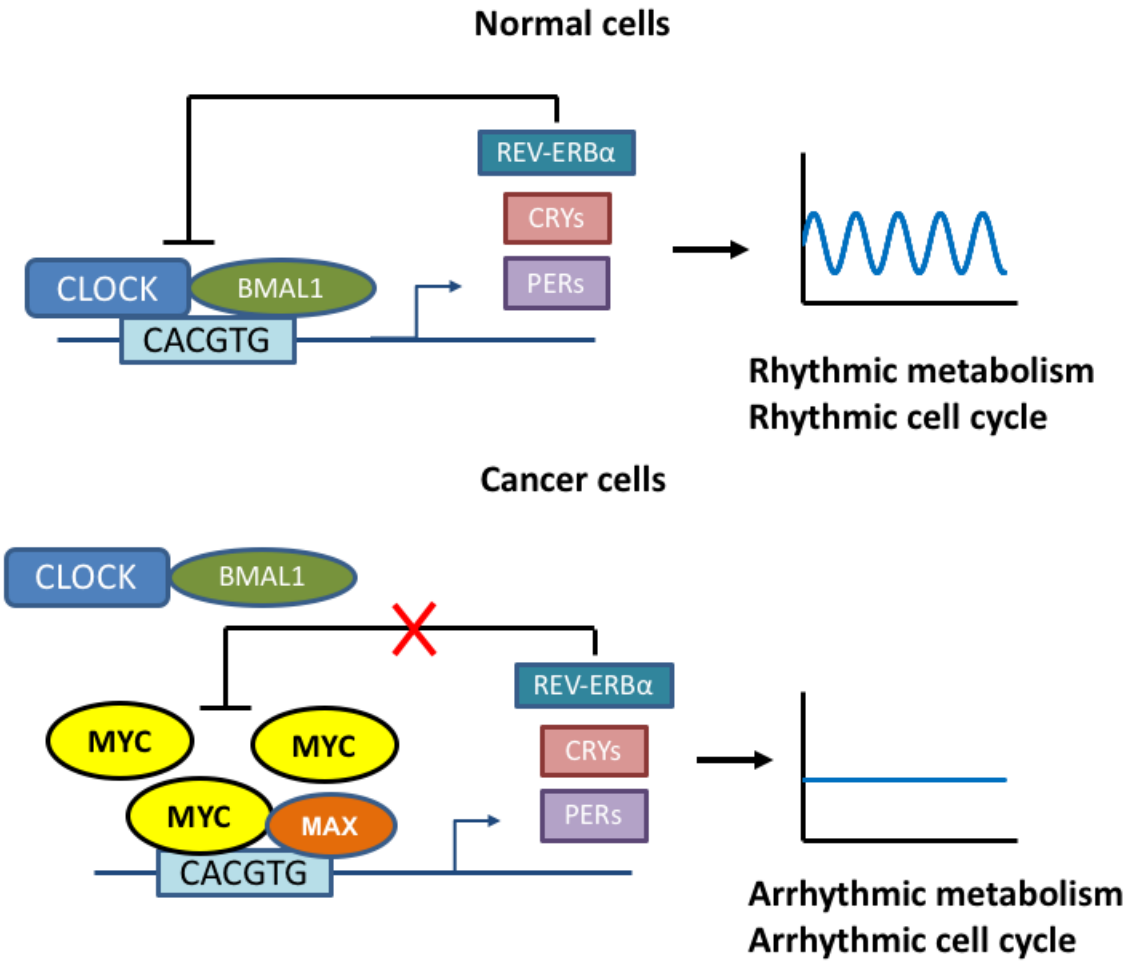

Figure 20. Hypothetical mechanism of Myc-mediated circadian disruption. A schematic representation of rhythmic control of "E-box" containing circadian repressor genes by CLOCK::BMAL1 in normal cells and MYC-dependent, sustained control of "E-box" containing circadian repressor genes in cancer cells.

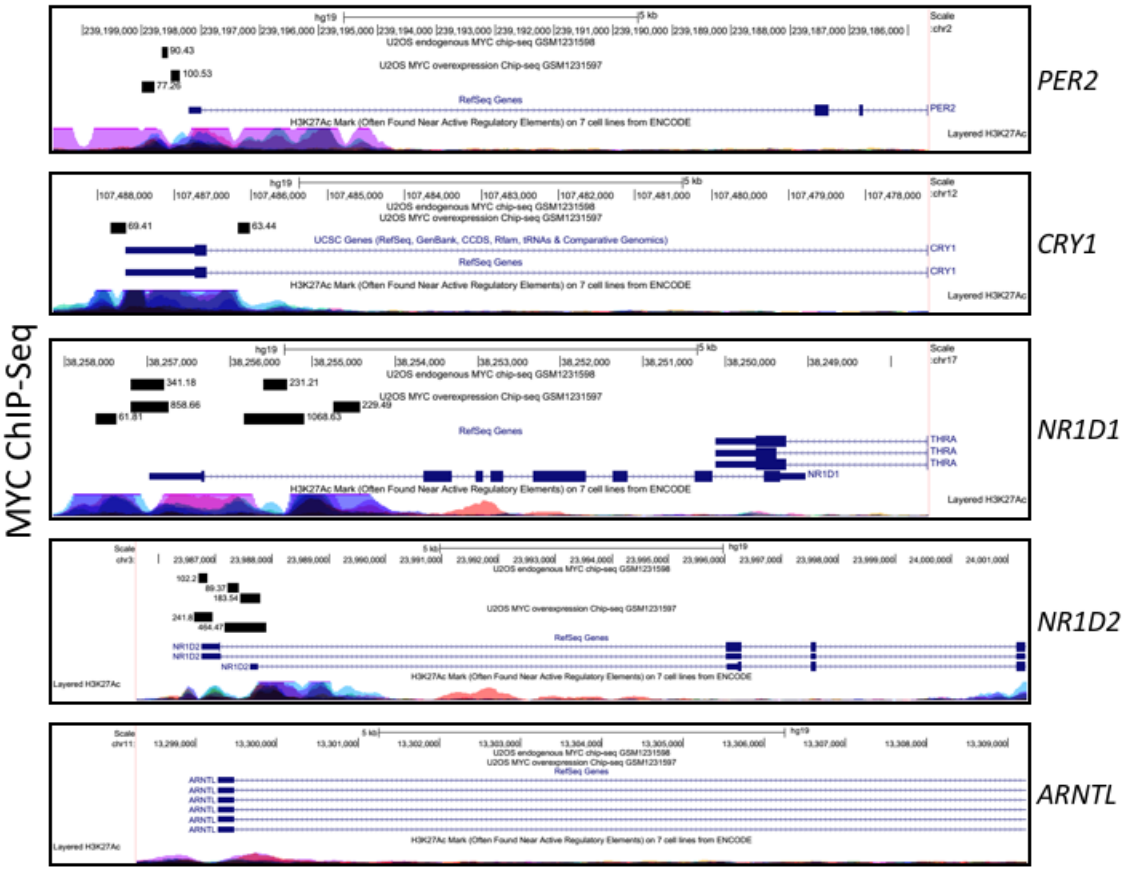

Figure 21. Circadian repressor genes are direct MYC targets.
The results of an endogenous MYC and doxycycline-inducible overexpressed MYC ChIP-Seq experiment (Walz et al., 2014) were loaded onto the February 2009 assembly of the USCS Genome Browser. Endogenous and inducible MYC binding to the promoters of *PER2*, *CRY1*, *NR1D1* (REV-ERBα), *NR1D2* (REV-ERBβ), and *ARNTL* (BMAL1) were assessed, indicated by black boxes above the gene, and numbers indicate quantified peak intensities. Below the gene, layered H3K27Ac peaks from the ENCODE project indicate sites of active transcription

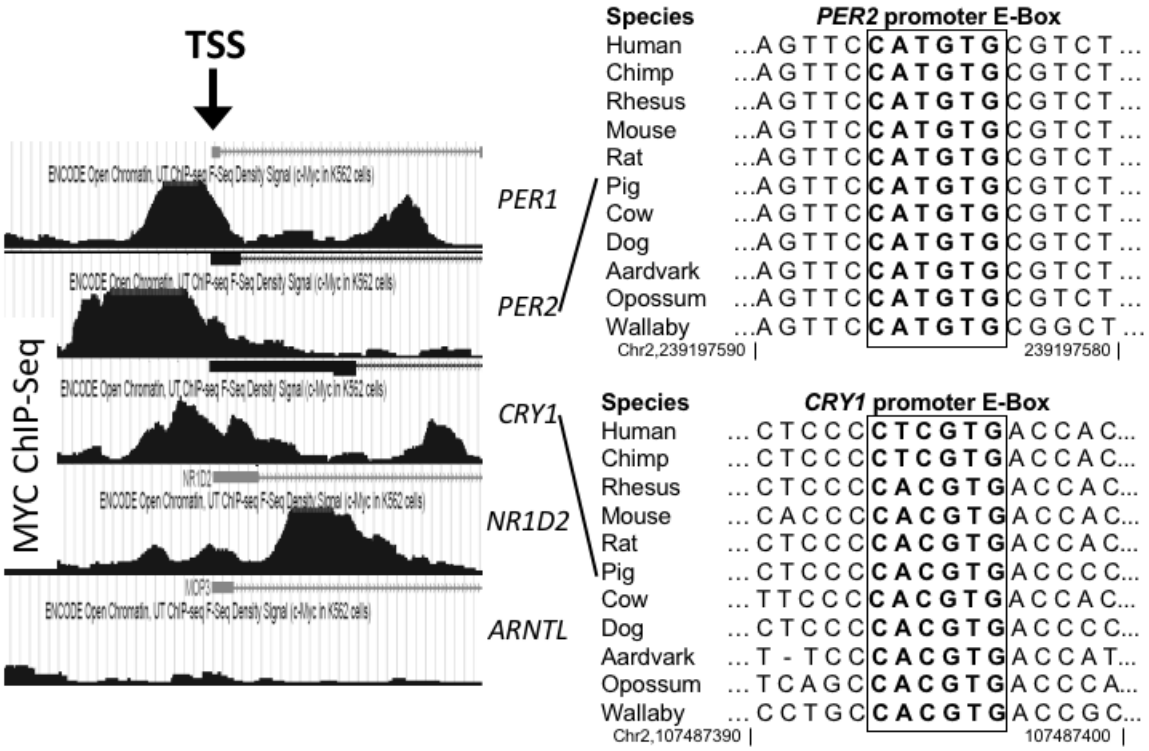

Figure 22. MYC directly engages the E-box promoter elements of circadian rhythm genes.

The UCSC Genome Browser Human March 2006 and February 2009 assemblies, which contain the results of a MYC CHIP-Seq experiment from the ENCODE project, were queried for c-Myc binding to the regulatory elements of *PER1*, *PER2*, *CRY1*, *NR1D2* (REV-ERBβ), and *ARNTL* (BMAL1) in K562 chronic myelogenous leukemia cells. Arrow indicates transcriptional start site (TSS). Similar binding data were observed in GM12878, HeLa, HepG2, and HUVEC (Dunham et al., 2012). The canonical E-box sequence of the promoter MYC binding peak in *PER2* and *CRY1* was identified (boxed sequence), and conservation was compared to other mammalian species. The sequence was not conserved in frog and chicken (Siepel et al., 2005).

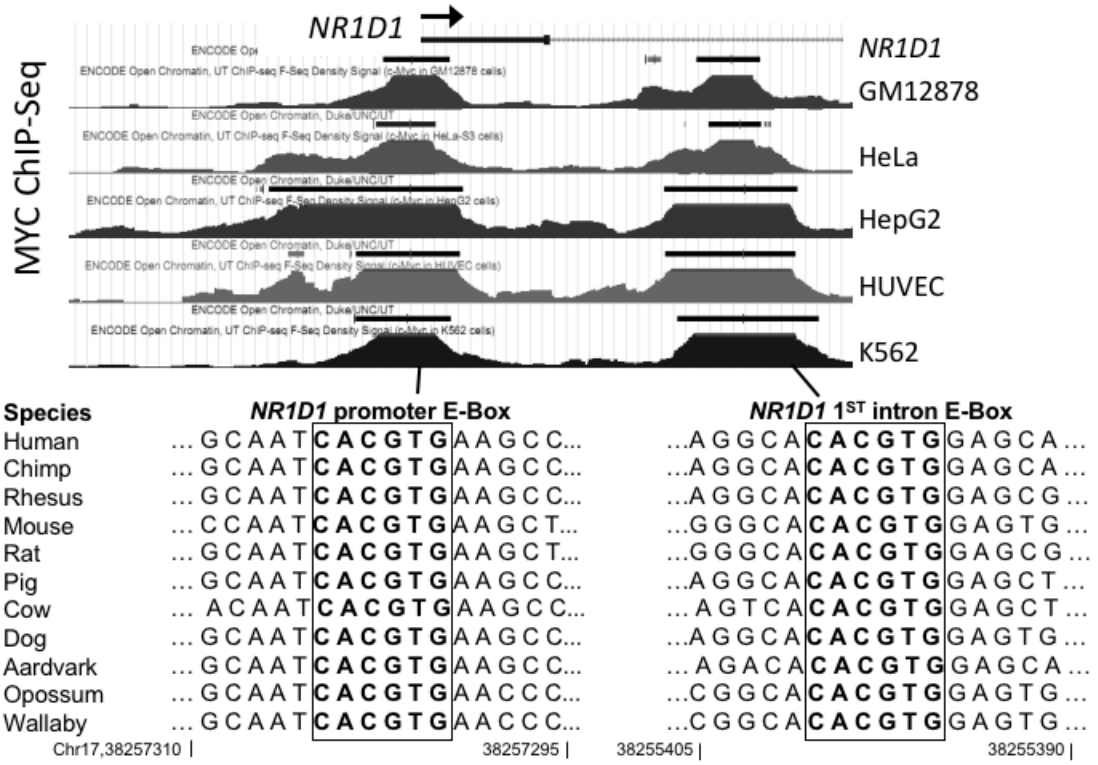

Figure 23. MYC directly engages the E-box promoter elements of REV-ERBα.

ENCODE data (Dunham et al., 2012; Kent et al., 2002) was queried for MYC binding to REV-ERBα (*NR1D1*) promoter in multiple cell lines. MYC showed strong binding to canonical E-Box element (Zeller et al., 2006) in the promoter region of NR1D1 in GM12878 (lymphoblastoid), HeLa (cervical cancer), HepG2 (kidney cancer), K562 (chronic myelogenous leukemia lines), and HUVEC (Human Umbilical Vein Endothelial Cells) cells. The canonical E-box sequence of each MYC binding peak in *NR1D1* was identified (boxed sequence), and conservation was compared to other mammalian species. The sequence was not conserved in frog and chicken (Siepel et al., 2005).

BMAL1::Luc oscillation in MYC-ON cells (Fig. 24C). In contrast, mRNA levels of *BMAL1* were rescued partially by either *REV-ERBα* or *REV-ERBβ* silencing and were completely rescued by siRNAs targeting both *REV-ERBα* and *REV-ERBβ* (Fig. 25). Strikingly, while in synchronized U2OS MYC-ER cells, the blunted oscillation of *BMAL1::Luc* in MYC-ON cells can be partially rescued by silencing REV-ERBα or REV-ERBβ, knockdown REV-ERBα and REV-ERBβ simultaneously results in a nearly complete rescue of *BMAL1::Luc* oscillation (Fig. 26). These data suggest that the elevation of *REV-ERBα* and *REV-ERBβ*, but not *PER2* and *CRY1*, are the critical repressors lead to *BMAL1* suppression in MYC overexpressing cells.

To determine whether REV-ERBα is directly regulated by MYC in the cell model we used, we performed Chromatin immunoprecipitation (ChIP) experiment using anti-MYC antibody in U2OS MYC-ER cells. Indeed, MYC directly binds to *REV-ERBα* promoter but not at the site 2Kb upstream of *REV-ERBα* promoter (Fig. 27). In mHCC 3-4 cells, Myc-mediated *BMAL1* suppression was similarly restored with siRNA targeting against *Rev-erbα* (Fig. 28A). In addition, silencing *Rev-erbα* also rescue *BMAL1::Luc* level in mHCC 3-4 c12 cells (Fig. 29). To further assess whether MYC directly activate *Rev-erbα* promoter activity, we transduced a luciferase reporter downstream of human *REV-ERBα* promoter into mHCC 3-4 cells (*REVα::Luc*). As expected, luciferase level is higher in mHCC 3-4 *REVα::Luc* cells when MYC is induced (Fig. 28B). Together, our results have demonstrated that *REV-ERBα* is a direct MYC target in both U2OS MYC-ER cells and mHCC 3-4 cells.

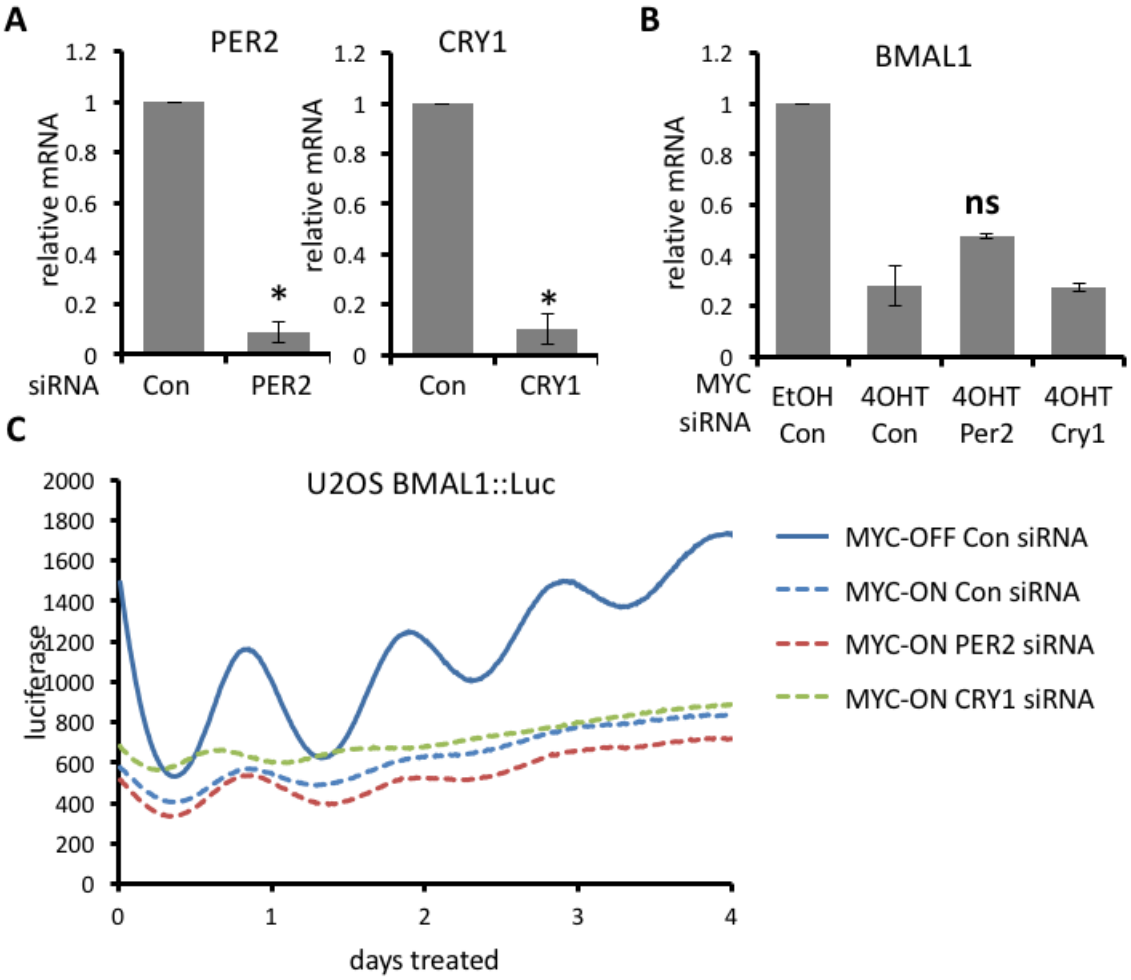

Figure 24. *PER2* and *CRY1* are not necessary for MYC disruption of BMAL1 promoter oscillation.

(A) mRNA levels (normalized to expression of *β2M*) for *PER2* or *CRY1* determined by RT-PCR in U2OS MYC-ER cells transfected with either non-targeting siRNA (Con), siRNA against *PER2*, or *CRY1* for 48 hr with 4OHT (MYC-ON) being added to cells 24 hr after transfection. Means and SDs from at least three experiments are shown. *p < 0.05 for Con versus siPER2 or siCRY1. (B) BMAL1 mRNA expression (normalized to expression of *β2M*) in U2OS MYC-ER transfected as described in (A) with siRNAs indicated at the bottom. *p < 0.05 by Student's t test for MYC-ON versus MYC-OFF. ns = not significant.

(C) U2OS MYC-ER cells were transfected with siRNAs as indicated in the figure, synchronized with dexamethasone and monitored using a LumiCycle luminometer. Data are representative of two or more experiments.

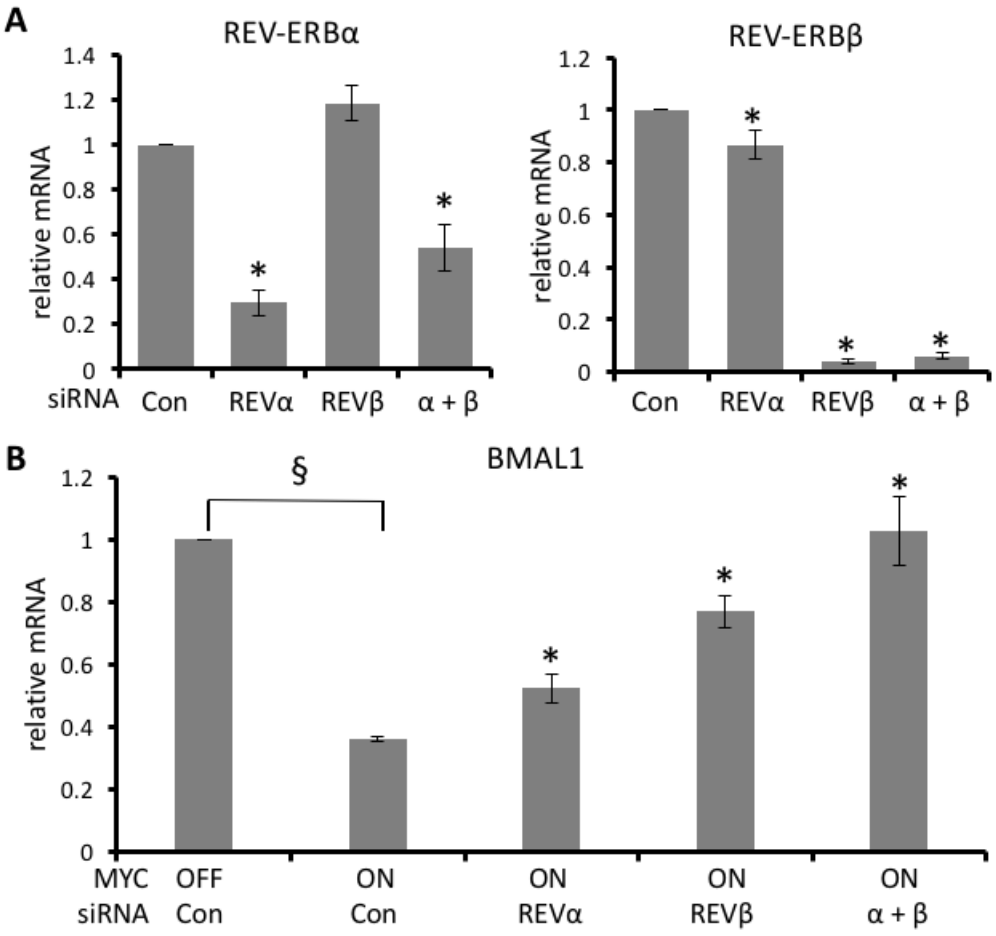

Figure 25. REV-ERBα and β are necessary for MYC disruption of BMAL1 expression

(A) mRNA levels (normalized to expression of *β2M*) for REV-ERBα or REV-ERBβ determined by RT-PCR in U2OS MYC-ER cells transfected with either non-targeting siRNA (Con), siRNA against REV-ERBα, REV- ERBβ, or both REV-ERBs (α**+**β**)** for 48 hr with 4OHT (MYC-ON) being added to cells 24 hr after transfection. Means and SDs from at least three experiments are shown. *$p < 0.05$ for siREV versus control.
(B) BMAL1 mRNA levels (normalized to expression of *β2M*) in U2OS MYC-ER transfected with the indicated siRNAs (bottom) as described in (A) and cultured with 4OHT (MYC-ON) or EtOH (MYC-OFF) after 24 hr. Means and SDs from at least three experiments are shown. *$p < 0.05$ by Student's t test for siREV or Con MYC-ON versus Con MYC-OFF. §, $p < 0.05$ siREV versus Con MYC-ON.

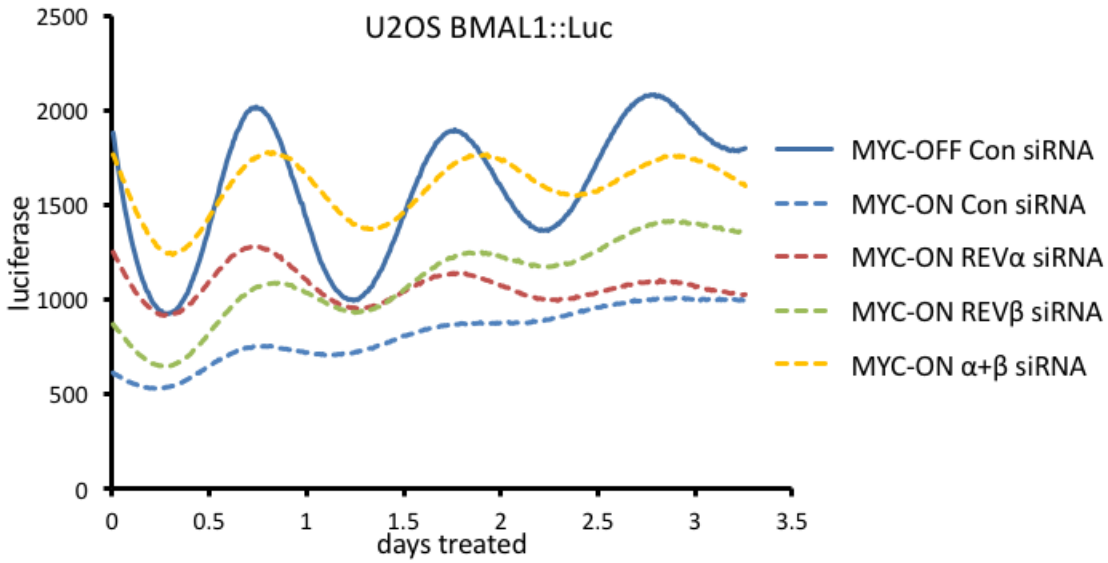

Figure 26. REV-ERBα and β are necessary for MYC disruption of BMAL1 promoter oscillation.

U2OS MYC-ER cells transfected with the indicated siRNAs for 48 hr, cultured with 4OHT (MYC- ON) or EtOH (MYC-OFF), synchronized with dexamethasone, and monitored using a LumiCycle luminometer. Data are representative of two or more experiments. RLU = relative light units.

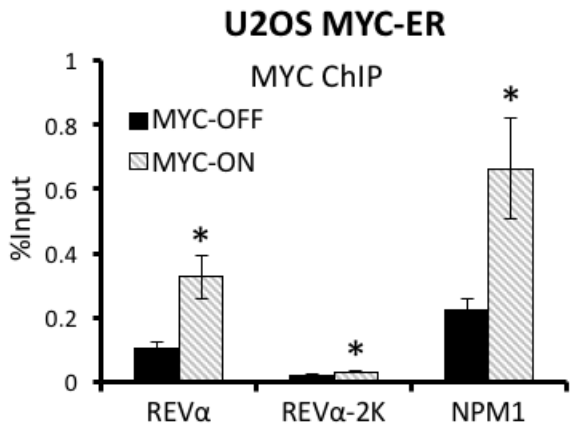

Figure 27. *REV-ERBα* is a direct MYC target gene in U2OS MYC-ER cells
U2OS MYC-ER expressing cells were treated with 4OHT (MYC-ON) or EtOH control (MYC- OFF) for 24 hours, and cells were fixed, lysed, sonicated, and chromatin was immunoprecipitated (ChIP) by anti-MYC according to manufacturer's instructions (Sigma Imprint Ultra Chromatin Immunoprecipitation Kit, Sigma). The following sites were targeted: the REV- ERBα promoter centered on the promoter E-box region (REVα, 81 bp fragment), 2Kb upstream of REV-ERBα transcription start site (REVα-2k, 99 bp fragment), and the promoter of the canonical MYC target nucleophosmin 1 (*NPM1*)(O'Donnell et al., 2005). Means and SDs from technical triplicates are shown. *$p < 0.05$ by Student's t test of 4OHT-treated samples relative to EtOH-treated samples. Data are representative of three or more experiments.

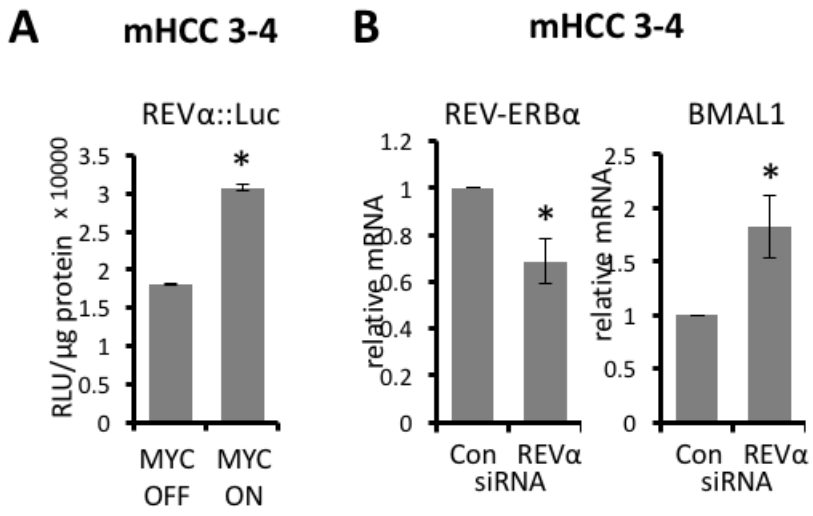

Figure 28. MYC directly upregulates *REV-ERBα* to suppress *BMAL1* in mHCC-3-4 cells.

(A) mHCC 3-4 cells were stably transduced with a promoterless luciferase construct driven by the -1156 to +31 region of the REV-ERBα promoter (REVα::Luc). Cells were cultured with (MYC-OFF) or without tetracycline (MYC-ON) for 48 hours. Luminescence was recorded using a luminometer. RLU: relative light unit. Means and SDs from triplicate samples are shown, and *$p < 0.05$ by Student's t test for MYC-ON vs. MYC-OFF. Data are representative of three or more experiments. (B) mHCC 3-4 cells cultured with media control (no tetracycline, MYC-ON) were transfected with either 60nM non-targeting siRNA (Con) or 60 nM siRNA against *REV-ERBα* (REVα) for 48 hours. mRNA was collected, reverse-transcribed to cDNA, and expression of REV-ERBα and BMAL1 were determined by quantitative real-time PCR, normalized to expression of *β2M*. Means and SDs from at least three experiments are shown.

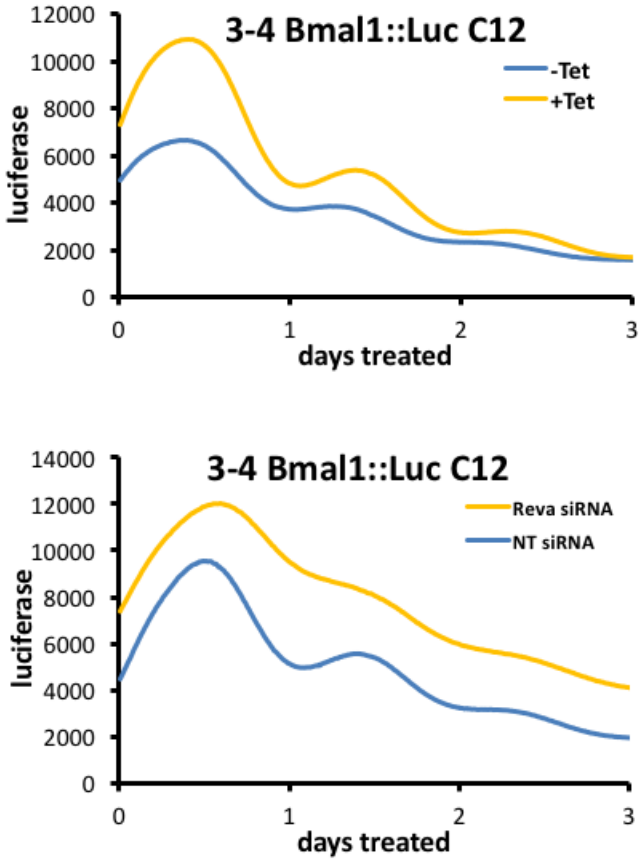

Figure 29. REV-ERBα and β are necessary for MYC suppression of BMAL1 promoter activity in mHCC 3-4 C12 cells

(A) mHCC 3-4 C12 cells treated with tetracycline (+Tet) or control (-Tet) and synchronized with dexamethasone. BMAL1 promoter activity luminescence was continuously measured (every 10 min) in a LumiCycle luminometer.

(B) mHCC 3-4 cells transfected with the REV-ERBα siRNAs (Reva) for 48 hr, synchronized with dexamethasone, and monitored using a LumiCycle luminometer. RLU = relative light units.

Discussion

In this Chapter, we provide evidence that MYC directly upregulates several negative regulators of BMAL1, including PER2, CRY1 and REV-ERBs from public available ChIP-Seq data in a number of different cancer cell lines. While PERs and CRYs form heterodimer and translocate to the nucleus to inhibit CLOCK::BMAL1 activity, REV-ERBs repress BMAL1 transcription directly (Preitner et al., 2002; Relogio et al., 2011). When we knockdown these BMAL1 repressors individually, we found only knockdown of REV-ERBα or REV-ERBβ but not PER2 or CRY1 is able to rescue BMAL1 oscillation and expression in U2OS MycER cells, suggesting REV-ERBs are the major downstream factors that act on *BMAL1* suppression. REV-ERBα's strong effect on clock suppression has been documented in earlier study where they achieve liver-specific *Bmal1* knockdown in mouse by constitutively expressed *Rev-erbα* in mouse liver (Kornmann et al., 2007). In fact, our earlier data showed overexpression of mutant $MYC^{\Delta 106}$, which lacks transactivation domain of MYC, resulted in elevation of *BMAL1* promoter activity (Fig. 18). This dominant negative effect due to overexpression of mutant $MYC^{\Delta 106}$ reveal that MYC effect on *BMAL* oscillation is from transcriptional repressors. Furthermore, silencing both *REV-ERBα* and *REV-ERBβ* achieve nearly full rescue of both expression level and oscillation of *BMAL1*, indicating both proteins are responsible for *BMAL1* suppression. Our data documented a novel mechanism in which MYC induces a nature clock repressor as a way to constitutively shut down clock and perhaps clock-controlled biological processes (Fig. 30).

A

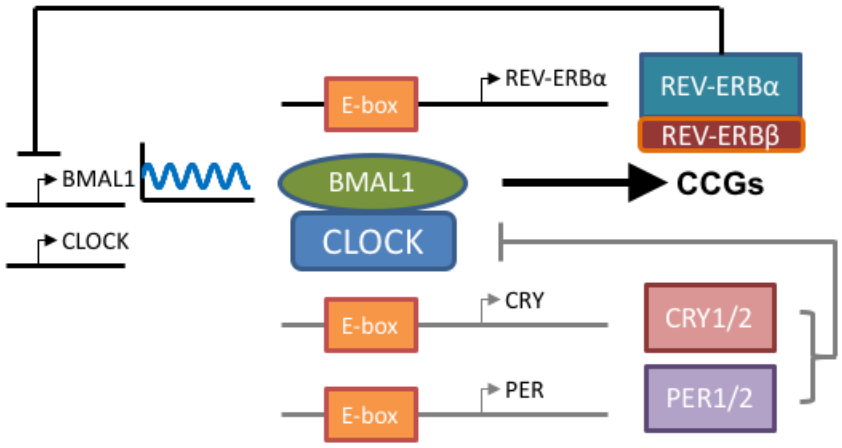

B

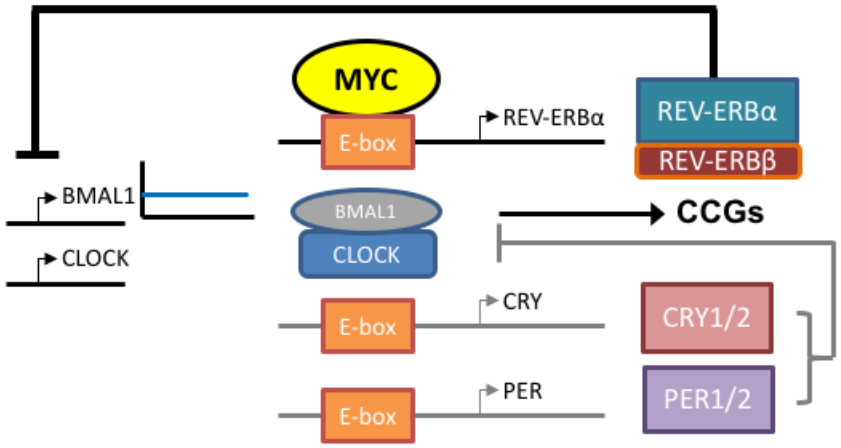

Figure 30. Model of Circadian Rhythm Disruption by MYC
(A and B) Summary diagram of normal molecular clock (A) and molecular clock disrupted by MYC (B).

Although knockdown of *REV-ERBα* is able to partially rescue *BMAL1* suppression, knockdown both *REV-ERBα* and *REV-ERBβ* are required to fully restore *BMAL1* expression and oscillation. Indeed, REV-ERBβ has been shown to collaborate with REV-ERBα to regulate both clock and metabolism in mouse embryonic fibroblasts as well as mouse liver (Bugge et al., 2012). In addition, circadian wheel-running behavior is only completely disrupted in *Rev-erbα*, *Rev-erbβ* double knockout mice but not in mice that loss either *Rev-erbα* or *Rev-erbβ* alone (Cho et al., 2012). Overall, our data and observations from others suggest that REV-ERBα and REV-ERBβ are not just functionally redundant but have collaborative effect on clock and metabolism.

Chapter 4

The role of BMAL1 and REV-ERBα in human neuroblastoma

To test the translational connection of c-MYC disruption of circadian clock in cancer cells, we further investigate whether N-MYC also suppresses the molecular clock by upregulating REV-ERBα. N-MYC belongs to the same family as c-MYC and shares similar sequence and structural components as c-MYC and L-MYC, another oncogene that has been linked to lung adenocarcinoma (Fig. 31) (Brodeur et al., 1984; Nau et al., 1985). N-MYC is an oncogene that drives extremely aggressive childhood cancer neuroblastoma (Brodeur et al., 1984; Kohl et al., 1984). Thus, understanding the role of N-Myc in circadian clock can potentially provide clues for better risk assessment and developing new therapeutic approach to the patients with neuroblastoma.

N-MYC has been studied in numerous literature that it drives overlapping target genes as c-MYC (Boon et al., 2001; Malynn et al., 2000). Many neuroblastoma cell lines are addictive to N-MYC expression, and suppression of N-MYC leads to arrested tumor growth (Jiang et al., 2011). Amplification of N-MYC in neuroblastoma has been shown in a number of different clinical trials that predict poorer prognosis of neuroblastoma patients (Brodeur et al., 1984; Kushner et al., 2014; Slavc et al., 1990). However, how overexpressed N-MYC in neuroblastoma affects the molecular clock remains poorly understood.

In this chapter, we first look at the relevance of c-MYC and REV-ERBα in the context of human leukemia. We then did detailed studies to determine whether REV-ERBα acts as a target gene downstream of N-MYC and we found that *REV-ERBα* is directly regulated by overexpressed N-Myc in two neuroblastoma cell lines. In collaboration with Dr. John Maris, we further analyze the expression of *REV-ERBα* and *BMAL1* in human neuroblastoma tumor samples. Elevated *REV-ERBα* and reduced *BMAL1* were associated

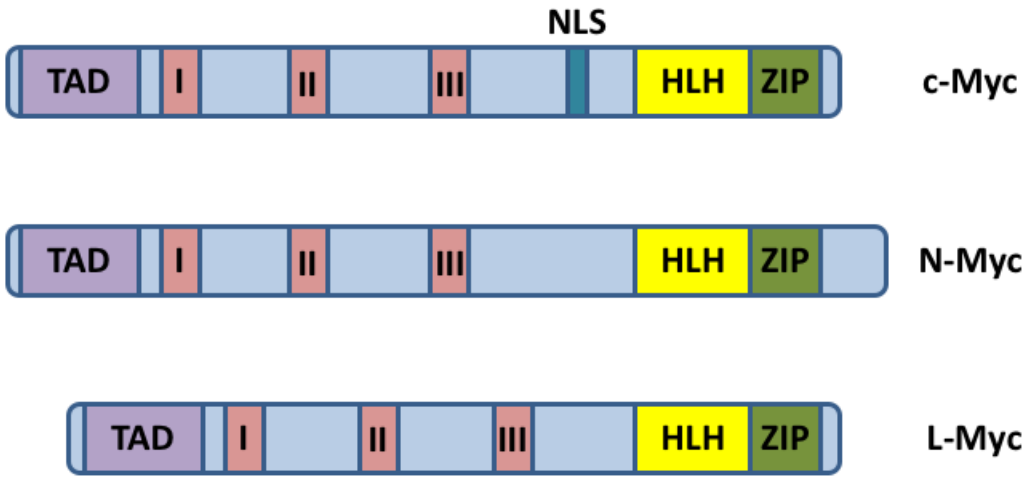

Figure 31. Domain structures of MYC family members.

Figure was adapted from
http://www.cellsignallingbiology.org/csb/004/csb004fig4_Myc_structure.htm
TAD = Transactivation domain, NLS= nuclear localization signal, HLH= basic helix-loop-helix motif, ZIP=basic leucine zipper domain

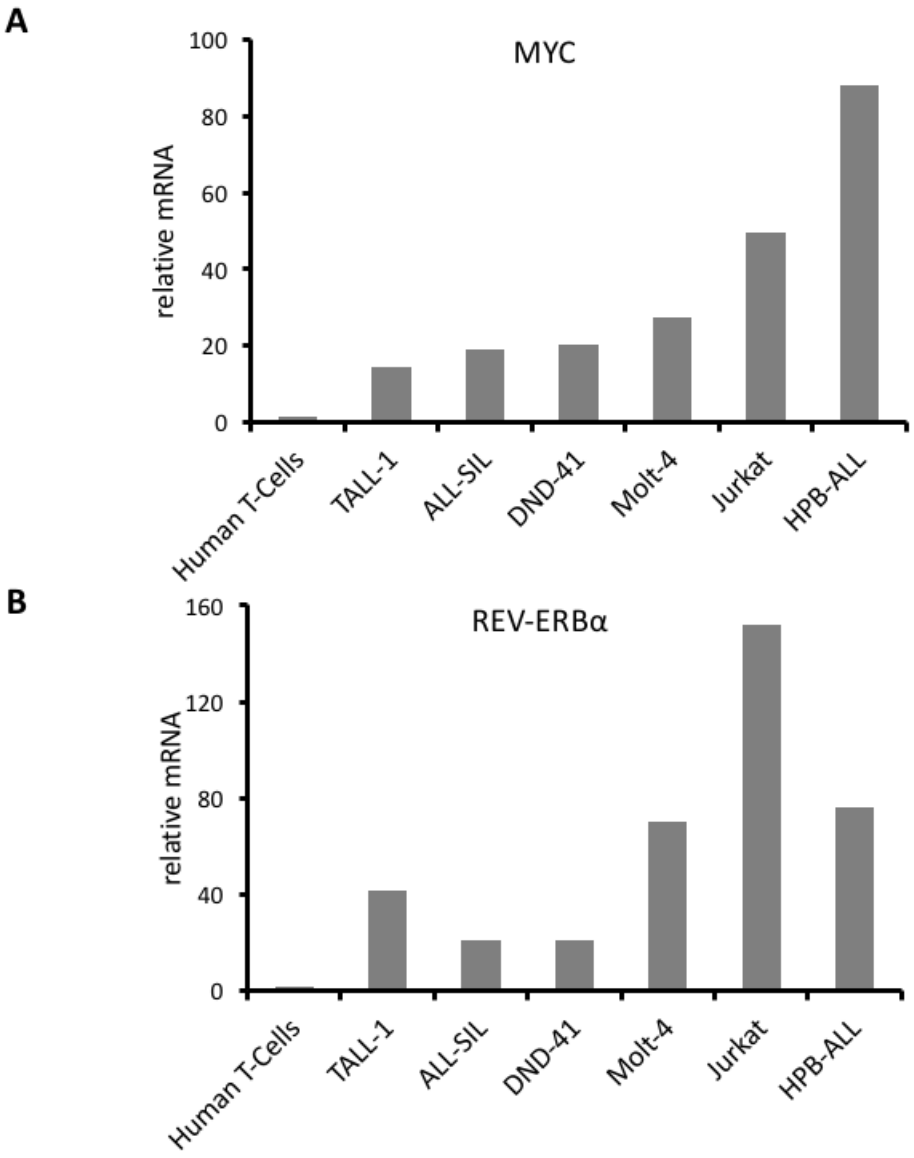

Figure 32. Oncogenic *MYC* correlates with elevated *REV-ERBα* in human T-acute lymphoblastic leukemia (T-ALL)

Human primary T-cells were activated for 48 hours with 10µg/ml anti-CD3 and 2.5 µg/ml anti-CD28, and mRNA from the activated human T-cells along with six human T-cell acute lympoblastic leukemia (T-ALL) cell lines (T-ALL1, ALL-SIL, DND-41, Molt-4, Jurkat, and HPB-ALL) was extracted, reverse-transcribed to cDNA, and (A) MYC and (B) REV-ERBα expression were determined by real-time quantitative PCR, normalized to expression of *ß2M*. Data are from a single experiment.

with more aggressive tumor. Strikingly, elevated *REV-ERBα* and reduced *BMAL1* also correlate with poorer prognosis of neuroblastoma patients from two independent patient cohorts. Lastly, we observed decrease in colony formation in in two patient-derived neuroblastoma cell lines upon BMAL1 overexpression, suggesting that BMAL1 is a tumor suppressor in neuroblastoma.

Materials and Methods

Plasmids

The promoter region of human REV-ERNα (NR1D1) corresponding to bases -1156 to +31, where 0 is the ATG start site, or a region exactly 2000 bases upstream of this, were cloned from U2OS BMAL1::Luc genomic DNA harvested by DNEasy Blood and Tissue Kit (Qiagen, Gaithersburg, MD, USA) using the Phusion ™ High-Fidelity DNA Polymerase (New England Biolabs, Ipswitch, MA), and inserted into the pGL4.15 promoterless luciferase construct (Promega, Madison, WI, USA). The inserts in the resulting vector were sequenced by the University of Pennsylvania DNA Sequencing Facility and confirmed to not have mutations.

pCMV6-ARNTL (RC207870) and its empty vector pCMV-entry vector (PS100001) were purchased from Origene (Rockville, MD, USA).

Cell Culture

Shep N-MYC-ER (Ushmorov et al., 2008), SKNAS N-MYC-ER (Valentijn et al., 2005), Shep, NLF, and Kelly were cultivated in Dulbecco's modified Eagle's medium (DMEM,

Mediatech, Manassas, VA, USA, starting glucose concentration of 25 mM and starting glutamine concentration of 4 mM). Media was supplemented with 10% fetal bovine serum (FBS, HyClone, Logan, UT, USA or Life Technologies, Grand Island, NY, USA) and 1X Penicillin/Streptomycin (Mediatech) for all cells. Some Shep N-MYC-ER, and SKNAS N-MYC-ER cells were treated with 500 nM 4-hydroxytamoxifen (Sigma, St. Louis, MO, USA) or ethanol control.

Primary human T-cells were cultured in RPMI 1640 medium (Mediatech) supplemented with 10% FBS (Gemini Bioproducts, West Sacramento, CA), 100 µ/mL Penicillin/Streptomycin (Life Technologies), 2 mM L-Glutamine (Life Technologies), and 55 µM -mercaptoethanol (Life Technologies). Cells were activated for 48 hours on plates coated with 10µg / ml anti-CD3 and 2.5 µg / ml anti-CD28 (both from Ebioscience, San Diego, CA, USA).

Human T-ALL lines were cultured in the following medium: RPMI 1640 medium (Mediatech) supplemented with 100 µ/mL Penicillin/Streptomycin (Life Technologies), 2 mM L-Glutamine (Life Technologies), and 55 µM -mercaptoethanol (Life Technologies). The following amounts of FBS were used: TALL-1: 15% FBS; ALL-SIL: 20% FBS; DND-41: 10% FBS; Molt-4: 10% FBS; Jurkat: 10% FBS; HPB-ALL: 20% FBS.

To generate Shep N-MYC-ER cells stably expressing luciferase reporter constructs, plasmids (REV-ERBα::Luc described above in pGL 4.27 [Promega (Baggs et al., 2009)] were linearized by digestion with Not1 (New England Biolabs) and purified by QIAquick PCR purification kit (Qiagen). Shep N-MYC-ER cells were then transfected with

linearized plasmids using Lipofectamine 2000 (Life Technologies) and selected with Hygromycin (Mediatech) at the following concentrations: 0.4 mg / ml for Shep N-MYC-ER.

All cell culture, except that during live-cell luminometer experiments (see Lumicycle section below), was conducted in a 5% CO2 humidified atmosphere.

ChIP

Chromatin immunoprecipitation was done by using Imprint® Ultra Chromatin Immunoprecipitation Kit, according to manufacturer's instructions (Sigma). Briefly, cells were washed in PBS, crosslinked in 1% Formaldehyde (Sigma), lysed, sonicated and then immunoprecipitated with rabbit anti-MYC antibody (Abcam, Cambridge, MA, USA). Myc-bound DNA fragments were reverse crosslinked, eluted and then amplified by quantitative RT-PCR. Primer pairs for ChIP assay were: REV-ERBα, 5'-GCTTTGCCAGGCAGAAAGGGTAAA-3' and 5'-GCAACGACAAGACTGTCGGGATTT-3'; REV-ERBα minus 2K, 5'-TGGCTTTCATGTTTCCCAGGCA-3' and 5'- TCCCAGTGCTTCTAGAGAGGGTTT-3'; NPM1, 5'-GCTACATCCGGGACTCACC-3' and 5'-GCTGCCATCACAGTACATGC-3'.

Luciferase

Cells were washed with PBS, lysed with 1X Passive lysis buffer (Promega) and dislodged by cell scraper. Cell lysates were then collected, mixed with luciferase assay reagent (Promega) and luciferase activity was measured by luminometer.

Real-Time PCR

All RNAs were extracted by RNeasy Plus Mini Kit (Qiagen) according to manufacturer's instruction and reversed to complementary DNA by using TaqMan Reverse Transcription Reagents (Life Technologies). cDNA was used as template to proceed to quantitative real time PCR (RT-PCR) with specific human or mouse primers. RT-PCRs were performed using the StepONE Plus system, 7900HT Real-time PCR System, or ViiA™ 7 Real-time PCR system (Life Technologies). Relative mRNA expression levels were normalized to β2M and analyzed using comparative delta-delta CT method. All RT-PCR primers are listed below:

Circadian mRNA Experiments

Circadian mRNA experiments for Shep N-MYC-ER, SKNAS N-MYC-ER, Shep, NLF, and Kelly were carried out in the media described above as a 'split timecourse'. 24 hours prior to the start of the experiment, half the cells were cultured in 0.1 μM dexamethasone (dex, Sigma), and at the start of the experiment, the other half of the cells were cultured in dexamethosone. At each timepoint, two plates were harvested representing 0 and 24 hours +dex, 4 and 28, etc, to arrive at a 52 hour timecourse. mRNA was processed and analyzed as described above.

Colony suppression assay

Kelly and NLF cells were seeded in 6-well plate and transfected with either pCMV6-ARNTL vector or pCMV6-entry empty vector (Origene) with Lipofectamine LTX with Plus (Life technology) in triplicates with concentrations of 0.2 or 0.8 μg/ml, as noted in figure legend. After one day of transfection, both Kelly and NLF cells were

cultured in media containing 1mg/ml G418 (Mediatech) for 7-10 days. G418-containing media was changed every 2 days. Colonies were stained with crystal violet solution for 20 min at room temperature and washed with water to remove extra crystal violet solution. Plates were scanned and quantified with ImageJ, and representative images were uniformly contrasted.

Primary Neuroblastoma Data

For survival data, previously published data (Wang et al., 2006) for ninety-two human tumors was assessed for overall survival based on MYCN and NR1D1 expression. Survival analyses were performed using the methods of Kaplan and Meier. Patients were divided into groups based on tertiles of mRNA expression. For overall-survival (OS), time was defined as the time from diagnosis until the time of death from disease or until the time of last contact if death did not occur. Patients who were alive were censored at the time last known alive. Log-rank p-values < 0.05 were considered significant. For mRNA expression analyses of primary human neuroblastomas, we analyzed Affymetrix Exon ST array data of 240 tumors obtained at diagnosis (Pugh et al., 2013) as part of the Therapeutically Applicable Research to Generate Effective Treatments (TARGET) project of the National Cancer Institute Office of Cancer Genomics. Data were normalized as described previously. A Student's t-test was applied to assess expression differences across risk groups as defined by the Children's Oncology Group (COG), accounting for MYCN amplification status. $P < 0.05$ was considered significant.

Results

REV-ERBα expression is upregulated in human T-cell acute lymphoblastic leukemia cell lines

Given our observation that MYC overexpression renders elevation of *REV-ERBα* transcripts, we further analyze expression of *REV-ERBα* in T-lineage acute lymphoblastic leukemia where *c-MYC* is often overexpressed.

T-lineage acute lymphoblastic leukemia (T-ALL) is a childhood blood cancer where more than half of them exhibit deregulation of PI3K/AKT pathway ultimately leads to elevated *c-MYC* RNA (Goldman and McGuire, 1992; La Starza et al., 2014). We compare mRNA expression of *c-MYC* and *REV-ERBα* in activated human primary T cells versus six human T-ALL cell lines (courtesy Dr. Jeffrey Rathmell, Vanderbilt University, TN) and found *c-MYC* is highly upregulated in all T-ALL cell lines compare to human activated T cells (Fig. 32A). Interestingly, elevation of *REV-ERBα* transcripts is observed in all T-ALL cell lines which nicely correlate with the level of MYC overexpression (Fig. 32B). This observation has revealed that perhaps *REV-ERBα* is a downstream target of MYC in human T-ALL cell lines.

REV-ERBα is a direct N-MYC target

Our previous results have demonstrated that *REV-ERBα* is directly upregulated by MYC in U2OS cells and mHCC 3-4 cells, we further ask a question whether *REV-ERBα* is also a direct target of N-MYC. To address this question, we used two human neuroblastoma cell lines: Shep N-MYC-ER and SKNAS N-MYC-ER (Ushmorov et al., 2008; Valentijn et al., 2005). Both cell lines do not have *MYCN* amplification, however, they harbor

ectopic N-MYC-ER construct which overexpresses N-MYC in the presence of estrogen analog 4-hydroxytamoxifen (4OHT). Two canonical c-MYC targets *ODC1* and *NAMPT* are induced in both Shep N-MYC-ER and SKNAS N-MYC-ER with activation of ectopic N-MYC, further demonstrated that N-MYC shares c-MYC target genes (Fig. 34). We further assess whether *REV-ERBα* is similarly upregulated by N-MYC. Indeed, when N-MYC is induced in Shep N-MYC-ER cells, *REV-ERBα* mRNA is elevated (Fig. 33A). Chromatin immunoprecipitation revealed that N-MYC binds to *REV-ERBα* promoter but not 2 KB upstream of the promoter (Fig. 33B). In addition, elevated N-MYC is able to activate *REV-ERBα* promoter as demonstrated by increased luciferase activity in Shep N-MYC-ER *REVα::Luc* cells in the presence of 4OHT (Fig. 33C). In two N-MYC amplified human neuroblastoma cell lines (NLF and Kelly), *REV-ERBα* mRNA is also significantly higher compare to parental Shep cells (Fig. 36).

Consistent with what we observed in U2OS cells and mHCC 3-4 cells, *BMAL1* mRNA is downregulated significantly and the oscillation is dampened in Shep N-MYC-ER (Fig. 33, 35) and SKNAS N-MYC-ER (Fig. 34, 35) when N-MYC is induced. Similarly, *PER2* is highly upregulated with high N-MYC in both cell lines (Fig. 34, 35). Furthermore, the expression of *PER1*, *CRY1* and *REV-ERBβ* elevates in response to high N-MYC as expected (Fig. 34). In contrast to robust *Bmal1* transcript oscillation in parental Shep cells, where N-MYC is low, NLF and Kelly exhibit disrupted Bmal1 oscillation (Fig. 36B). These observations further corroborate that in the presence of high N-MYC, upregulated *REV-ERBα* suppresses Bmal1 expression and oscillation.

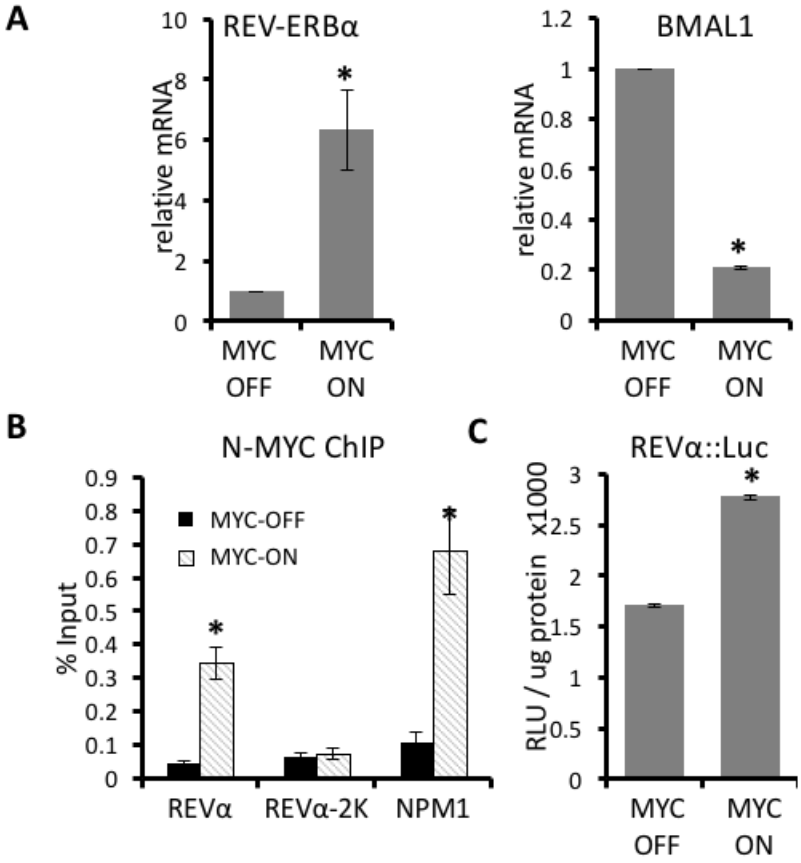

Figure 33. N-MYC Directly Upregulates REV- ERBα

(A) *REV-ERBα* and *BMAL1* mRNA expression (normalized to expression of *β2M*) determined by RT-PCR in Shep N-MYC-ER expressing neuroblastoma cells with MYC-ON or MYC-OFF. Means and SDs from at least three experiments are shown. *p < 0.05 by Student's t test for MYC-ON versus MYC-OFF. (B) Chromatin immunopreciptitation (ChIP) analysis with anti-N-MYC antibody in MYC-ON versus MYC-OFF in Shep N-MYC-ER cells. ChIP signals (% input) are shown for the Rev-erbα promoter E- box region (REVα, 81 bp region), 2 kb upstream of REV-ERBα transcription start site (REVα-2k), and the promoter of the canonical MYC target nucleophosmin 1 (*NPM1*). Means and SDs from tech- nical triplicates are shown. *p < 0.05 by Student's t test for MYC-ON versus MYC-OFF. Data are representative of three or more experiments. (C) Activity of the REV-ERBα promoter::luciferase construct (-1156 to +31 region) in Shep N-MYC-ER-expressing cells expressing under MYC-ON versus MYC-OFF conditions. RLU: relative light unit. Means and SDs from triplicate samples are shown, and *p < 0.05 by Student's t test for MYC- ON versus MYC-OFF. Data are representative of three or more experiments.

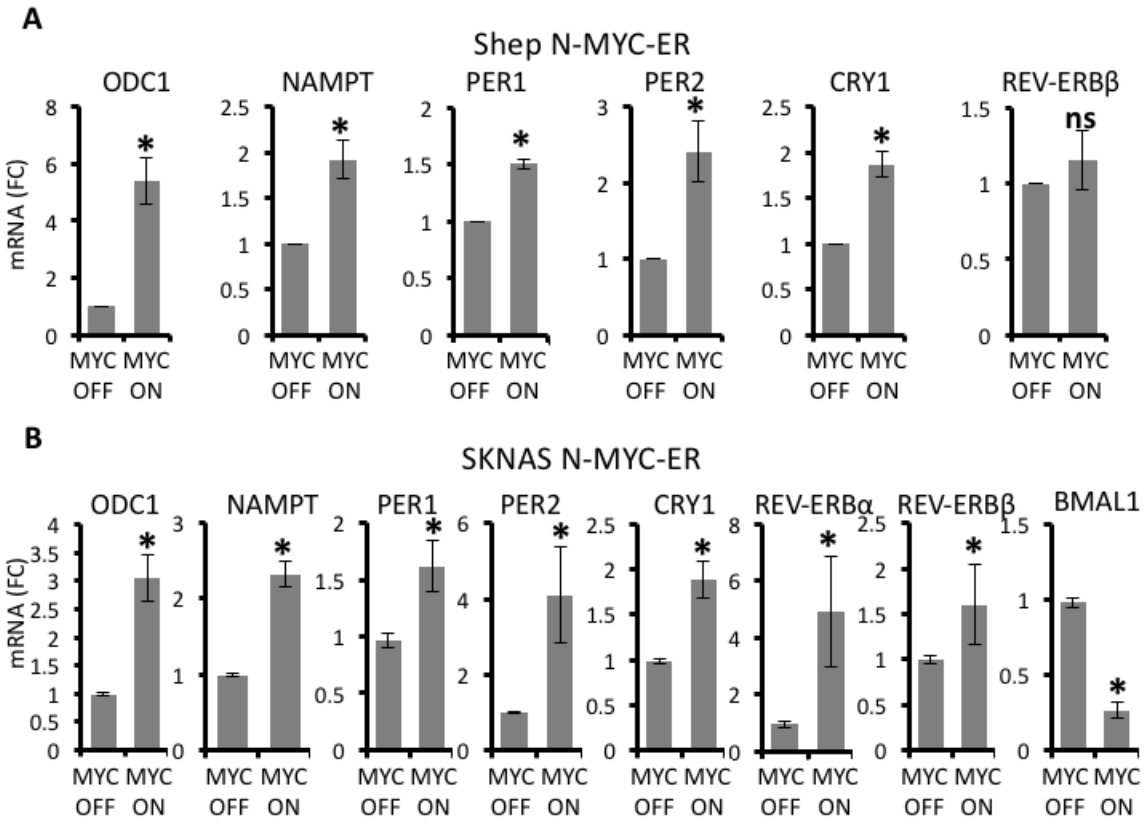

Figure 34. Oncogenic N-MYC upregulates canonical MYC targets and circadian genes

(A) Shep cells stably expressing N- MYC-ER were treated with 500 nM 4OHT to activate N-MYC-ER (MYC-ON) or EtOH control (MYC-OFF) for 24 hours. mRNA was harvested and reverse transcribed to cDNA and expression of *ODC1*, *NAMPT*, *PER1*, *PER2*, *CRY1*, and *REV-ERBβ* was determined by quantitative real-time PCR, normalized to expression of *β2M.* mRNA (FC) = Fold Change (B) SKNAS neuroblastoma cells stably expressing N-MYC-ER were treated with 500 nM 4OHT to activate N-MYC-ER (MYC-ON) or EtOH control (MYC-OFF) for 24 hours, mRNA was harvested and reverse transcribed to cDNA, and expression of *ODC1*, *NAMPT*, *PER1*, *PER2*, *CRY1*, *REV-ERBα*, *REV-ERBβ*, and *BMAL1* was determined by quantitative real-time PCR, normalized to expression of *β2M*. *$p < 0.05$ by Student's t test for MYC-ON versus MYC-OFF. ns = not significant.

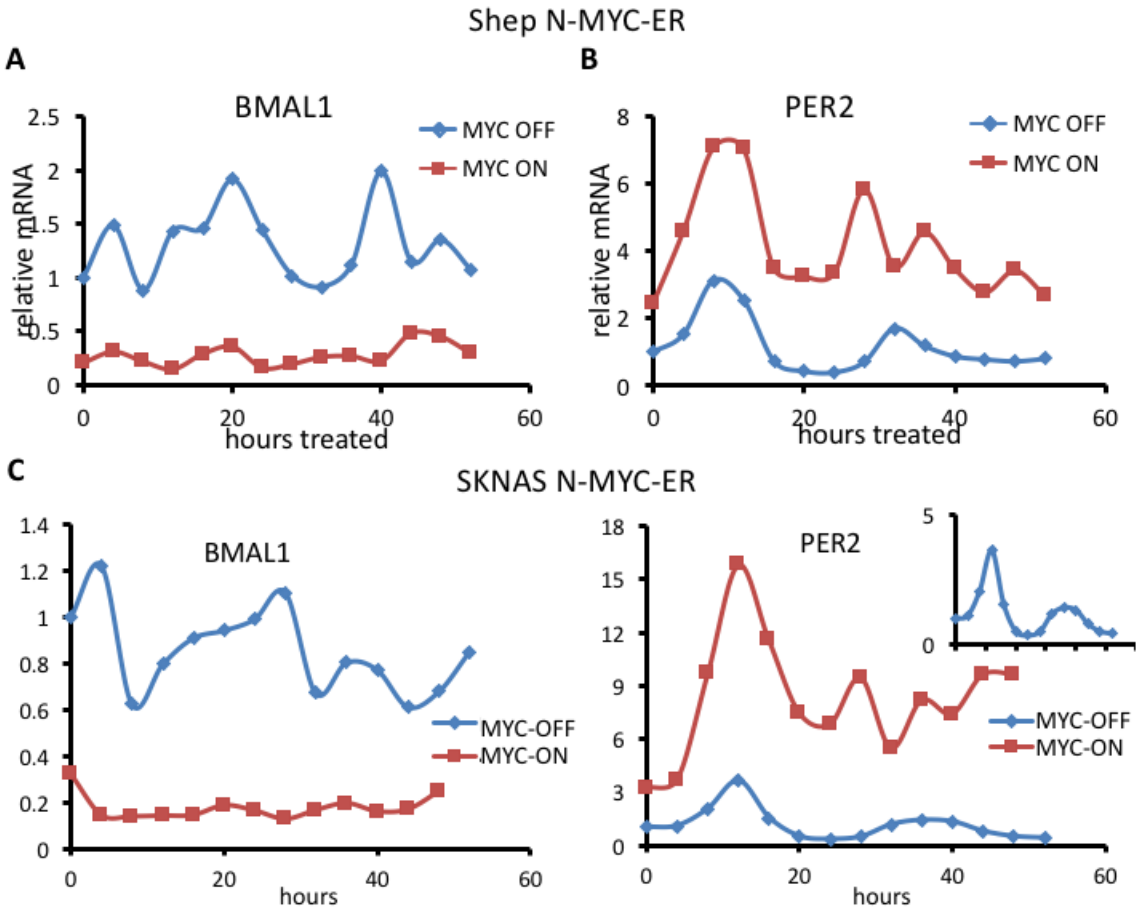

Figure 35. Oncogenic N-MYC disrupts circadian oscillation.
SKNAS N-MYC-ER-expressing cells were cultured with 4OHT (MYC- ON) or EtOH (MYC-OFF) control for 24 hours, then cultured with EtOH or 4OHT and synchronized with dexamethasone. mRNA was collected every four hours for 52 hours, reverse-transcribed to cDNA, and endogenous *BMAL1* expression (left panel) or *PER2* expression (right panel) was determined by quantitative real-time PCR, normalized to expression of the non-circadian gene *β2M*. **INSET** for *PER2* graph is EtOH (MYC-OFF) treated cells, with a smaller Y axis to demonstrate *PER2* oscillation. Data are from a single experiment.

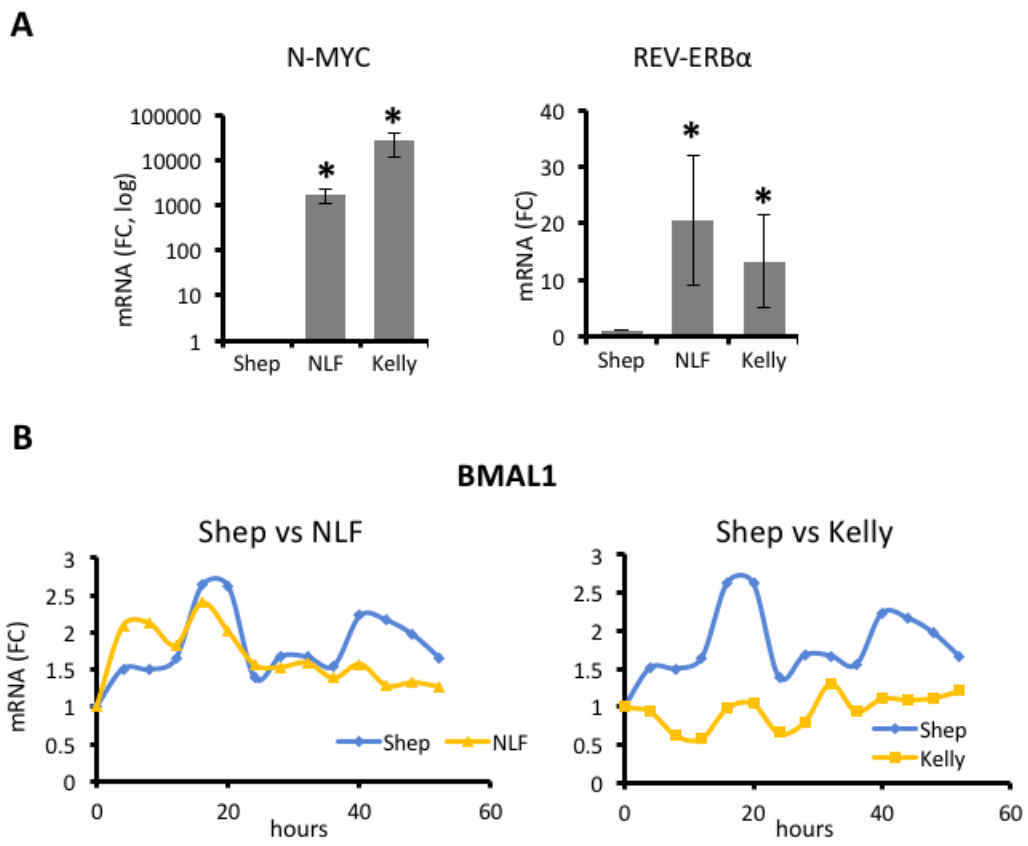

Figure 36. N-MYC expression correlates with high REV-ERBα expression and disrupted BMAL1 oscillation

(A) Shep neuroblastoma, with single copy *MYCN* (N-MYC), or NLF and Kelly neuroblastoma, with amplified *MYCN*, were harvested for mRNA, which was reverse-transcribed to cDNA. Expression of *MYCN* and *REV-ERBα* was determined by quantitative real-time PCR, normalized to expression of *β2M*. *Note log scale for MYCN expression*. means and SDs from at least three experiments are shown. *$p < 0.05$ by Student's t test of N-MYC amplified cells to Shep cells (B) Shep neuroblastoma, with single copy *MYCN* (N-MYC), or NLF and Kelly neuroblastoma, with amplified *MYCN*, were synchronized with 0.1 µM dexamethasone. mRNA was collected every four hours for 52 hours, reverse- transcribed to cDNA, and endogenous *BMAL1* expression was determined by quantitative real- time PCR, normalized to expression of the non-circadian gene *β2M*. Shep cell *BMAL1* expression was compared to NLF (left panel) or Kelly (right panel). Data are representative of two or more experiments.

High REV-ERBα and low BMAL1 associate with poor prognosis in neuroblastoma patients

The increased *REV-ERBα* expression in response to high MYC has implied that upregulating *REV-ERBα* with consequently suppression of *BMAL1* may have potential survival benefit for N-MYC-overexpressing tumor cells. To assess the relationship between expression of *REV-ERBα* and *BMAL1* in the tumor samples and the associated patient outcome, we analyze the expression of *REV-ERBα* and *BMAL1* in a neuroblastoma patient cohort. Tumors that are graded as high risk tend to have significantly higher *REV-ERBα* mRNA level and lower *BMAL1* expression (Fig. 37D, 37E). Consistent with previous studies, high N-MYC is linked to poor patient outcome (Chan et al., 1997). Surprisingly, tumors that express high *NR1D1* (*REV-ERBα*, Fig. 37B) and low *ARNTL* (*BMAL1*, Fig 37C) are also correlated with poor prognosis. Furthermore, in a separate cohort with 476 neuroblastoma patients, patients who have neuroblastoma with *NR1D1* (*REV-ERBα*) expression higher than median had poorer overall survival than did patients who had neuroblastoma with NR1D1 expression lower than median (Fig. 37 F). Patients who had neuroblastoma with *ARNTL* (*BMAL1*) expression higher than median consistently live longer than those who had neuroblastoma with lower *ARNTL* expression (Fig. 37G). These data suggest that the suppression of *BMAL1*, most likely through upregulation of *REV-ERBα*, is critical for the growth of neuroblastoma both in cell culture and in patient samples.

Colony suppression assay with BMAL1 overexpression

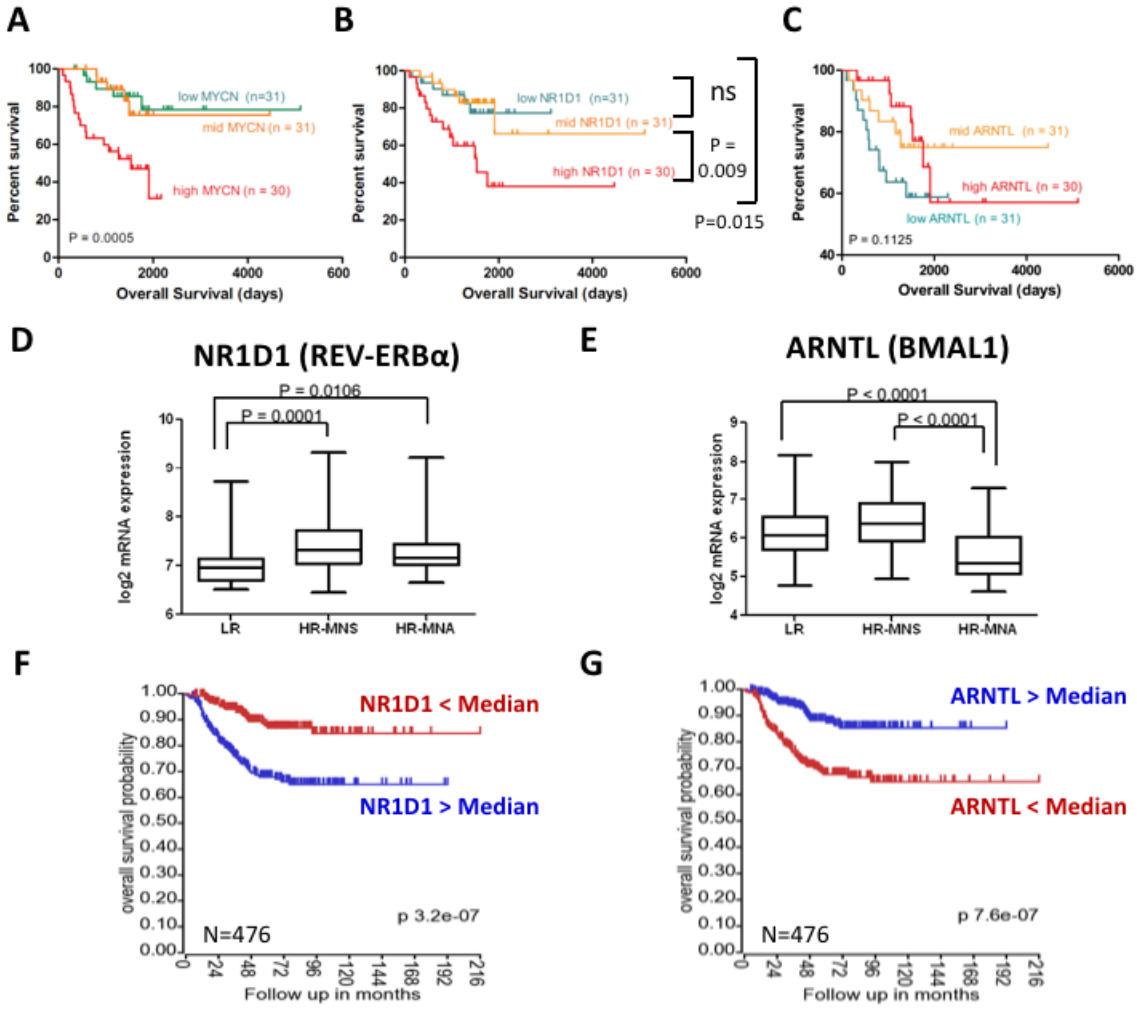

Figure 37. High-risk neuroblastoma exhibits increased REV- ERBα and decreased BMAL1 and these features correlate with poor prognosis.

(A,B,C) Kaplan-Meier survival analysis of patients with neuroblastoma expressing different levels of *MYCN* (A), (REV-ERBα) *NR1D1* (B) or (BMAL1) *ARNTL* (C) analysis grouped by tertiles based on individual gene expression. Log rank p values are shown. (D, E) *NR1D1* is significantly overexpressed (D) and BMAL1 (*ARNTL*) is repressed (E) in high-risk *MYCN*-amplified neuroblastoma compared to low- and intermediate-risk tumors (from a sample group of 240 tumors total). Box and whisker plot of *NR1D1* and *ARNTL* expression in primary neuroblastomas based on Children's Oncology Group (COG) risk groups and *MYCN* amplification status. LR, low-risk; HR-MNS, high-risk, non-amplified MYCN; HR-MNA, high risk, amplified MYCN. Whiskers represent 5th and 95th percentiles respectively (F,G) In a separate cohort of 476 patients, (F) higher than median expression of NR1D1 or (G) lower than median expression of ARNTL were both correlated with worse prognosis, as plotted and visualized by Kaplan-Meier analysis.

Since suppression of *BMAL1* appears to be beneficial for the growth of neuroblastoma, we sought to determine whether BMAL1 has the ability to suppress tumor growth. To test this, we transiently transfect pCMV6-EV or pCMV6-ARNTL vector in human neuroblastoma cell line NLF and Kelly, where *MYCN* is amplified and *BMAL1* expression is normally low, and assess colony suppression. Elevated BMAL1 expression can be detected by immunoblot after transient transfection (Fig. 38A). Interestingly, colony formation is greatly reduced in both cells with BMAL1 overexpression, indicating BMAL1 indeed acts as a putative tumor suppressor in human neuroblastoma (Fig. 38B, 38C).

Discussion

Our findings demonstrate that REV-ERBα is crucial for N-MYC-mediated *BMAL1* suppression, which in turns promotes tumor progression in human neuroblastoma. We provide evidence that elevated *REV-ERBα* expression is correlated with c-MYC-overexpressed T-ALL as well as *MYCN*-amplified neuroblastoma. In addition, we found N-MYC directly upregulates *REV-ERBα* in N-MYC inducible cell line. Intriguingly, both high *REV-ERBα* expression and low *BMAL1* expression predict poor prognosis of patients with neuroblastoma in two independent patient cohorts. Finally, constitutively overexpressed BMAL1 is sufficient to suppress colony formation in neuroblastoma cell lines. Overall, there is a solid link between loss of clock and cancer progression in N-MYC driven neuroblastoma.

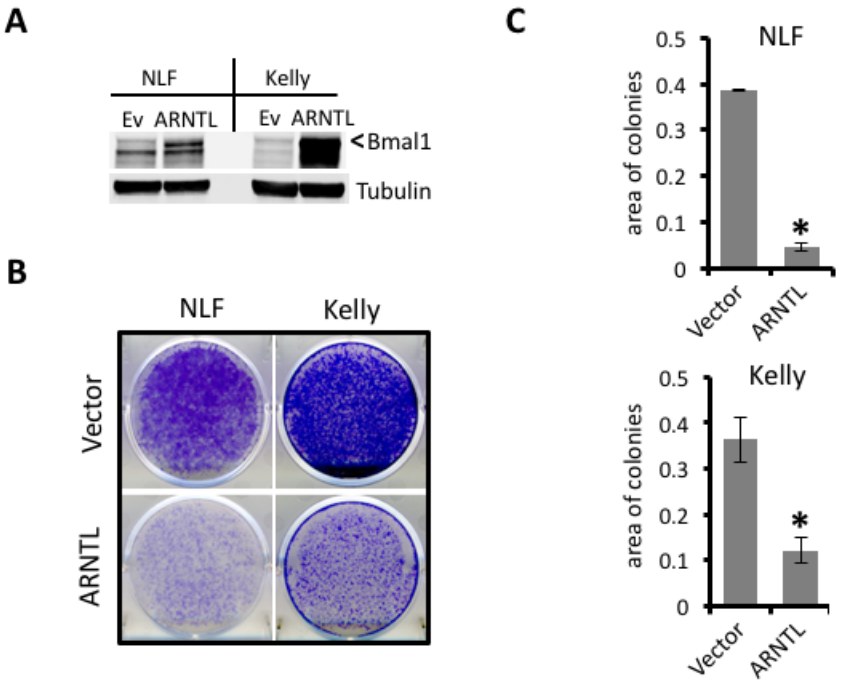

Figure 38. Overexpression of BMAL1 suppress colony formation in N-MYC-amplified neuroblastoma cell lines.

(A) Ectopic expression of BMAL1 (*ARNTL*, specific band indicated by <) in the high *MYCN* neuroblastoma cell lines NLF and Kelly was determined by immunoblotting, with Tubulin serving as a loading control (B) Colony suppression assay of cells treated with 1 mg/ml G418 showed that ectopic expression of *ARNTL* suppressed colony formation capacities of NLF and Kelly cells as compared with vector control (ev). (C) Quantitation of colony suppression by *ARNTL* determined by area of colonies on culture plates measured by ImageJ. n = 3, error bars represent SD. *$p < 0.05$ by Student's t test.

The first report implicated that *REV-ERBα* is a potential oncogene is done in breast cancer (Kourtidis et al., 2010). The gene encodes REV-ERBα, *NR1D1*, is located within 17q12-21 amplicons that containing *ERBB2*. *ERBB2* is overexpressed in approximately 30% of breast cancers, suggesting upregulating *REV-ERBα* could exhibit in a broad breast cancer population (Kourtidis et al., 2010). REV-ERBα has been shown to promote fatty acid synthesis in these *ERBB2*-postive breast cancer cell lines (Kourtidis et al., 2010). Interestingly, based on our observation that overexpression of BMAL1 suppress colony formation in neuroblastoma cell lines, we postulated that REV-ERBα-tumor promoting effect is largely from *BMAL1* suppression. Recent study also supported our finding that the promoter of *BMAL1* is epigenetically silenced in ovarian cancer cell lines and overexpression of BMAL1 inhibits tumor cell growth (Yeh et al., 2014).

Chapter 5

Metabolic alteration of MYC-disrupted molecular clock in U2OS cells

MYC orchestrates major cellular metabolic pathways, particularly enzymes that are involved in glycolysis, the TCA cycle, fatty acid synthesis and nucleotide synthesis (Hsieh et al., 2015; Stine et al., 2015). Given our observation that MYC disrupts molecular clock circuitry by upregulating *REV-ERBs* to suppress *BMAL1* expression and oscillation, it stands to reason that the disruption of the molecular clock can affect metabolism. There are multiple pieces of evidence that lead to this hypothesis. First, as extensively reported, BMAL1 has a central role in regulating metabolism (Bass, 2012). Knockdown of *BMAL1* leads to disrupted oscillation of metabolic processes (Kennaway et al., 2013). Since MYC suppresses *BMAL1*, the metabolic processes driven by the molecular clock are likely to be affected. Second, as discussed in Chapter 1, MYC induces the expression of key enzymes in the metabolic pathway by binding to the E-box within their promoters, which is the same site to which CLOCK::BMAL1 heterodimer binds to regulate its target genes(Yoshitane et al., 2014). The combination of high level of MYC and reduced level of BMAL1 may dramatically change the dynamic of transcription factor occupancy and gene expression as demonstrated from the observation of USF1 in Clock mutant mice (Shimomura et al., 2013). Third, rapid growing cells will require high metabolic activity to support their growth. Thus, releasing expression of rate-limiting enzymes from circadian control may be critical to maintain constant, heightened metabolic flux.

In this chapter, we provide evidence that MYC reprograms metabolic processes in U2OS MYC-ER cells and alters the metabolic circadian profile. We also demonstrated that circadian glucose oscillation in MYC-OFF cells is disrupted by MYC, which in turns promotes rapid consumption of glucose, lactate, pyruvate, glutamine and glutamate for

biosynthesis. Finally, oscillation of phospho-AMPK, a surrogate of cellular energetics, is also disrupted by MYC.

Material and Methods

Plasmids

c-MYC-ER™ wt and Δ106-143, which are responsive to tamoxifen and 4-hydroxytamoxifen but not to estrogen, were received in the pBabe-puro vector courtesy of Dr, Linda Penn, Ontario Cancer Institute, University Health Network, University of Toronto, Canada) and were described previously (Littlewood et al., 1995). c-MYC-ER™ wt and Δ106-143 were subcloned into pBabe-Zeo (Morgenstern and Land, 1990) (courtesy of Dr. Robert Weinberg, Whitehead Institute for Biomedical Research, Cambridge, MA, USA, Addgene plasmid 1766). Retrovirus was generated in 293T cells using the pCMV-VSVG and pUMVC vectors (Stewart et al., 2003) (courtesy of Dr. Robert Weinberg, Addgene plasmids 8449 and 8454).

Cell Culture

U2OS cells with BMAL1::luciferase vector were kindly shared by Dr. John Hogenesch (Baggs et al., 2009). U2OS cells were cultivated in Dulbecco's modified Eagle's medium (DMEM, Mediatech, Manassas, VA, USA, starting glucose concentration of 25 mM and starting glutamine concentration of 4 mM). Media was supplemented with 10% fetal bovine serum (FBS, HyClone, Logan, UT, USA or Life Technologies, Grand Island, NY, USA) and 1X Penicillin/Streptomycin (Mediatech) for

all cells. Some U2OS MYC-ER™ were treated with 500 nM 4-hydroxytamoxifen (Sigma, St. Louis, MO, USA) or ethanol control.

For U2OS MYC-ER metabolomics, cells were plated three days prior to sample harvest and allowed to grow to confluence. Two days before harvest, cells were treated + 500 nM 4OHT (MYC-ON) or ethanol (MYC-OFF) (without changing media), and one day prior to harvest, cells were synchronized with 0.1 uM dexamethasone (without changing media). During experiment, cells were collected every two hours by washing with cold PBS, scraping into a small volume of cold PBS, spinning down cells into a pellet, and snap-freezing. At each timepoint, 1 mL of media was spun down to clear it of debris, and also snap frozen. Pellets and media were extracted for NMR as described below.

U2OS BMAL1::Luc cells were stably transduced with MYC-ER™, MYC-ER™ Δ106-143, or pBabe-Zeo empty vector retrovirus using the plasmids and methods described above. Infected cells were selected for with 100 µg/ml Zeocin (Life Technologies) for two weeks, then continually cultured in Zeocin except during experiments.

All cell culture, except that during live-cell luminometer experiments (see Lumicycle section below), was conducted in a 5% CO2 humidified atmosphere.

Cell and media extraction for NMR analysis

U2OS cell pellets were thawed on ice and extracted using a modified Bligh-Dyer method (Bligh and Dyer, 1959; Tambellini et al., 2013). Briefly, a methanol: chloroform (2:1) mixture (300µl) was added to cell pellets, then vortexed and sonicated for 15 min.

Chloroform and water (100µl each) was then added and samples were again vortexed. Organic and aqueous layers were partitioned by centrifugation at 13,300rpm, for 7mins at 4°C. 100µl of the aqueous layer was dried in a speed vacuum for 4hrs until dry and immediately prepared for NMR analysis as described below.

Media samples (50µl each) were centrifuged at 14000 rpm for 20 min, and the supernatant was prepared for NMR as described below. Liquid chromatography-mass spectrometry (LC-MS) - grade Acetonitrile, Methanol, Chloroform was purchased from Fisher Scientific (New Jersey, USA).

NMR Spectroscopy and Quantitative Profiling

The samples were dissolved in 200 µl phosphate buffer (final pH ~7.1) containing Sodium-2,2-Dimethyl2-Silapentane-5-Sulfonate (DSS, Cambridge Isotope Limited, Andover, MA) (Cambridge Isotope Limited, Cambridge, UK 0.175 mM for media samples and 0.255 mM for cell samples) and 10% D2O for field frequency lock purpose (Cambridge Isotope Limited, Cambridge, UK). The samples were transferred to NMR tubes (3mm I.D, Bruker Biospin, Billerica, MA). All NMR spectra were acquired on Avance III HD 700 MHz NMR spectrometer from Bruker Biospin (Billerica, MA) equipped with a 3mm NMR triple resonance inverse probe and SampleJet cooled to 10oC for automated spectral acquisition.

For all 1-dimensional NMR spectra, the pulseprogram took the shape of first transient of a 2 dimensional NOESY and generally of the form RD-90-t-90-tm-90-ACQ. Where RD = relaxation delay, t = small time delay between pulses, tm = mixing time and ACQ = acquisition (Beckonert et al., 2007). The water signal was saturated using

continuous irradiation during RD and tm. The spectra were acquired using 76K data points and 14 ppm spectral width. 378 scans were performed and 1 second interscan (relaxation) delay and 0.1 second mixing time was allowed. The FIDs were zero filled to 128K; 0.1 Hz of linear broadening was applied followed by Fourier transformation.

NMR spectra were imported into Chenomx v 8.0. (Edmonton, Canada) for quantitative targeted profiling (Weljie et al., 2006). The processor module was used to phase and baseline correct the spectra followed by internal standard calibration and deletion of water region. The processed spectra were then imported to the profiler module for targeted profiling. Quantified data from this process were exported for further analysis.

Principal Component Analysis of metabolites

NMR spectra was profiled using Chenomx v8.0 (Edmonton, Canada) and the profiled data from all the spectra consisting of concentration values from the metabolites was used as the input dataset for Principal Component Analysis (PCA). PCA was performed in Simca-P 13.0 (Umetrics AB, Sweden). The data was mean centered and autoscaled prior to implementing the algorithm. Auto scaling was performed by dividing each variable by its standard deviation. The quality of the model was judged by the goodness of fit (R2) and goodness of prediction (Q2) based on a 1/7th round of cross-validation.

Quantitative Analysis of Metabolite Oscillations

Output concentrations from the NMR analysis were imported into the R statistical framework (Team, 2015), and were noted to have significant temporal change in overall concentrations. Thus a detrending algorithm was applied from the pracma R package

(Borchers, 2015) prior to assessment of rhythmicity in the metabolite data. Oscillations were assessed using the non-parametric JTK_CYCLE algorithm (Hughes et al., 2010), testing for period lengths between 22 and 26 hours corresponding to circadian events. The default cosine function was used to assess rhythmic patterns and tested against the experimental data as a function of both period length, phase and amplitude. Rhythms were considered significant if the Benjamini-Hochberg corrected false discovery rate (BH.Q) was < 0.05 (Benjamini and Hochberg, 1995).

Results

U2OS MYC-ER cells display distinct metabolites clustering between MYC-ON and MYC-OFF state

After observing that elevated MYC suppresses the molecular clock in a number of different cell lines, we further sought to determine the functional impact on metabolism, particularly the major biological processes that have been previously documented to be regulated by circadian rhythm. To this end, we cultured U2OS MYC-ER cells in both MYC-ON and MYC-OFF states, synchronized them with dexamethasone and then harvested both the cell pellets and supernatant media every two hours. Metabolites from cell pellets and media were extracted and analyzed by nuclear magnetic resonance (NMR) spectroscopy.

Principle component analysis (PCA) of all time points has revealed that despite the variance between time points, the overall clustering of MYC-ON and MYC-OFF cells are

very distinctive (Fig. 39). This observation is consistent with what has been reported in literature regarding rewiring of metabolism by oncogenic MYC (Dang, 2013).

Oscillation of glucose metabolism is abolished in MYC-ON cells

NMR spectroscopy allows us to observe selective metabolites in a quantitative way, including glucose, glutamine, pyruvate, lactate and glutamine. Each metabolite was measured over a 48-hour time course in 2-hour intervals, and the resulting metabolite concentrations as a function of time subjected to JTK analysis to evaluate the period and the robustness of oscillation. As expected, glucose level is greatly reduced in MYC-ON cells both in the cell and in the media, suggesting that MYC induces high flux of glycolysis (Fig. 40). Strikingly, intracellular glucose level in MYC-OFF cells exhibits a 24-hour oscillation which has a p-value of 0.052 in JTK analysis (Fig. 40). This circadian oscillation, however, is dampened in MYC-ON cells (Fig. 40). Interestingly, glucose level also appears to oscillate in the media with the trough at 12 hour and 26 hour, matching with the timing of peak glucose level intracellularly (Fig. 40). Low level of intracellular and extracellular glucose indicates that in addition to the molecular clock disruption, MYC also induces several glycolytic enzymes allowing cells to consume glucose rapidly, perhaps for macromolecular synthesis. End-products of glucose metabolism, such as pyruvate and lactate, also appears to oscillate in MYC-OFF cells (Fig. 40). The timing of the highest concentration of pyruvate and lactate correlates with the trough of intracellular glucose level (Fig. 40), suggesting BMAL1-controled glucose metabolism is affecting the entire glycolytic pathway. Pyruvate level decreased overtime

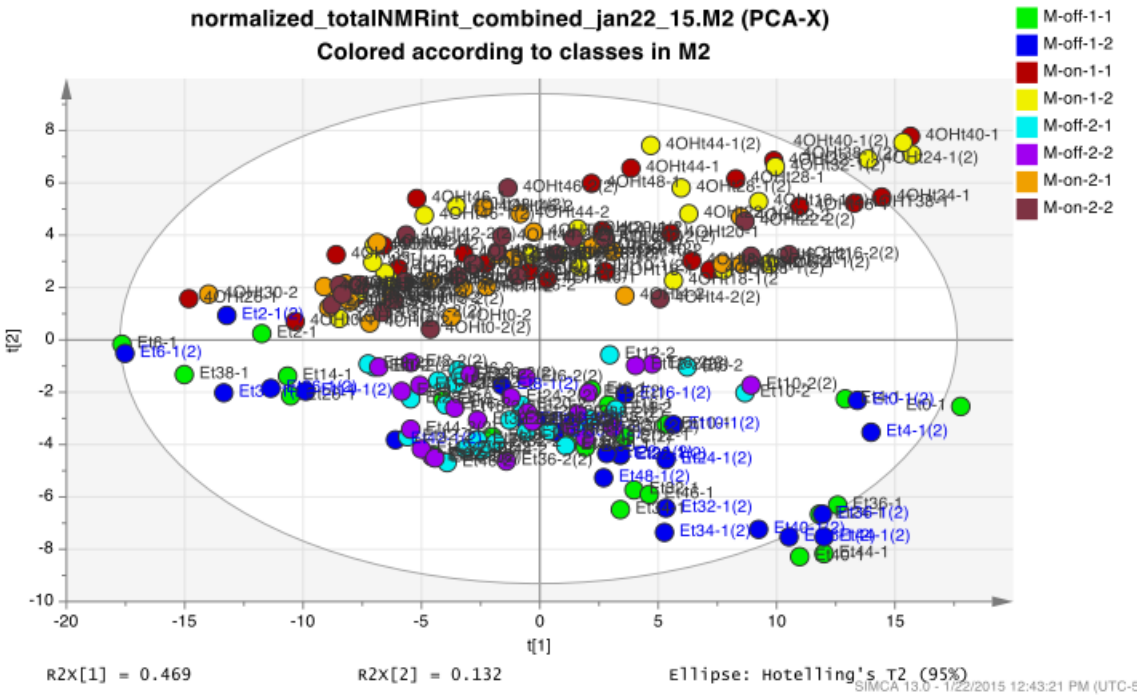

Figure 39. Principal component analysis of metabolites from U2OS MYC-ER cells

NMR spectra were acquired in a time-series experiment with 2-hr intervals from synchronized U2OS cells with MYC-OFF (EtOH, M-off on the diagram) or MYC-ON (4OHT, M-on on the diagram). NMR spectra was then profiled using Chenomx v8.0 (Edmonton, Canada) and the profiled data from all the spectra consisting of concentration values from the metabolites was used as the input dataset for Principal Component Analysis (PCA). Each dot represents NMR signal from either MYC-ON or MYC-OFF cells at each time point.

in the culture media of MYC-ON cells and was not detected intracellularly in both conditions, further indicating rapidly consumption for TCA cycle fueling and biosynthesis pathways (Fig. 40). Compared with gradual accumulation of lactate in MYC-OFF cells, lactate remains low in MYC-ON cells (Fig. 40). Low intracellular lactate is possibly a consequence of increased lactate export through MYC-mediated monocarboxylate transporter 1 (MCT1) overexpression (Doherty et al., 2014), which is further reflected by increased lactate accumulation in the culture media of MYC-ON cells (Fig. 40). Similarly, the level of glutamine within cells of both MYC states did not reach the detection threshold of NMR. Glutamine derived glutamate, however, was rapidly consumed in MYC-ON cells intracellularly and extracellularly (Fig. 40). Our observations suggest that both glutamine and glutamate were likely used for biosynthesis. Collectively, disruption of BMAL1 by MYC profoundly alters cellular metabolism, featured by enhanced glycolysis flux, which prepares cancer cells to fulfill metabolic demands required for rapid growth.

MYC disrupts oscillation of AMPK phosphorylation

Since glycolysis is the most important metabolic pathway to generate ATPs, changes in glycolytic flux can alter cellular energetic status. Given the observation that MYC disrupts normal oscillation of glucose metabolism, we next sought to determine the effect of circadian disruption by MYC on cellular energetics. We use phosphorylation of AMP-activated protein kinase (AMPK) as a measure of cellular energetics. AMPK plays a critical role in maintaining cellular energy homeostasis (Hardie and Alessi, 2013). When

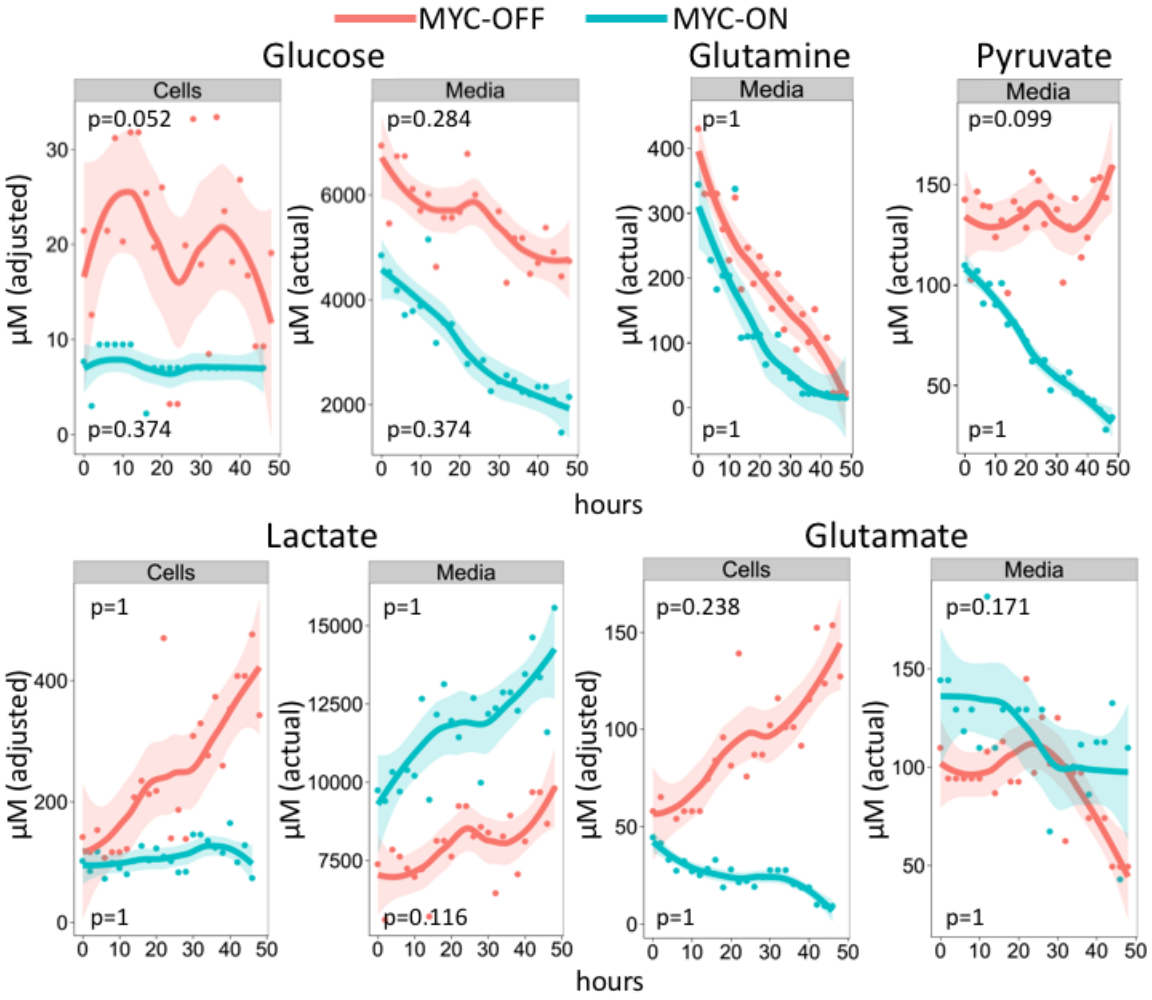

Figure 40. MYC Suppresses circadian oscillation of glucose metabolism and alters glutamine metabolism in U2OS Cells

Cellular (Cells) or media metabolite (top labels) levels determined by NMR spectroscopy are shown for a time-series experiment with 2-hr intervals from U2OS with MYC-OFF (EtOH) or MYC-ON (4OHT), 24 hr after initial dexamethasone synchronization. Concentrations for metabolites represent the *adjusted* concentration for cells, based on extraction volume, or the *actual* concentration of media metabolites. For each metabolite profile, the time-series data were plotted using the JTK v2 algorithm after linear detrending, and rhythmicity was assessed via a non-parametric cosine function fit. The colored bands represent 95% confidence intervals from the locally weighted scatterplot smoothing function that generated the curves. p values indicate the significance of the cosine wave fit to experimental data. Note that MYC-ON media 24-hr sample and MYC-ON cells 48-hr sample were excluded due to inconsistencies in sample measurements.

cells don't have enough energy, ATP level will drop and AMP will accumulate. Elevated level of AMP promotes AMPK phosphorylation and activates it. Activated AMPK will suppress anabolic pathways that consume ATPs and induce catabolic pathways that generate ATPs. Interestingly, immunoblot showed phospho-AMPK peaks at 12 hours and 40 hours in MYC-OFF cells, the exactly same time points when glucose level is highest in the cell (Fig. 41). When glucose level is high, less glucose was used and less ATPs were being generated. As a result, accumulation of AMP activates AMPK. However, the oscillation of phospho-AMPK is not evident in MYC-ON cells, where BMAL1 is greatly reduced (Fig. 41). This observation further demonstrates that loss of clock leads to enhanced glycolysis and increased cellular energetics. Hexokinase 1 (HK1), the first rate-limiting enzyme of glycolysis, shows a slight oscillation in MYC-OFF cells (Fig. 41). However, in MYC-ON cells, hexokinase 2 (HK2) is dramatically induced and no oscillation is appreciable (Fig. 41). Once again, our data support that MYC concurrently suppresses clock-controlled glucose metabolism and activates MYC-induced glycolytic pathway, which results in heightened metabolism in tumor cells.

MYC disrupts NAMPT and NAD^+ oscillation

Previous study has shown that NAMPT robustly oscillates every 24 hour in mouse liver and white adipose tissue (Nakahata et al., 2009; Ramsey et al., 2009). Its oscillation is abolished in Clock mutant mice, suggesting NAMPT is regulated by clock (Nakahata et al., 2009; Ramsey et al., 2009). Interestingly, NAMPT is also one of the canonical MYC target genes (Menssen et al., 2012). When we examine mRNA expression of *NAMPT* in

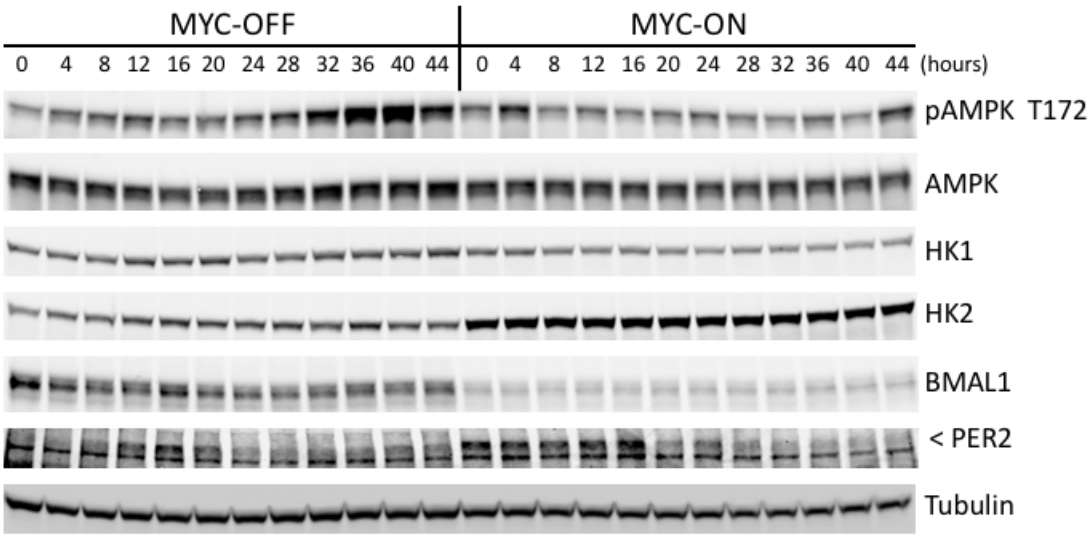

Figure 41. MYC Suppresses Circadian Oscillation of cellular energetics.
Synchronized U2OS MYC-ER cells were harvested after treatment and lysates were processed for immunoblots of hexokinase 1 (HK1), hexokinase 2 (HK2), phospho-AMP kinase (pAMPK Thr172), AMP-kinase (AMPK), BMAL1, and PER2 (indicated by <). Tubulin serves as a loading control. Data are representative of two individual experiments.

U2OS MYC-ER cells, *NAMPT* appears to oscillate with a period of 36 hour in MYC-OFF cells (Fig. 42A). When MYC is induced, *NAMPT* transcript elevates and loses its oscillation (Fig 42A). NAMPT is the rate limiting enzyme in NAD^+ salvage pathway and knockdown of NAMPT reduces NAD^+ levels (Menssen et al., 2012). NAD^+ is an important co-factor in many metabolic pathways, thus alteration of its level results in profound metabolic effects (Canto and Auwerx, 2011; Chiarugi et al., 2012; Hara et al., 2007). We next examine whether disruption of NAMPT expression affects NAD^+ levels from our circadian metabolomic experiment. Interestingly, NAD^+ in MYC-OFF cells seems to oscillate approximately every 14 hour (Fig. 42B), which is similar to NAD^+ oscillation in mouse liver that has been documented in the literature (Ramsey et al., 2009). In MYC-ON cells, however, intracellular NAD^+ level dramatically increases and spikes up and down every 8-12 hour, consistent with the pattern of *NAMPT* transcript in MYC-ON cells (Fig. 42B). In addition, *Nampt* mRNA oscillate robustly with a period approximately 24 hours in mHCC 3-4 c12 cells when MYC is off, but the oscillation is gone when MYC is induced (Fig. 42C). Collectively, here we showed that high MYC elevates and accelerates *NAMPT* oscillation, which leads to "ultradian" oscillating NAD^+ levels in cancer cells. However, whether MYC-induced ultradian oscillation of NAD^+ levels has functional impact on overall cell metabolism in cancer cell would require further investigation.

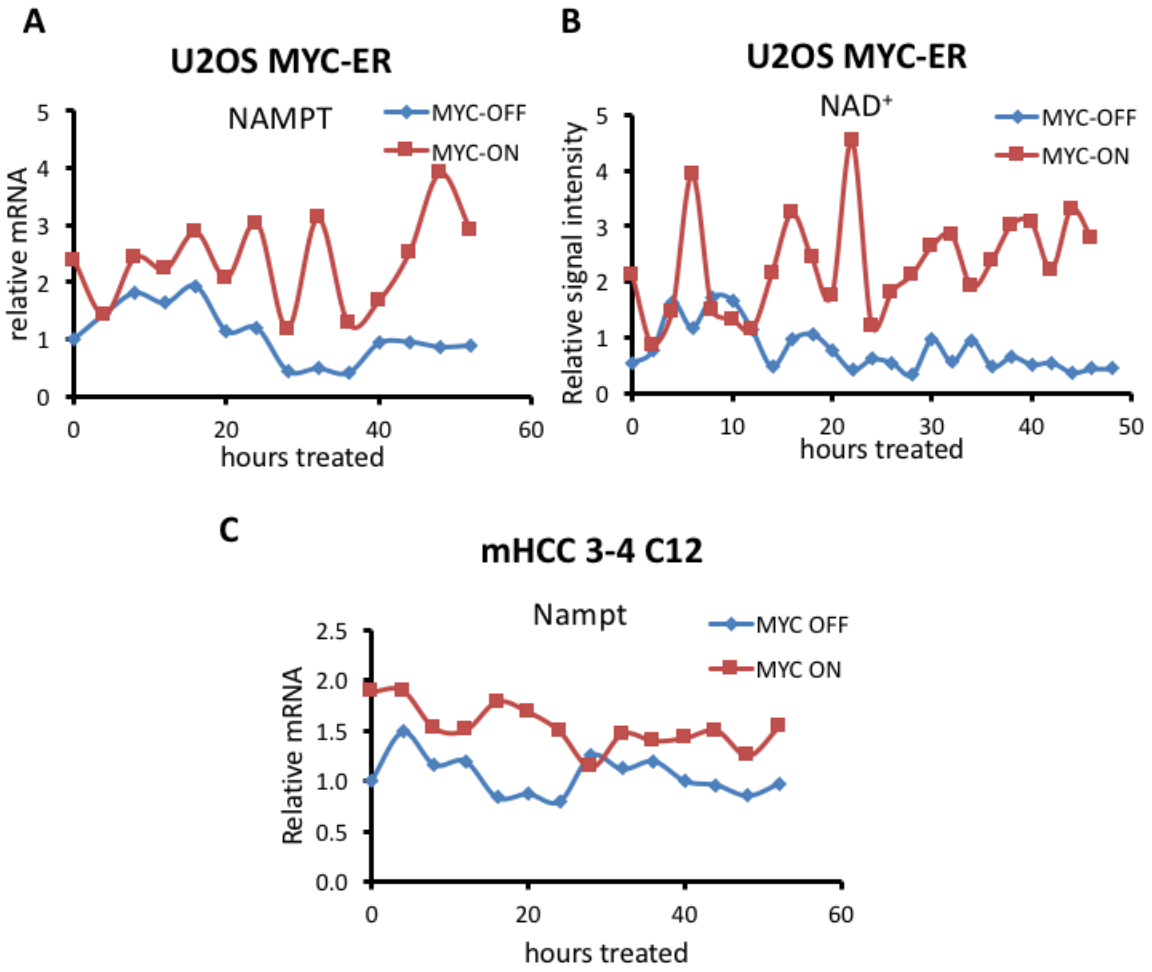

Figure 42. MYC disrupts NAMPT oscillation and induces NAD⁺ spikes.
(A) Time series (every 4 hr) expression of NAMPT mRNA (relative to *b2M*) determined by RT-PCR in U2OS MYC-ER cells treated with 4-hydroxytamoxifen (4OHT, MYC-ON) or ethanol (EtOH, MYC-OFF) control and synchronized with dexamethasone. (B) Cellular NAD^+ determined by LC-MS are shown for a time-series experiment with 2-hr intervals from U2OS with MYC-OFF (EtOH) or MYC-ON (4OHT), 24 hr after initial dexamethasone synchronization. (C) Time series (every 4 hr) expression of BMAL1, PER1, PER2, REV-ERBα, NAMPT mRNA (relative to β2M) determined by RT-PCR in synchronized mHCC 3-4 cells C12 cells treated with (+Tet, MYC-OFF) or without (-Tet, MYC-ON) tetracycline

Discussion

Circadian rhythm synchronizes and regulates metabolism to ensure organismal fitness (Bass, 2012). Obesity, liver steatosis and other metabolic disorders often arise in animal models lacking the molecular clock regulators (Kennaway et al., 2013; Paschos et al., 2012). In MYC-driven cancer cells, as we showed in previous chapters, molecular clock regulator *BMAL1* is profoundly suppressed. As a result, we would surmise that clock-controlled metabolism is similarly disrupted. Here, we have demonstrated that MYC indeed releases metabolism from circadian constraints and reprograms metabolic pathways to promote rapid growth. By using a high-resolution time course metabolomics analysis, we revealed that there is circadian oscillation of intracellular glucose level in synchronized U2OS cells. The oscillation, however, is eliminated when MYC is induced. MYC activation leads to hexokinase II elevation, which in turns increases glycolytic flux. Significant reduction of glutamine, glutamate, pyruvate and loss of pAMPK oscillation suggest that MYC-driven cells are undergoing biosynthesis. Overall, MYC's ability to suppress *BMAL1* provides a convenient metabolic switch from homeostasis to unrestricted growth.

Chapter 6

Investigation of *Drosophila* Myc in fly circadian behavior

We have observed that overexpressed MYC in mammalian cancer cells can suppress *BMAL1* oscillation and expression through upregulating *REV-ERB*α. We sought to determine whether *Drosophila* Myc will alter the molecular clock in the similar way as mammalian cancer cells. *Drosophila* Myc (called dMyc) is a transcriptional factor that is highly conserved with functional properties similar to mammalian MYC, including regulation of cell growth, development, and metabolism (Demontis and Perrimon, 2009; Grewal et al., 2005). However, the role of dMyc in the *Drosophila* molecular clock and metabolism is not known. *Drosophila* is a great *in vivo* model for Myc disruption of circadian rhythm for the following reasons: First, *Drosophila* Myc has similar function and gene regulatory mechanism as mammalian MYC. Second, *Drosophila* exhibits well-conserved molecular clock circuitry that resembles mammalian clock (Fig. 43). Finally, *Drosophila* exhibits robust circadian locomotor activity that is easy to monitor.

In this chapter, we demonstrate that both gain-of-function and loss-of-function of dMyc can disturb circadian locomotor behavior in flies. Using the Drosophila Activity Monitoring system, we show that overexpression of dMyc specific in Pigment Dispersing Factor (PDF) and Cryptochrome (Cry) expressing cells results in a higher percentage of arrhythmic flies. In these flies, dMyc overexpression also induces several E-box containing genes, such as *cycle* (*cyc*), *timeless* (*tim)*, *cryptochrome* (*cry*) and clockwork orange (*cwo*), however, the expression of *Drosophila BMAL1* homolog *clock* (*clk*) was not altered. Morphological analysis of neurons required for circadian locomotor behavior in the dMyc-overexpressing flies showed decreased PDF staining in the dorsal projection while the cell bodies remain unchanged. Preliminary metabolic profiling of the heads from these flies using GC-MS revealed that high dMyc leads to significant consumption

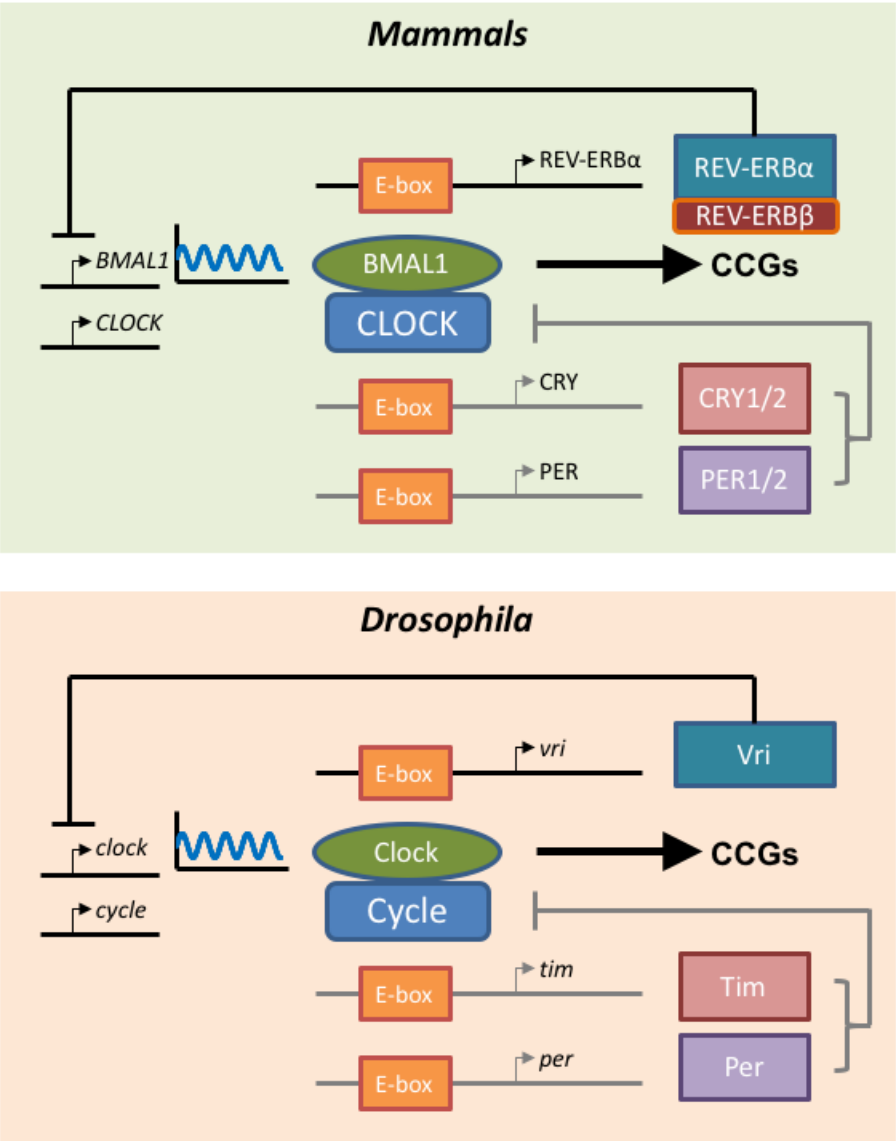

Figure 43. Molecular clock circuitry in mammals versus *Drosophila*

of valine and leucine, accompanied with accumulation of urea. Whether molecular clock perturbation or metabolic alteration resulting from high dMyc is the underlying mechanism of locomotor arrhythmicity requires further investigation.

Interestingly, adult dMyc hypomorph flies also display higher percentage of arrhythmic circadian activity, which can be rescued by additional deletion of dMnt, a known suppressor of dMyc activity. In contrast to dMyc overexpression, loss of dMyc does not alter the mRNA expression and oscillation of clock-controlled genes. However, Per staining in small lateral ventral neurons (sLNvs), the central clock cells in *Drosophila*, is dramatically diminished specifically in arrhythmic dMyc hypomorph flies. Reduced Per staining in sLNvs of arrhythmic dMyc mutant flies is not observed in dMyc mutant flies with dMnt deletion, suggesting endogenous dMyc activity is essential for circadian behavior. Our results have demonstrated a novel role of dMyc in modulating *Drosophila* circadian locomotor behavior potentially through directly regulating components of the core molecular clock as well as an indirect effect on metabolism.

Materials and Methods

Fly stocks

pdf-Gal4, *tim*-UAS-Gal4, *tim*-Gal4, cry^{24}-Gal4 and dm^{P0} lines were provided by the Bloomington Stock Center. UAS-Myc UAS-p35 and dm^{4} were kindly shared by Dr. Julie Secombe (Albert Einstein College of Medicine, NY). $dm^{4}dmnt^{1}$ were provided by Dr. Robert N. Eisenman (Fred Hutchinson Cancer Research Center). dm^{4} and $dm^{4}dmnt^{1}$ line were balanced with FM7i, Act-GFP. *pdf*-Gal4; cry^{24}-Gal4 lines were generated from

crossing *pdf*-Gal4 to cry^{24}-Gal4. dm^{P}/Y and its sibling control *w*/Y were generated by backcrossed dm^{P0} line from Bloomington Stock Center with isogenic wild type line (w^{ISO31}). Flies that used for the experiments were grown at 25 ºC.

Locomotor activity assay

Circadian locomotor activity assays were measured using the *Drosophila* Activity Monitoring System (Trikinetics). Approximately 5- to 7-day-old adult flies were entrained to light-dark (LD) 12 hour: 12 hour (12:12) cycles for three days, then transferred to constant darkness (DD) for 7-8 days. Collected activity data were analyzed using Clocklab software (ActiMetrics). Individual periods were calculated from 7-8 days activity data during DD using chi-square periodogram. Rhythm strength was determined by FFT analysis, then categorized as arrhythmic (<0.01), weakly rhythmic (0.01-0.03) and rhythmic (>0.05). Periods and rhythm strength were only calculated from rhythmic and weakly rhythmic flies.

Immunohistochemistry

Five-day-old adult flies were entrained to LD 12:12 cycle for 3 days and then transferred to DD. Brain dissection were done on day 4 or day 5 in DD. Five to ten brains of each genotype at each time point were stained. Adult fly brains were dissected and fixed for 30-60 min in 4% formaldehyde made in PBS with 0.3% Triton-X (PBST). Fixed brains were quickly rinsed twice in PBST, washed 3 x 10 min with PBST, followed by blocking with 5% normal donkey serum in PBST (NDST) for 1 hour. Brains were then incubated with primary antibody diluted in NDST at 4 ºC overnight. Brain samples were then washed 3 x 10 min with PBST, incubated with secondary antibody diluted in NDST at

room temperature for 2 hours, washed with 3 x 10 min PBST again and mounted with Vectashield. A Leica TCS SP5 confocal microscope was used to acquire images for immunostained brain. Primary antibodies used include: rabbit anti-PDF (kindly shared by Dr. Amita Sehgal) and Guinea Pig anti-Per (kindly shared by Dr. Amita Sehgal). Secondary antibodies used include: Alexa-Flour 448 goat anti-rabbit IgG (Life Technologies), Alexa-Flour 448 goat anti-Guinea Pig IgG (Life Technologies), Cy3 donkey anti-rabbit (Jackson ImmunoResearch Laboratories, West Grove, PA), Cy3 donkey anti-mouse (Jackson ImmunoResearch Laboratories)

Quantitative real-time PCR

Five- to Seven- day old adult flies were entrained to LD 12:12 cycle for 3-5 days. Approximately 20 flies were collected on dry ice at each time points on the last day of LD. Adult fly heads were homogenized in TRIzol® Reagent using VMR Pellet Mixers for 10 sec. Total RNA was then extracted according to manufacturer's instruction (TRIzol; Life Technologies) and reversed to complementary DNA by using TaqMan Reverse Transcription Reagents (Life Technologies). cDNA was used as template to proceed to quantitative real time PCR (RT-PCR) with specific *Drosophila* primers. RT-PCRs were performed using the ViiA™ 7 Real-time PCR system with a SYBR Green kit (Life Technologies). Relative mRNA expression levels were normalized to actin and analyzed using absolute quantification method. Standard curve used for quantification was determined by serial dilution of mixed samples from all time points. Primers used in the experiments were *dMyc* forward (5'-GAGCAACAACAGGCCATCGATATAG-3'), *dMyc* reverse (5'-CCTTCAGACTGGATCGTTTGCG-3'), *per* forward (5'-CGTCAATCCATGGTCCCG-3'), *per* reverse (5'-CCTGAAAGACGCGATGGTG-3'),

tim forward (5’-GCTGCGCCTTGTTTTCCTT-3’), *tim* reverse (5’-ATGATGTTCAGATCCTGCTGGA-3’), *pdp* forward (5’-TTTGAACAGCTTGAAAGCGC-3’), *pdp* reverse (5’-GAGATTTCCTGCCTGAGCTGG-3’), *vri* forward (5’-CGACTCTCTCGATGAACGGC-3’), *vri* reverse (5’-ACGGATGCAAGTTAGAAGCCTC-3’), *actin* forward (5’-GCGCGGTTACTCTTTCACCA-3’), *actin* reverse (5’-ATGTCACGGACGATTTCACG-3’), *cry* forward (5’-GCAGTACGTCCCGGAGTTGA-3’), *cry* reverse (5’-AGGGCTCGTGAACAAATTCCT-3’), *clk* forward (5’-TTCTCGATGGTGTTCTCGGTG-3’), *clk* reverse (5’-AGTTCGCAAAGCCAACGG-3’), *cyc* forward (5’-GTACGTTTCCGATTCGGTGT-3’), *cyc* reverse (5’-CTCTGTGGAACGTCGGTCTT-3’), *cwo* forward (5’-CAGGACTTTTGCCACCGACTATTG-3’), *cwo* reverse (5’-CTGCCGCCGCCTGCTGAC-3’), E75-PA forward (5’-CGGTAATCTGCACATTGTCGC-3’), E75-PA reverse (5’-TGCTTCAGCTGTTGGCTCTTG-3’), E75-PB forward (5’-TGCAACATCATCCGGAGGAT-3’), E75-PB reverse (5'-TCCTCCAGATGCAGCATCTCA-3’), E75-PC forward (5'-GACTTCTGTGATCTGCAGCACG-3’), E75-PC reverse (5'-CGACCTGTTACCCCCAAAATG-3’), E75-PD forward (5'-GCGAAGAACTCCCGATATTGAA-3’), E75-PD reverse (5'-TGAACTCACAGGTCTCGAGGTG-3’)

Western blot analysis

Five- to Seven- day old adult flies were entrained to LD 12:12 cycle for 3-5 days. Approximately 8-10 flies were collected on dry ice at each time points on the last day of LD. Adult fly heads were lysed and homogenized in 1X Passive Lysis Buffer (Promega) diluted in PBS supplemented with protease inhibitors and phosphatase inhibitor okadaic acid. Sample buffer (Thermo Cat:39000) was added to each sample. All samples were then boiled and spinned. Equaled-volume of supernatant from each sample was loaded into the Criterion pre-cast gradient gels (Bio-Rad, Hercules, CA, USA). Proteins were transferred onto nitrocellulose membranes using iBlot® Gel transfer system (Thermo). Primary antibodies used include: mouse anti-dMyc (kindly shared by Dr. Robert N. Eisenman), rabbit anti-α-Tubulin (Cell Signaling, Danvers, MA, USA) and Guinea Pig anti-Per (kindly shared by Dr. Amita Sehgal). Secondary antibodies used include: Peroxidase AffiniPure Goat Anti-Guinea Pig IgG (Jackson ImmunoResearch Laboratories), Goat anti-Mouse IgG1, HRP conjugate (Thermo). Immunoblots were then developed using ECL substrate (Thermo).

Results

Overexpressed dMyc affects circadian locomotor activity in a cell-specific manner

To study the effect of dMyc overexpression on the *Drosophila* molecular clock, we took advantage of the well-establish *Drosophila* GAL4/UAS (upstream activating sequence) system. This system allows us to ectopically express transgene in a specific cell type and requires two transgenic fly lines. In the "driver" fly line, the yeast transcriptional activator GAL4 is placed downstream of a cell-specific promoter. In the "UAS-transgene

fly" line, the transgene is placed downstream of a UAS activation domain that containing GAL4-binding sites. The otherwise silent transgene is activated in the progeny of UAS-transgene flies crossed to the "driver" flies that express GAL4. By using this system, we overexpress dMyc specifically in clock cells and observe the changes in circadian locomotor behavior to assess the effect of dMyc on the molecular clock in flies. Known clock-cell specific drivers including *pdf*-Gal4, *tim*-UAS-Gal4 and *tim*-Gal4 are used to cross with either isogenic wild type (w^{ISO31},+) , UAS-p35 (p35) or UAS-dMyc UAS-p35 (Myc+p35) flies. p35 is *Drosophila* homolog of *BCL2*, which has been documented previously to rescue overexpressed dMyc-induced life span shortening (Greer et al., 2013). Overexpressing both dMyc and p35 allows us to observe the effects of dMyc on the molecular clock without the confounding cell apoptotic effect that introduced of dMyc overexpression alone (Greer et al., 2013).

To assess the circadian locomotor behavior of these flies, we use the Drosophila Actogram Monitoring system. Each fly was loaded into a single glass tube and placed in a monitor housed in an incubator with controlled light/dark or dark/dark schedules. An infrared beam directed across the tube allows computers connected to the monitors to record every time when the fly interrupts the beam. The collected data is then plotted on actograms, which displayed the activities of a single fly over several days (Fig. 44A, C, E).

We first overexpressed dMyc with use of the *pdf*-Gal4 driver, which is expressed only in ventral lateral neurons that are critical for circadian behavior. Pdf-Gal4-mediated dMyc overexpression leads to decreased percentage of rhythmic flies from 100% to 87% and decreased rhythm strength in rhythmic flies (Table 3, Fig 44A, B). Since Pdf-Gal4

Table 3. Circadian locomotor rhythmicity of dMyc-overexpressing flies in Constant Darkness

Genotype	n	no. Rhythmic	% Rhythmic	Period (h)	Std. error	FFT	Std. error
w/Y;+;UAS-Myc, UAS-p35/+	32	32	100	23.80	0.04	0.04	0.004
w/Y;*pdf*-G/+;*pdf*-G/+	32	32	100	24.01	0.04	0.06	0.005
w/Y;*pdf*-G/+;*pdf*-G/UAS-Myc, UAS-p35	30	26	87	24.13	0.10	0.02	0.002
*cry*24-G/Y;*pdf*-G/+;+	31	31	100	24.49	0.05	0.10	0.008
*cry*24-G/Y;*pdf*-G/+;+/UAS-p35	28	25	89	24.60	0.05	0.04	0.004
*cry*24-G/Y;*pdf*-G/+;+/UAS-Myc, UAS-p35	26	8	31	24.46	0.07	0.03	0.004
w/Y;TUG/+;+	32	32	100	24.49	0.04	0.05	0.005
w/Y;TUG/+;+/UAS-Myc, UAS-p35	32	32	100	23.97	0.06	0.07	0.009
yw/Y;*tim*-G/+;+	54	30	56	25.32	0.11	0.01	0.001
yw/Y;*tim*-G/+;+/UAS-Myc, UAS-p35	69	21	30	24.77	0.07	0.01	0.001
w/Y;*tim*-G/+;+/UAS-p35	32	29	91	24.52	0.08	0.04	0.004
w/Y;*tim*-G/+;+//UAS-Myc, UAS-p35	64	49	77	24.06	0.05	0.04	0.003

w: w^{ISO31}*;yw: y*^{1}*,w*^{1118}*;tim*-G*: tim-Gal4;*TUG*: tim*-(UAS)-*Gal4;cry24*-G*: cry-Gal4* (line 24)*;pdf*-G*: pdf-Gal4*

Table 3. Summary of circadian locomotor rhythmicity in dMyc-overexpressing flies. FFT= fast Fourier transform

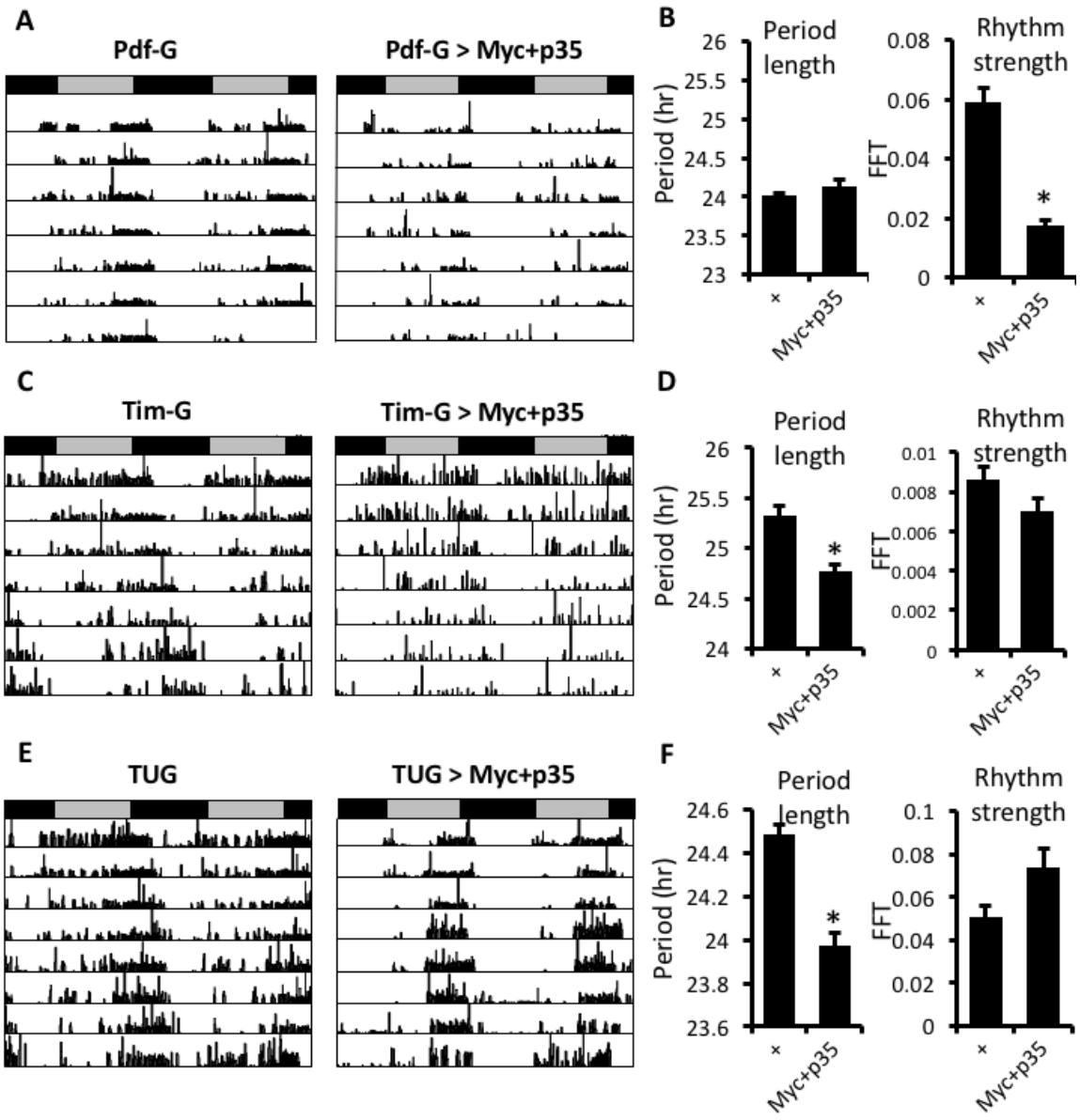

Figure 44. Circadian locomotor rhythmicity in dMyc-overexpressing flies.
(A, C, E) Representative actogram of Pdf-G and Pdf-G > Myc+p35 (A), Tim-G and Tim-G > Myc+p35 (C), TUG and TUG > Myc+p35 (E) flies. (B, D, F) Period length (determined by chi-square) and rhythm strength of Pdf-G and Pdf-G > Myc+p35 (B), Tim-G and Tim-G > Myc+p35 (D), TUG and TUG > Myc+p35 (F) flies. *$p < 0.05$ by Student's t test for Myc+p35 flies versus +.

expression is very limited, we subsequently used the *tim*-UAS-Gal4 (TUG) (Blau and Young, 1999) to expresses dMyc in other clock cells in addition to ventral lateral neurons. This TUG driver line has 5 UAS sites upstream of the transcription start site of *tim* promoter, so that Gal4 proteins produced downstream of *tim* promoter would positively regulate its own expression to diminish oscillatory *tim* promoter activity. However, overexpression of dMyc by TUG did not have any effect on either the period length or rhythm strength (Table 3 Fig. 44E, F). To express dMyc more broadly and at a higher level, *tim*-Gal4 driver was used. Overexpression of dMyc by *tim*-Gal4 causes a nearly 200- to 500-fold increase in *dMyc* transcripts in fly heads that peak at ZT 18, consistent with the peak expression of timeless transcript (Fig. 45) (Sehgal et al., 1995). Western blot also showed significantly increased dMyc protein in *tim*-Gal4> UAS-Myc+p35 flies compare to Gal4 or UAS controls (Fig. 45). Broader expression of dMyc by *tim*-Gal4 resulted in lower percentage of rhythmic flies (30%) compare to Gal4 control (56%) (Table 3, Fig. 44C, D). Notably, overexpression of dMyc by both TUG and *tim*-Gal4 shortens period length significantly, suggesting a possibility that Per expression might be affected by high level of dMyc since mutation of Per alters the period of circadian locomotor activity (Konopka and Benzer, 1971). Interestingly, use of both Cry24-Gal4 and Pdf-Gal4 driving dMyc expression (Cry24Pdf-G>Myc+p35) in ventral lateral neurons as well as Cry-expressing cells resulted in loss of rhythm in about 70% of the flies and weaker rhythm in the rhythmic flies (Table 3, Fig. 46A). These observations indicate that dMyc indeed affects *Drosophila* circadian behavior; however, the severity of perturbation on *Drosophila* circadian behavior appears to not correlate with the level of dMyc overexpression but instead where dMyc is expressed.

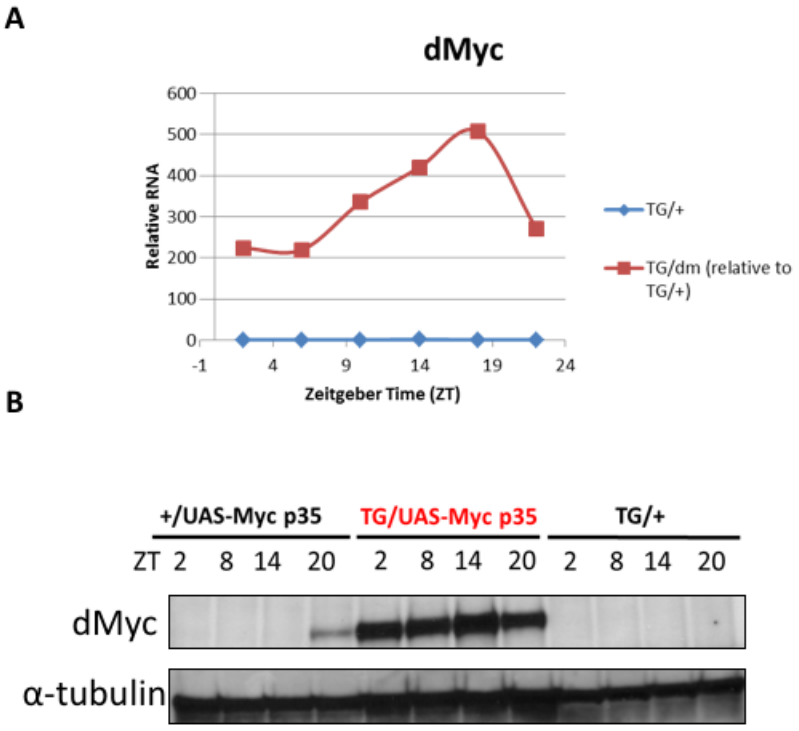

Figure 45. *Drosophila* Myc overexpression using Tim-Gal4 driver.
(A) Time series (every 4 hr) expression of dMyc mRNA (normalized to expression of actin*)* by quantitative real time PCR (qRT-PCR) and (B) dMyc protein by Western Blot from fly heads of Tim-Gal4/UAS-dMyc+p35 flies, Tim-Gal4/+ flies or UAS-Myc+p35/+ flies. α-tubulin serves as loading control. Flies were entrained in light-dark 12hr-12hr cycle for 3-5 days. On the last day of entrainment, flies were snapfrozen every 4-6 hour and the heads were used to extract mRNA or protein.

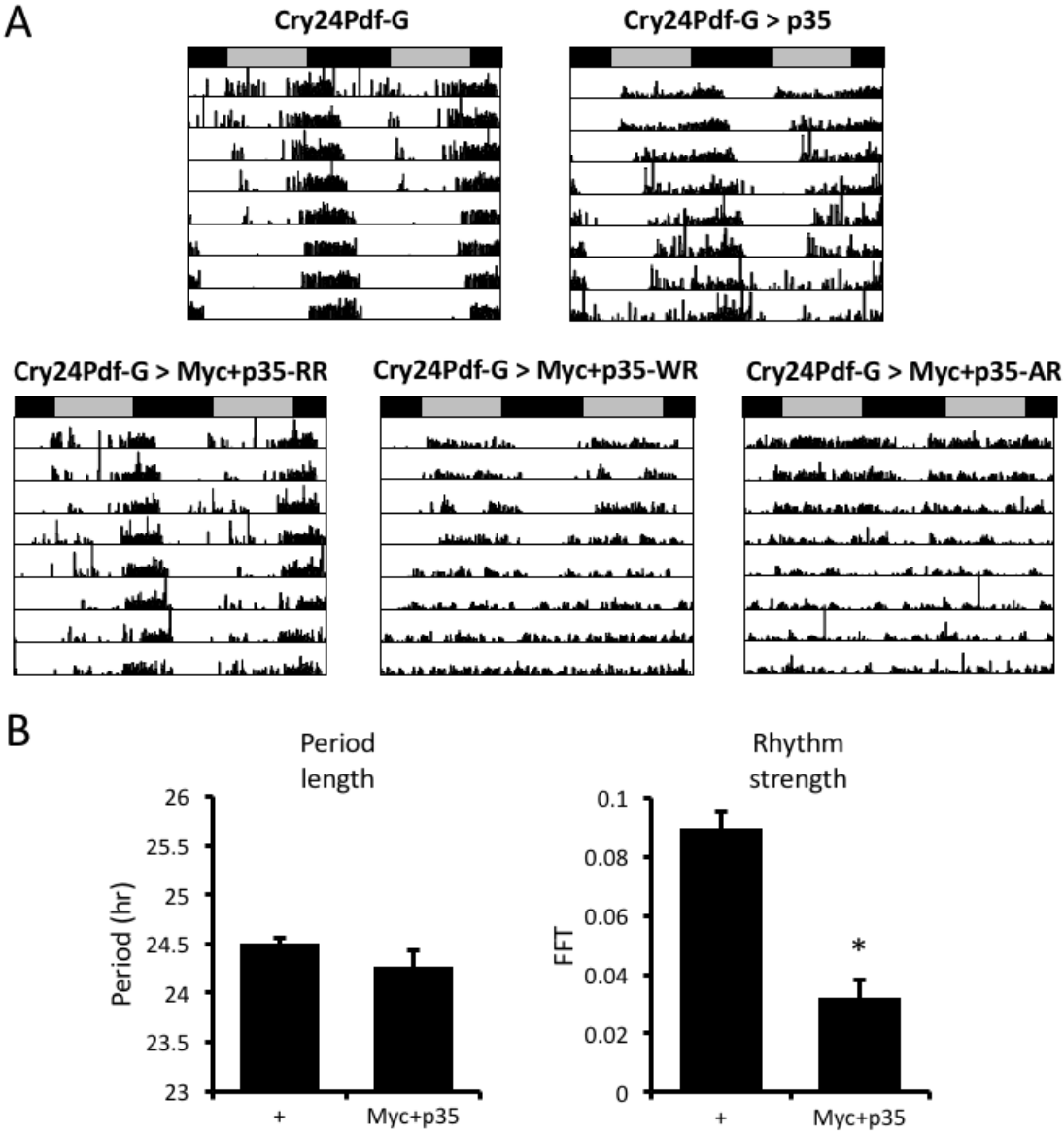

Figure 46. Circadian locomotor rhythmicity in dMyc-overexpressing flies.
(A, C, E) Representative actogram of Pdf-G and Pdf-G > Myc+p35 (A), Tim-G and Tim-G > Myc+p35 (C), TUG and TUG > Myc+p35 (E) flies. (B, D, F) Period length (determined by chi-square) and rhythm strength of Pdf-G and Pdf-G > Myc+p35 (B), Tim-G and Tim-G > Myc+p35 (D), TUG and TUG > Myc+p35 (F) flies. *$p < 0.05$ by Student's t test for Myc+p35 flies versus + (wild type).

Overexpressed dMyc induces negative regulators but does not suppress *clk*

To delineate the underlying mechanism of dMyc-mediated behavior perturbation, we first examined transcript levels of genes involved in the molecular clock in whole head extracts of *tim*-Gal4> UAS-Myc+p35 flies compared to Gal4 control flies. Consistent with what we observed in mammalian cancer cells (Fig. 9 and 16), dMyc induces most of the negative regulators, including *per*, *tim*, *vri* and *cwo* (Fig. 47A). Western blot from whole head lysates also demonstrated a significant increase in Per protein levels (Fig. 47B). However, *clk* mRNA is not suppressed but slightly induced by dMyc in these flies (Fig. 47A). Similarly, mRNA of *tim*, *cry* and *cwo* are induced in Cry24Pdf-G>Myc+p35 flies compare to control and *clk* is also not suppressed (Fig. 48). Our findings support the idea that dMyc indeed affects the molecular clock components in flies, however, *Drosophila clk* appears to be more resistant to dMyc overexpression than its homolog in mammalian cancer cells.

In Chapter 3, we provide evidence that MYC suppresses *BMAL1* through upregulation of *REV-ERBα*. Interestingly, *Drosophila REV-ERBα* homolog *E75* has recently been identified and observed to analogously suppress *clk* (Kumar et al., 2014). We sought to determine whether dMyc regulates *E75* in flies by examining the mRNA levels of all four isoforms of *E75*. To our surprise, transcript levels of all isoforms of *E75* are unchanged in Cry24Pdf-G>Myc+p35 flies compared to control (Fig. 49), suggesting that MYC-REV-ERB*α*-BMAL1 regulation that we observed in mammalian cancer cells is not conserved in *Drosophila*.

A

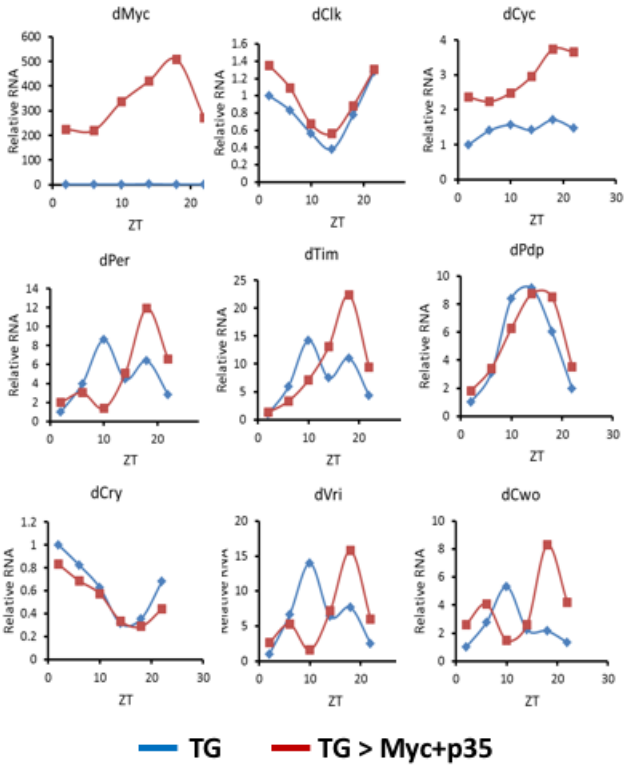

B

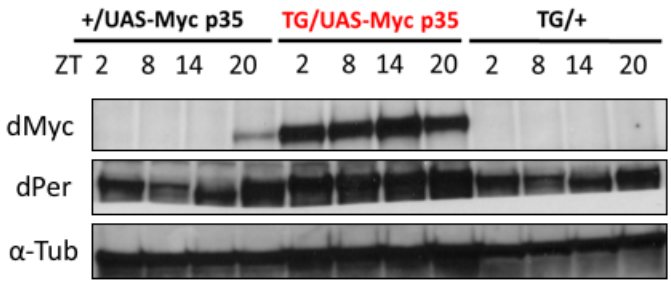

Figure 47. dMyc overexpression alters circadian genes expression using Tim-Gal4 driver.

(A) Time series (every 4 hr) expression of dMyc and core clock genes by qRT-PCR in heads of TG/+ and TG/Myc+p35 flies (B) dMyc and dPer protein level determined by Immunoblot in heads of TG/Myc+p35 flies compare to TG/+ and +/UAS-Myc p35 flies. Flies were entrained in light-dark 12hr-12hr cycle for 3-5 days. On the last day of entrainment, flies were snapfrozen every 4-6 hour and the heads were used to extract mRNA or protein.

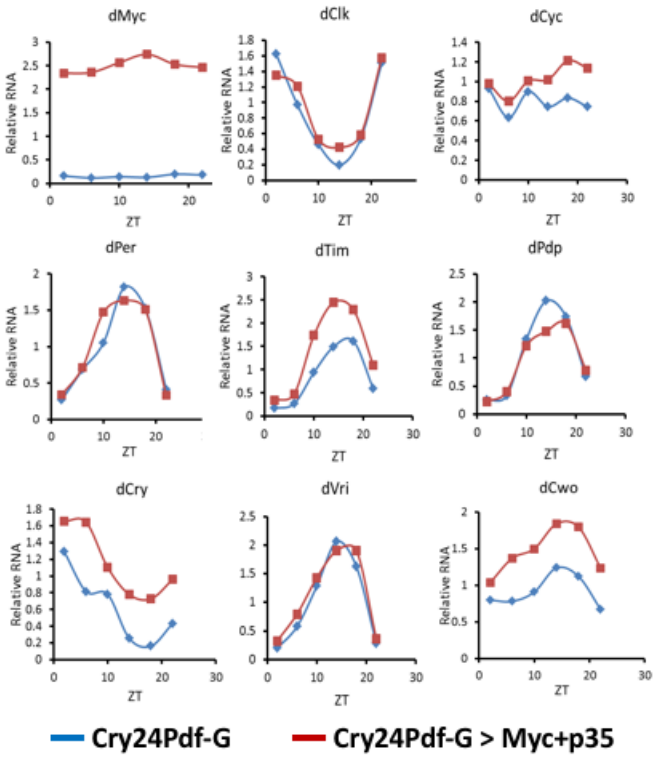

Figure 48. dMyc overexpression alters circadian genes expression using Cry24Pdf-Gal4 driver.

Time series (every 4 hr) expression of dMyc and core clock genes by qRT-PCR in heads of Cry24Pdf-G/+ and Cry24Pdf-G/Myc+p35. Flies were entrained in light-dark 12hr-12hr cycle for 3-5 days. On the last day of entrainment, flies were snapfrozen every 4-6 hour and the heads were used to extract mRNA.

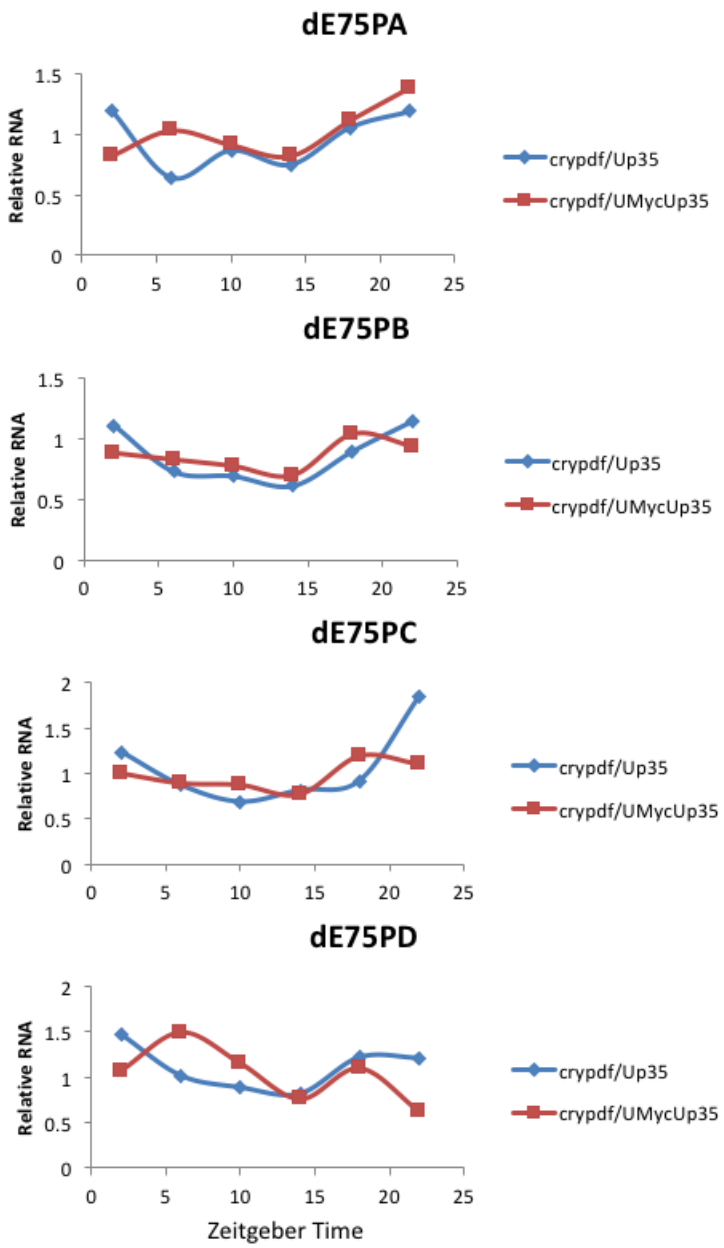

Figure 49. dMyc overexpression does not affect dE75 expression using Cry24Pdf-Gal4 driver

Time series (every 4 hr) expression of four isoforms of *Drosophila* REV-ERBα homolog dE75 (dE75PA, dE75PB, dE75PC, dE75PD) by qRT-PCR in heads of Cry24Pdf-G/+ versus Cry24Pdf-G/Myc+p35. Flies were entrained in light-dark 12hr-12hr cycle for 3-5 days. On the last day of entrainment, flies were snapfrozen every 4-6 hour and the heads were used to extract mRNA or protein.

dMyc overexpressing flies showed shortening of PDF dorsal projection

The minor change of *clk* mRNA expression upon dMyc overexpression is insufficient to explain the dramatically increased arrhythmicity that we observed in Cry24Pdf-G>Myc+p35 flies. Since dMyc affects cell growth and apoptosis, we next examined the morphology of the ventral lateral neurons, which can be visualized by PDF staining through immunohistochemistry (IHC) of fly brain. While there is no gross abnormalities of the cell bodies of both large ventral lateral neurons (l-LNvs) and small ventral lateral neurons (s-LNvs), we noted shortening of the dorsal projections (Fig. 50, arrows) from s-LNvs in Cry24Pdf-G>Myc+p35 flies compare to control (Fig. 50). Interestingly, shortening of the dorsal projections from sLNvs has been observed in both *clk* mutant flies and *cyc* mutant flies (Park et al., 2000), suggesting Clk-mediated PDF expression or clock neuron development is likely to be affected in these flies. We also assayed Per protein expression in fly brain, however, no difference in Per protein expression was observed (Fig. 50)

dMyc overexpression does not affect axonal development

To further investigate whether the shortening of the dorsal projections from sLNvs is due to defects of axonal development, we took advantage of the marker UAS-mCD8-GFP, which is a fusion protein of mouse lymphocyte marker CD8 and the green fluorescence protein (GFP) (Lee and Luo, 1999). Since mCD8 is a transmembrane protein, it labels the cell surface, particularly axons and dendrites due to their high surface area. Recombining UAS-mCD8-GFP with either UAS-p35 or UAS-Myc;UAS-p35 flies and then crossing

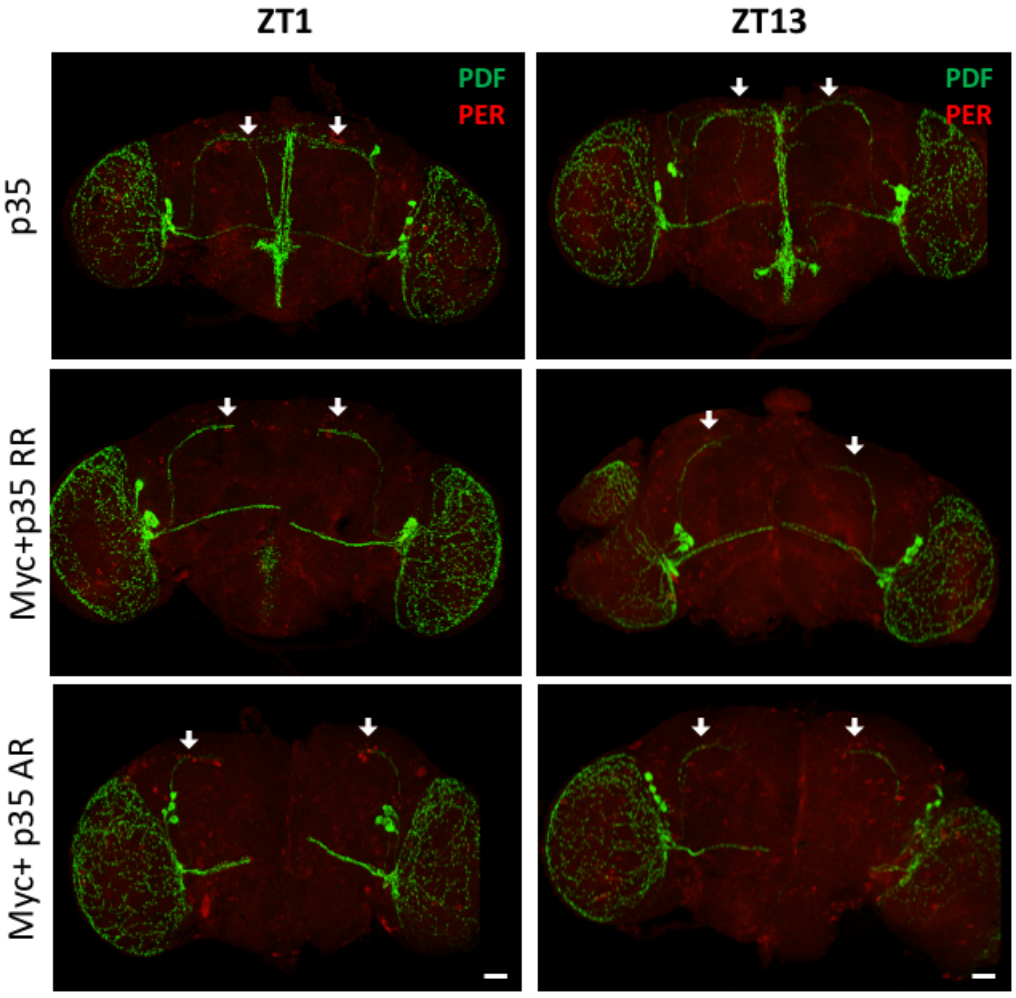

Figure 50. dMyc overexpression decreases PDF immunostaining of the s-LNv dorsal projections.

Representative confocal image of brains dissected from control flies (CryPdfG > p35), rhythmic (RR) or arrhythmic (AR) dMyc-overexpressing flies (CryPdfG > Myc+p35) subjected to immunofluorescence staining using antibodies directed against the PDF (green) and PER (red) proteins at ZT1 and ZT13. *arrows:* dorsal projections from s-LNvs. Scare bars, 40 µm.

with Cry24Pdf-G drivers allows us to visualize neuronal processes of Cry and Pdf expressing cells in dMyc overexpressing flies versus control flies. Consistent with our IHC data, Cry24Pdf-G>Myc+p35 flies exhibit shorter dorsal projections from sLNvs with less intense PDF staining (Fig. 51). In contrast, we found that there is no difference in abundance of mCD8-labeling axons/dendrites (Fig. 51, white rectangle), suggesting dMyc overexpression does not affect overall axonal development from Cry and Pdf expressing cells, instead, specifically reduce PDF staining at the dorsal projections.

Overexpressed dMyc alters metabolism in fly head

As mentioned in Chapter 1, MYC orchestrates a number of metabolic pathways. In addition, alteration of cellular energetic status, such as the ratio of NAD+/NADH or ATP/AMP was shown to feed back to the circadian clock (Lamia et al., 2009; Rutter et al., 2001). We thus hypothesized that overexpression dMyc by Cry24Pdf-Gal4 alters metabolism in fly heads, which in turns contributes to increased arrhythmic behavior in these flies. Cry24Pdf-G>Myc+p35 and control flies were snapfrozen in dry ice at different Zeitgeber Times after entrainment. Polar metabolites in fly heads were extracted by methanol-chloroform, derivatized by MTBSTFA and analyzed by gas chromatography mass spectrometry (GC-MS). While the majority of amino acids do not change with dMyc overexpression, we noted that the concentration of valine, leucine and glutamine is significantly reduced (Fig. 52). In addition, significant increase of urea (3-5 folds) and acetic acid is observed in Cry24Pdf-G>Myc+p35 flies compare to control (Fig. 52). The observations support the idea that dMyc plays a previously unknown role in regulating

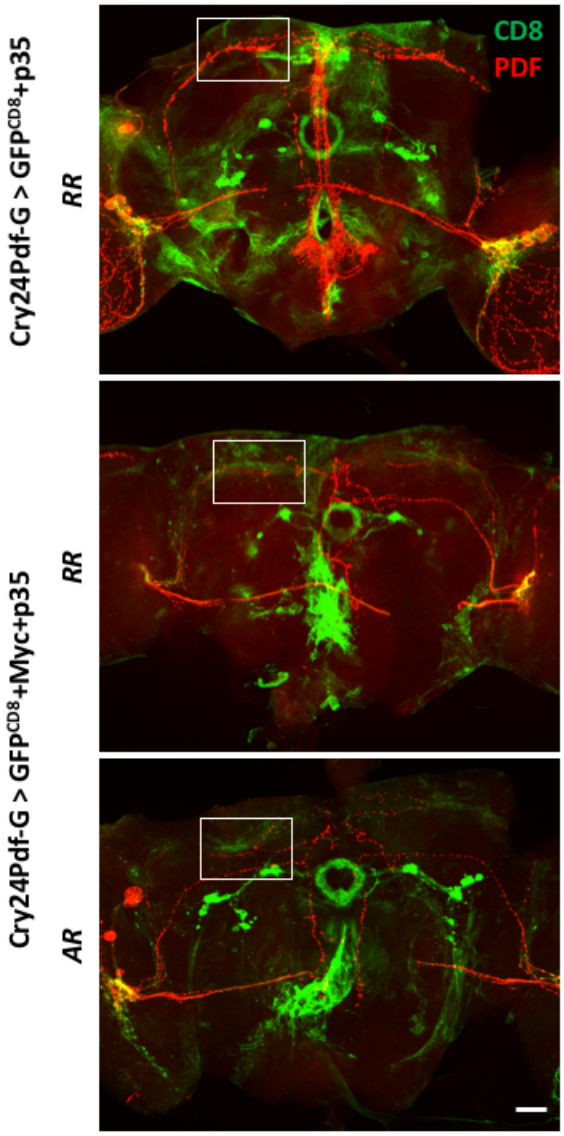

Figure 51. dMyc overexpression does not alter neuronal processes from the s-LNvs.

Representative confocal image of brains dissected from control flies (CryPdfG > GFP^{CD8}+p35), rhythmic (RR) or arrhythmic (AR) dMyc-overexpressing flies (CryPdfG > GFP^{CD8}+Myc+p35) subjected to immunofluorescence staining using antibodies directed against the PDF (red). *rectangle:* dorsal projections from s-LNvs. Scare bars, 40 µm.

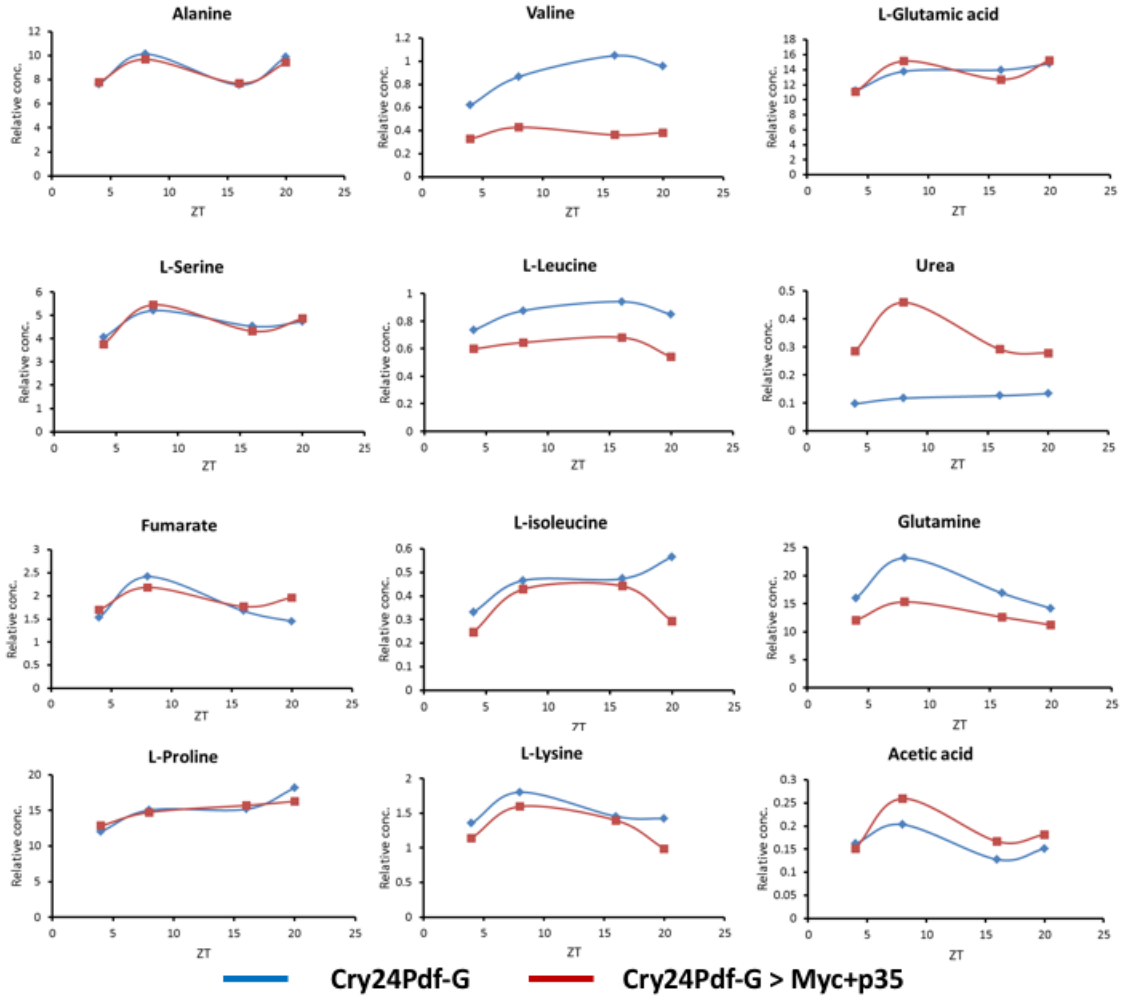

Figure 52. dMyc overexpression leads to decreased branch-chain amino acids and increased urea.

Polar metabolites analyzed by GC-MS in heads of Cry24Pef/+ or Cry24Pdf > Myc+p35 flies collected every 6 hour. Flies were entrained in light-dark 12hr-12hr cycle for 3-5 days. On the last day of entrainment, flies were snapfrozen every 6 hour and the heads were used to extract metabolites.

metabolism despite the fact that its expression is limited to Cry- and Pdf- expressing cells. However, further investigations are required to determine whether this alteration of metabolism mediates dMyc-induced arrhythmic behavior in flies.

Hypomorphic dMyc flies exhibit arrhythmic behavior

As we mentioned in previous chapters, an earlier study documented that endogenous mouse *Myc* exhibits circadian expression that is regulated by *Per2* (Fu et al., 2002). Loss of *Per2* in mouse leads to loss of *Myc* oscillation, which eventually leads to tumorigenesis (Fu et al., 2002). But how endogenous MYC affects circadian clock remains poorly understood. Loss of dMyc has been associated with small body size; however, little is known about whether dMyc is indispensable for circadian behavior. To study whether loss of dMyc affects *Drosophila* circadian locomotor behavior, we took advantage of several available dMyc mutants, including the the hypomorphic Myc fly (dm^{P0}, a result of insertion of a P-element within 100bp upstream of the transcription start site of dMyc) and a Myc null fly (dm^{4}, a result of deletion of the first two exons) (Fig. 53A) (Pierce et al. 2004, Development). dm^{P0}/Y flies are viable but exhibit smaller body size (Fig. 53B) compare to its sibling control *w*/Y, however, dm^{4} flies are lethal at early larva stage (Johnston et al., 1999). When we assayed the circadian locomotor behavior of dm^{P0}/Y compare to its sibling control *w*/Y, we found that while control flies exhibit robust circadian locomotor behavior, hypomorphic Myc flies displayed bimodal distribution in rhythmicity where about a third of flies were rhythmic, a third of flies were arrhythmic and the rest of flies were weakly rhythmic (Fig. 53C). Even among the

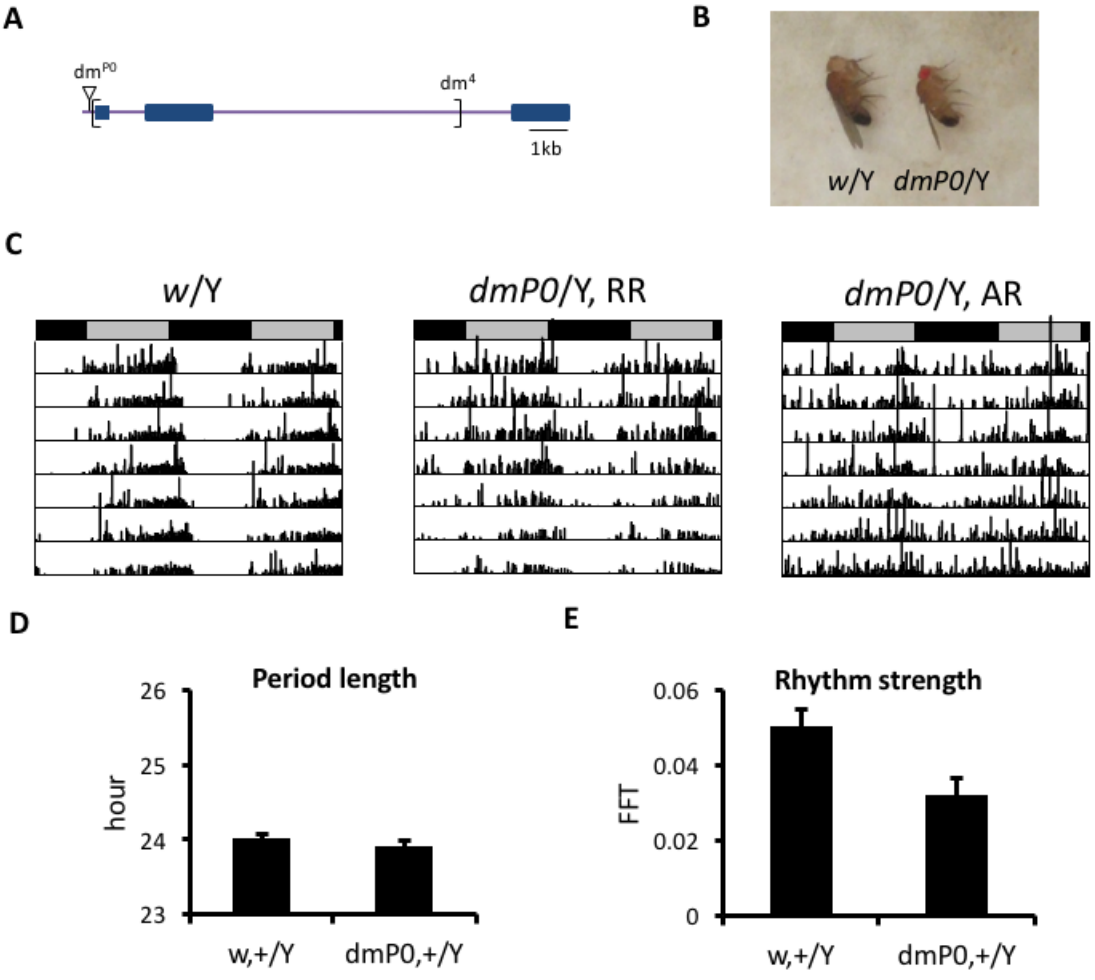

Figure 53. Hypomorphic dMyc flies exhibit dichotomous rhythmicity.
(A) Schematic illustration of the genetic strategy for engineering dMyc hypomorph dm^{P0} flies and dMyc null fly dm^{4}. Illustration is modified from Pierce *et al.* 2004, *Development* (B) picture of dmP0/Y fly versus its sibling control w/Y. (C) Representative actogram of w/Y, rhythmic (RR) dm^{P0}/Y and arrhythmic (AR) dm^{P0}/Y. (D, E) Period length (D) and rhythm strength of rhythmic dm^{P0}/Y flies compare with control flies w/Y.

rhythmic dm^{P0}/Y flies, rhythm strength also significantly decreased compare to sibling controls (Fig. 53E).

dMnt mutation rescues arrhythmicity of dMyc mutant flies

To verify the arrhythmic behavior in dm^{P0}/Y flies is due to lower dMyc activity, we sought to determine whether mutation of the dMyc repressor *Drosophila* Mnt in dMyc mutant background is able to rescue the arrhythmic phenotype. *Drosophila* Mnt (dMnt) is a homolog of mammalian MNT and is a member of the Mxd family. Mnt and other members in the Mxd family antagonize Myc function by dimerizing with Myc-binding partner Max and recruit mSin3 co-repressor (Hooker and Hurlin, 2006). The E-box within the promoter of a canonical Myc target gene ornithine decarboxylase (Odc) is bound by Mnt-Max complex in quiescent cells but is occupied by Myc-Max complex instead in proliferating cells (Nilsson et al., 2004). Knockdown Mnt using shRNA has been shown to accelerate cell proliferation even in Myc-null cells (Nilsson et al., 2004). Loss of dMnt in dMyc-null flies is also able to rescue growth arrest from the early larval stage to pupal stage (Pierce et al., 2008). These published data support a model in which Mnt-Max complex normally binds and represses Myc target genes and this repression can be relieved by overexpressing Myc or loss of Mnt.

Because dm^{4}/Y and $dm^{4}dmnt^{1}$/Y cannot form adult flies, we crossed dMyc male hypomorph flies (dm^{P0}/Y) with wild type female (W^{ISO31}), dMyc null female (dm^{4}/FM7) and dMyc null female with dMnt mutation ($dm^{4}dmnt^{1}$/FM7) to generate female

heterozygotes dm^{P0}/+, dm^{P0}/dm^{4} and $dm^{P0}/dm^{4}dmnt^{1}$, respectively. *dMyc* transcripts increase about 3-fold in fly heads from dm^{P0}/+ flies compared with dm^{P0}/dm^{4} flies (Fig. 54A). Unlike overexpressed dMyc protein, endogenous dMyc protein was not detectable either in fly heads from dm^{P0} or dm^{P0}/ dm^{4} flies with the anti-dMyc antibody (Fig. 54B). To determine the effects of the varying degrees of Myc activity possessed by our flies, we next examined their circadian locomotor behavior in these in constant darkness after entrainment. As expected, dm^{P0}/dm^{4} flies exhibit significantly reduced rhythmicity compare to dm^{P0}/Y flies (30% versus 94%) (Fig. 55A). Similar to dMyc hypormorphic dm^{P0}/Y flies, dm^{P0}/dm^{4} flies exhibit bimodal distribution of rhythmicity where 47% of flies are arrhythmic while 30% of flies remain rhythmic (Fig. 55A). Strikingly, dMnt mutation in dm^{4} background reduced the arrhythmicity from 47% down to 7% (Fig. 55A). There is no difference in period length between three female heterozygotes but rhythm strength of rhythmic flies is significantly reduced in dm^{P0}/dm^{4} flies and rescued in $dm^{P0}/ dm^{4}dmnt^{1}$ flies (Fig. 55C, D).

Molecular clock is not affected in dMyc mutant flies

To explore the underlying mechanism of arrhythmic behavior in dm^{P0}/dm^{4} flies, we first examined whether the transcripts levels of circadian clock components are altered in these flies. Interesting, despite a two-third reduction in *dMyc* mRNA expressed in the heads of dm^{P0}/dm^{4} flies (both rhythmic and arrhythmic flies), the mRNA level of most molecular clock components is not changed (Fig. 56). Since overexpressed dMyc elevates PER protein level (Fig. 47), we further assayed PER level by western blot in

A

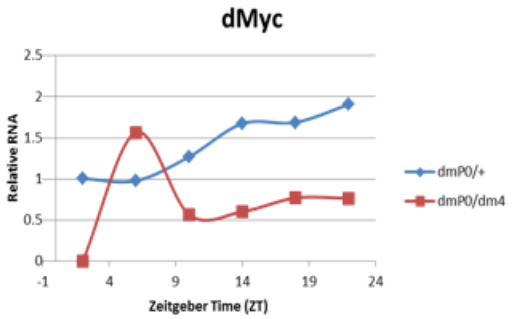

B

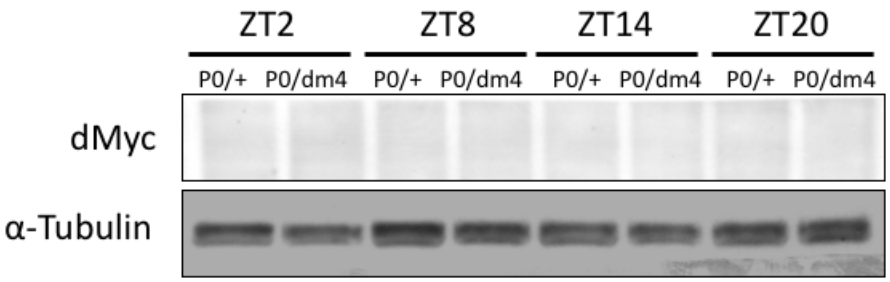

Figure 54. Endogenous *Drosophila* Myc level in Myc hypomorph flies.
(A) Time series (every 4 hr) expression of dMyc mRNA (normalized to expression of actin*)* by quantitative real time PCR (qRT-PCR) and (B) dMyc protein by Western Blot from fly heads of dmP0/+ or dm^{P0}/dm^{4} flies. α-tubulin serves as loading control. Flies were entrained in light-dark 12hr-12hr cycle for 3-5 days. On the last day of entrainment, flies were snapfrozen every 4-6 hour and the heads were used to extract mRNA or protein.

A

	RR	%	WR	%	AR	%	Total number
dmP0/+	29	94	2	6	0	0	31
dmP0/dm4	9	30	7	23	14	47	30
dmP0/dm4dmnt	19	63	9	30	2	7	30

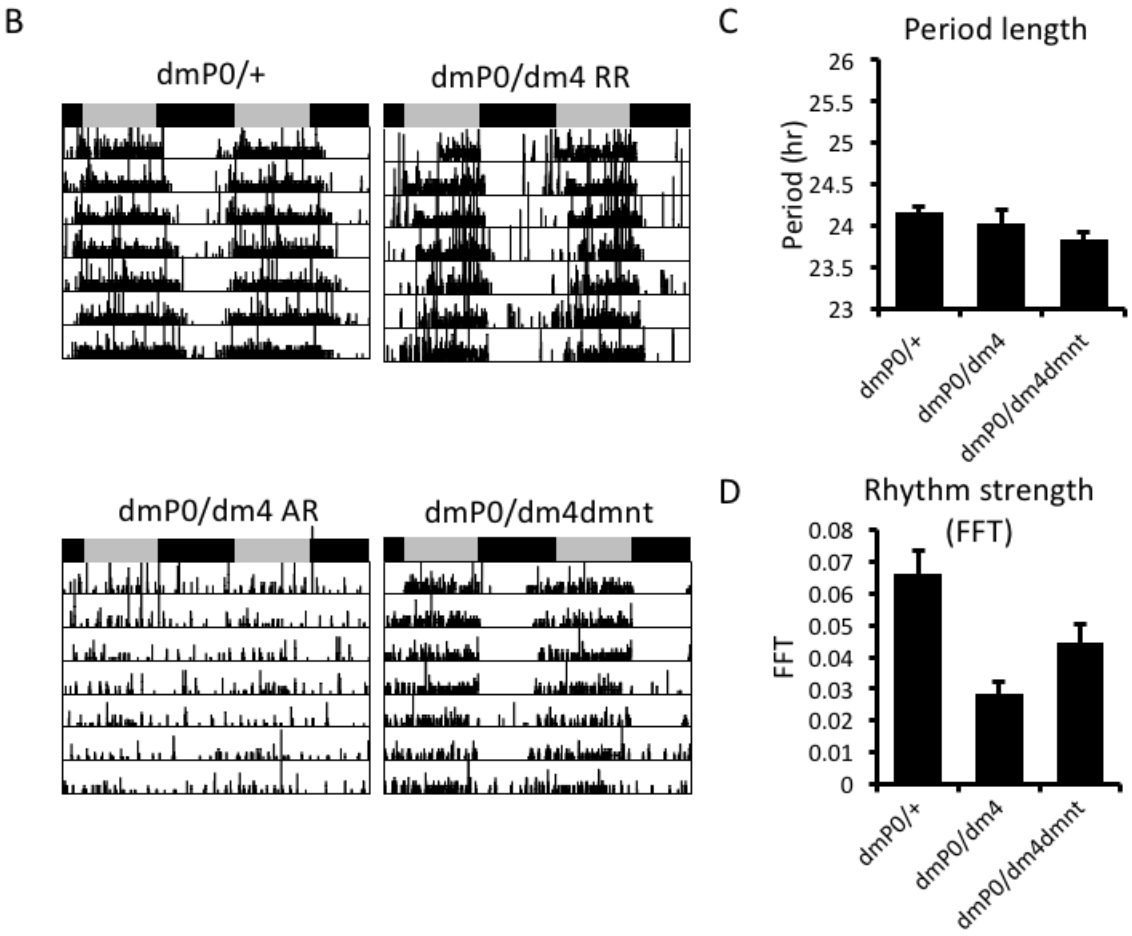

Figure 55. Hypomorphic dMyc flies exhibit dichotomous rhythmicity and can be rescued by dMnt mutation.

Summary of the circadian locomotor rhythmicity (A), period length (C) and rhythm strength (D) of dm^{P0}/+, dm^{P0}/dm^{4} and $dm^{P0}/dm^{4}dmnt^{1}$ flies. (B) Representative actogram of the dm^{P0}/+ rhythmic, dm^{4}/dm^{P0} rhythmic (RR) and arrhythmic (AR) and $dm^{P0}/dm^{4}dmnt^{1}$ rhythmic flies.

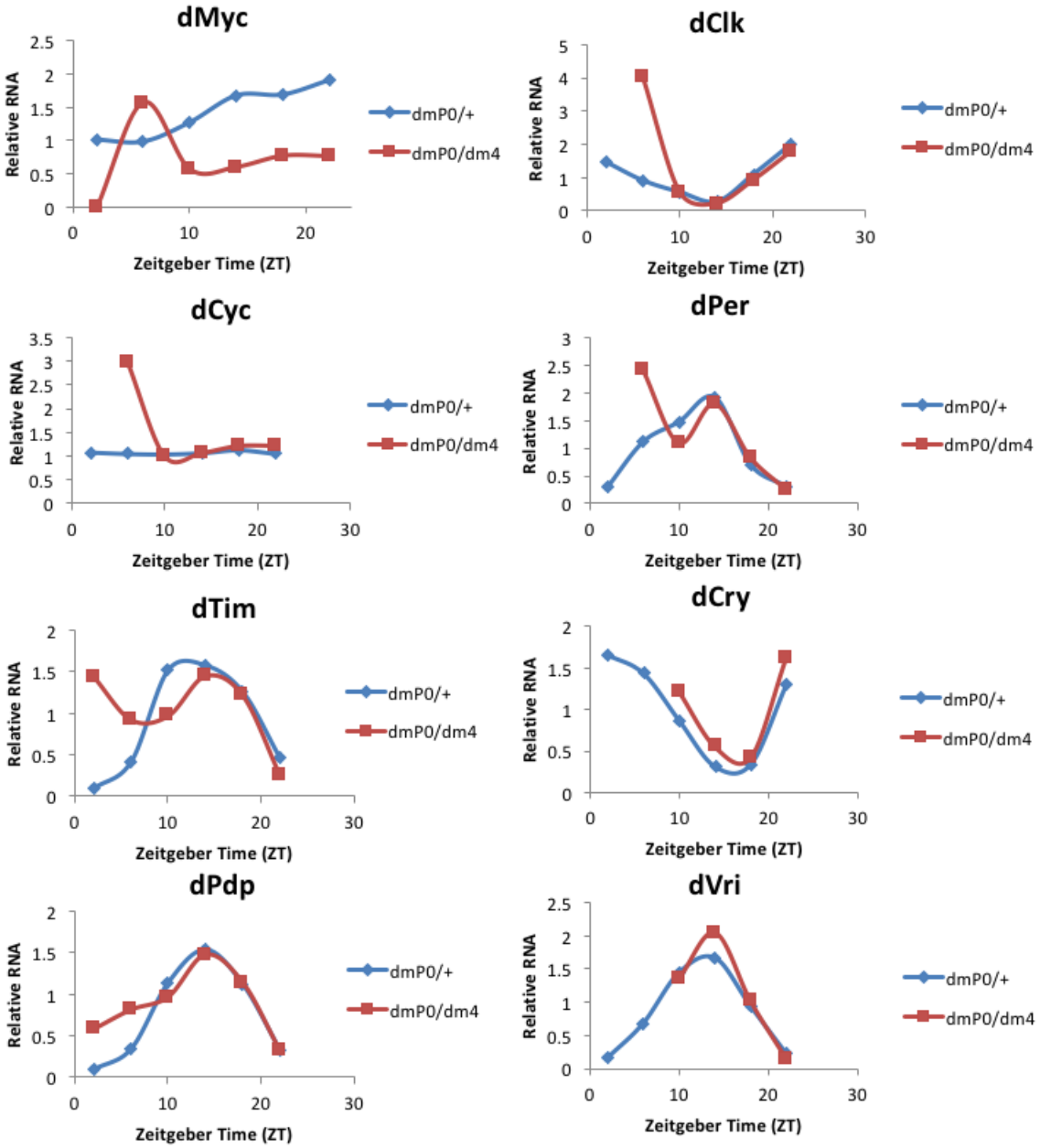

Figure 56. Loss of dMyc minimally alter circadian genes expression.
Time series (every 4 hr) expression of dMyc and core clock genes by qRT-PCR in heads of dm^{P0}/+ and dm^{P0}/dm^{4} flies. Flies were entrained in light-dark 12hr-12hr cycle for 3-5 days. On the last day of entrainment, flies were snapfrozen every 4-6 hour and the heads were used to extract mRNA.

dm^{P0}/+ and dm^{P0}/dm^{4} flies. However, there are no significant difference in PER protein expression between dm^{P0}/+ and dm^{P0}/dm^{4} flies (Fig. 57). Together, these results suggest that molecular clock expression is not affected in dm^{P0}/dm^{4} flies compare to dm^{P0}/+ control.

Loss of dMyc resulted in reduced sLNv Per expression in arrhythmic hypomorphic flies

As mentioned before, ventral lateral neurons are central clock cells in *Drosophila* that are crucial for maintaining rhythmic behavior in constant darkness. To investigate whether the clock protein oscillation is indeed unaffected in ventral lateral neurons, particularly in those arrhythmic flies, we compare PER protein in dissected fly brain from dm^{P0}/+, dm^{P0}/dm^{4} rhythmic, dm^{P0}/dm^{4} arrhythmic and $dm^{P0}/dm^{4}dmnt^{1}$ flies using immunohistochemistry. We focused on small ventral lateral neurons (sLNvs), because their Per expression is cyclic with nuclear Per expression reaching its peak at CT2 and minimum at CT14. At CT2, nuclear Per accumulation in sLNvs was dramatically reduced in arrhythmic dm^{P0}/dm^{4} flies but not in rhythmic dm^{P0}/dm^{4} flies relative to dm^{P0}/+ flies (Fig. 58). The reduced Per nuclear accumulation was also rescued in $dm^{P0}/dm^{4}dmnt^{1}$ flies (Fig. 58). We noticed similar pattern at CT20, where pan-cellular Per expression is the lowest in arrhythmic dm^{P0}/dm^{4} flies compare to its rhythmic dm^{P0}/dm^{4} siblings, dm^{P0}/+ and $dm^{P0}/dm^{4}dmnt^{1}$, suggesting that the decreased Per nuclear accumulation at CT2 in arrhythmic dm^{P0}/dm^{4} is not due to asynchrony, but overall decrease in Per expression at

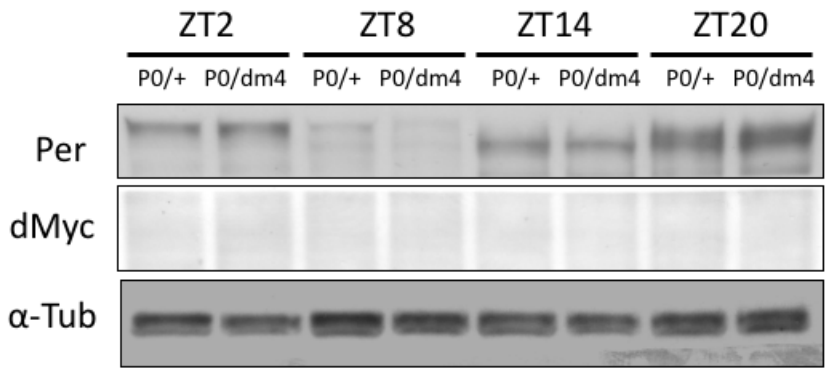

Figure 57. Loss of dMyc does not alter Per protein level from fly heads.
(A) dMyc and dPer protein level determined by Immunoblot in heads of dm^{P0}/+ and dm^{P0}/dm^{4} flies. Flies were entrained in light-dark 12hr-12hr cycle for 3-5 days. On the last day of entrainment, flies were snapfrozen every 6 hour and the heads were used to extract protein.

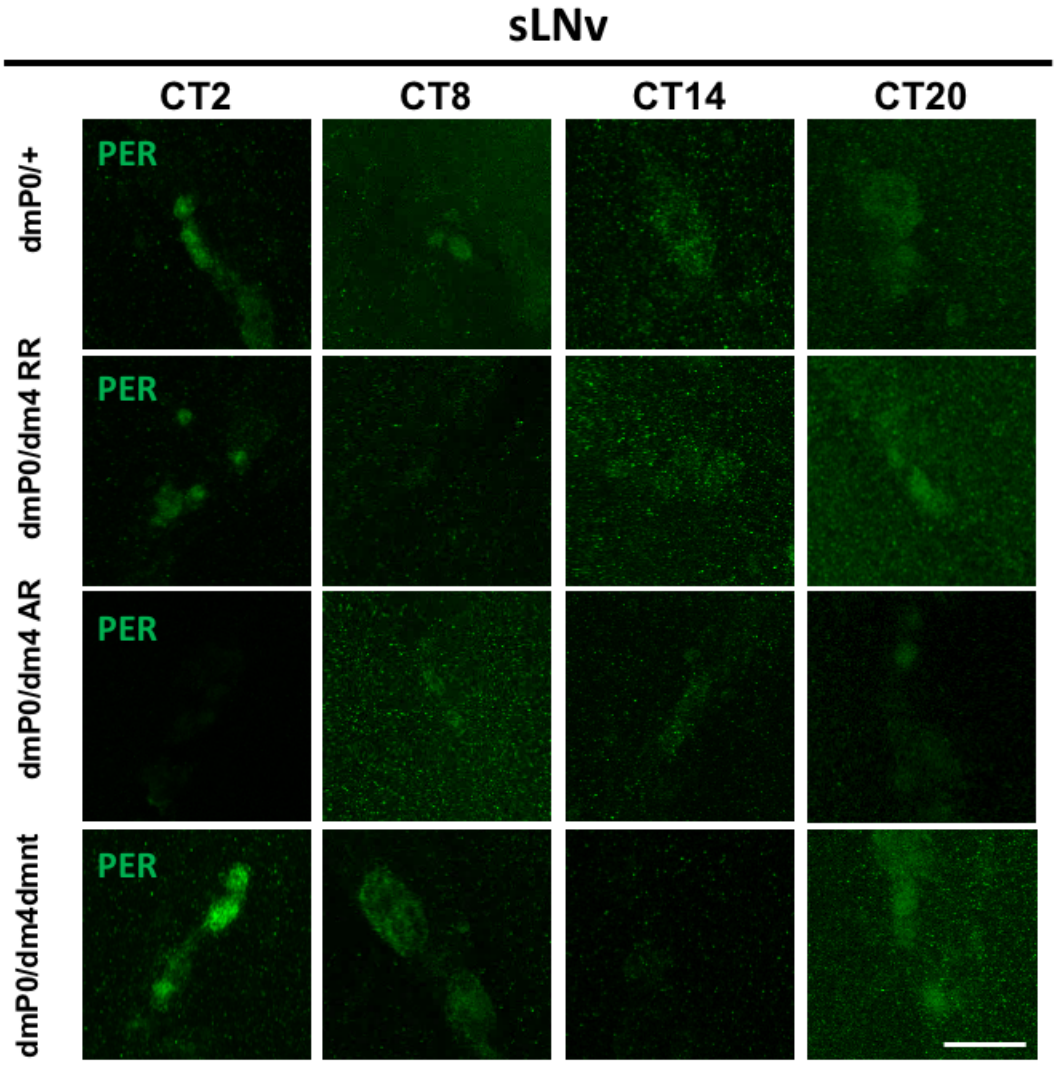

Figure 58. Loss of dMyc leads to reduced Per staining in sLNvs
Representative confocal image of brains dissected from dm^{P0}/+ rhythmic, dm^{4}/dm^{P0} rhythmic (RR) and arrhythmic (AR) and $dm^{P0}/dm^{4}dmnt^{1}$ rhythmic flies subjected to immunofluorescence staining using antibodies directed against the Per (green) proteins at CT2, 8, 14 and 20. Scare bars, 20 µm. Flies were entrained in light-dark 12hr-12hr cycle for 3 days, transferred to constant darkness (DD). Brains were dissected on DD day 4.

all time points. Our data therefore support that loss of dMyc attenuates Per expression in sLNvs in a subset of flies, contributing to their arrhythmic behavior.

Discussion

Many crucial functions of Myc are well-conserved in *Drosophila*, including regulation of growth, cell size and metabolism (Gallant, 2013). Myc's interaction with other members in the Myc family remains critical in target gene regulation, including its antagonism by dMnt (Pierce et al., 2008). In this chapter, we provide evidence that *Drosophila* Myc (dMyc) also plays a role in modulating circadian locomotor behavior in flies. We showed that overexpressing Myc in clock cells using Pdf-Gal4, *tim*-UAS-Gal4 and *tim*-Gal4 generally causes decrease of rhythm strength in rhythmic flies. Overexpressed dMyc induces mRNA level of several negative regulators and also induces PER protein expression. However, unlike Myc overexpression in mammalian cancer cells, overexpressed dMyc did not suppress *Drosophila clk* mRNA expression. We noticed that overexpressing dMyc specific in Pdf and Cry expressing cells resulted in loss of rhythm in more than 30% of flies. Although *clk* transcript level was not significantly altered in these flies, morphological analysis showed significant reduction of PDF expression in the dorsal projections from sLNvs, suggesting the molecular clock output PDF is affected by overexpressed dMyc. In addition, metabolomics analysis showed decrease of valine, leucine and glutamine and an increase in urea and acetate levels in heads of Cry24Pdf-G>Myc+p35 flies compare to controls. Together, our data indicated that overexpressed dMyc affects drosophila circadian behavior through both direct regulation of the

molecular clock expression as well as indirect regulation of clock output PDF and metabolite levels that feedback upon the clock.

Unlike the molecular clock in mammalian cancer cells suppressed by overexpressing Myc shown in Chapter 3, *Drosophila* circadian clock appears to be relatively resistant to elevated dMyc level. With over 200 to 500-fold *dMyc* transcript and significant elevation of dMyc protein in *tim*-G>Myc+p35 flies, the percentage of rhythmic flies only drops from 56% to 30%. Cry24Pdf-G>Myc+p35 flies showed a severely arrhythmic phenotype; however, *dMyc* transcript was only 3 folds higher than controls, suggesting dMyc-mediated disruption of circadian behavior in flies is dependent on where dMyc is expressed rather than on how much dMyc is expressed. The differences in consequences of Myc overexpression in cancer cells and Drosophila could be due to compensation and intact antagonistic regulation occurring in the whole organism.

The metabolic alteration we observed in Cry24Pdf-G>Myc+p35 flies is very interesting. With limited dMyc expression in specific cell groups, the reduction in valine, leucine and the accumulation of urea is surprising in its magnitude. A recent study observed a dramatically reduction of BCAA, particularly valine and leucine, in Arginase (Arg1)-deficient mice (Sin et al., 2013). Arginase is a rate-limiting enzyme in urea cycle, converting arginine to ornithine and urea. Correspondingly, Arg1-deficient mice exhibit hyperargininemia and hyperammonia. Although we did not observe hyperargininemia and hyperammonia in our fly heads, the accumulation of urea in fly heads suggests high urea cycle flux. However, further investigation is required to determine whether this metabolic alteration is correlated with loss of rhythm in Cry24Pdf-G>Myc+p35 flies.

Although overexpressing dMyc does not seem to recapitulate overexpressing mammalian MYC in cancer cells, our observation of increased arrhythmicity in dMyc mutant flies suggests that endogenous dMyc is critical for maintaining rhythmic behavior. Loss of Per expression in arrhythmic dMyc hypomorph flies suggest endogenous dMyc may serve to maintaining basal level of Per expression, the loss of which results in arrhythmic behavior (Konopka and Benzer, 1971). Interestingly, loss of dMyc does not ablate either rhythmicity or Per expression in all progenies, instead, we observe a dichotomous distribution of rhythmicity as well as Per expression. We speculate that normally dMyc is responsible for maintaining Per level that is sufficient to maintain rhythmic behavior. However, in dMyc mutant flies, low dMyc level fails to maintain Per level and Per expression level and rhythmicity is thereby determined by other factors. The observation of biphasic response of E2F to low level Myc induction from a recent study shed a light on this underappreciated gene regulation by MYC (Wong et al., 2011). In this study, single cell measurement of viral-mediated MYC overexpression showed that full activation of E2F only occurs within a very narrow range of Myc level. However, a broad distribution of E2F response occurs when MYC level is either too high or too low. We suspect that in dMyc mutant fly, there is a possible biphasic response of Per, which in turns lead to a dichotomous distribution of rhythmicity. However, further studies are needed to delineate the quantitative relationship between MYC and Per expression.

Reference

Baggs, J.E., Price, T.S., DiTacchio, L., Panda, S., Fitzgerald, G.A., and Hogenesch, J.B. (2009). Network features of the mammalian circadian clock. PLoS biology *7*, e52.

Balsalobre, A., Damiola, F., and Schibler, U. (1998). A serum shock induces circadian gene expression in mammalian tissue culture cells. Cell *93*, 929-937.

Bass, J. (2012). Circadian topology of metabolism. Nature *491*, 348-356.
Beckonert, O., Keun, H.C., Ebbels, T.M., Bundy, J., Holmes, E., Lindon, J.C., and Nicholson, J.K. (2007). Metabolic profiling, metabolomic and metabonomic procedures for NMR spectroscopy of urine, plasma, serum and tissue extracts. Nature protocols *2*, 2692-2703.

Benjamini, Y., and Hochberg, Y. (1995). Controlling the false discovery rate: a practical and powerful approach to multiple testing. Journal of the Royal Statistical Society Series B *57*, 289–300.
Beroukhim, R., Mermel, C.H., Porter, D., Wei, G., Raychaudhuri, S., Donovan, J., Barretina, J., Boehm, J.S., Dobson, J., Urashima, M.*, et al.* (2010). The landscape of somatic copy-number alteration across human cancers. Nature *463*, 899-905.

Blau, J., and Young, M.W. (1999). Cycling vrille expression is required for a functional Drosophila clock. Cell *99*, 661-671.

Bligh, E.G., and Dyer, W.J. (1959). A rapid method of total lipid extraction and purification. Canadian journal of biochemistry and physiology *37*, 911-917.

Boon, K., Caron, H.N., van Asperen, R., Valentijn, L., Hermus, M.C., van Sluis, P., Roobeek, I., Weis, I., Voute, P.A., Schwab, M.*, et al.* (2001). N-myc enhances the expression of a large set of genes functioning in ribosome biogenesis and protein synthesis. The EMBO journal *20*, 1383-1393.

Borchers, H.W. (2015). pracma: Practical Numerical Math Functions. R package version 1.8.3., http://CRAN.R-project.org/package=pracma.

Brodeur, G.M., Seeger, R.C., Schwab, M., Varmus, H.E., and Bishop, J.M. (1984). Amplification of N-myc in untreated human neuroblastomas correlates with advanced disease stage. Science *224*, 1121-1124.

Bugge, A., Feng, D., Everett, L.J., Briggs, E.R., Mullican, S.E., Wang, F., Jager, J., and Lazar, M.A. (2012). Rev-erbalpha and Rev-erbbeta coordinately protect the circadian clock and normal metabolic function. Genes & development *26*, 657-667.

Canto, C., and Auwerx, J. (2011). NAD+ as a signaling molecule modulating metabolism. Cold Spring Harbor symposia on quantitative biology *76*, 291-298.

Carroll, P.A., Diolaiti, D., McFerrin, L., Gu, H., Djukovic, D., Du, J., Cheng, P.F., Anderson, S., Ulrich, M., Hurley, J.B.*, et al.* (2015). Deregulated Myc Requires MondoA/Mlx for Metabolic Reprogramming and Tumorigenesis. Cancer cell *27*, 271-285.

Cerami, E., Gao, J., Dogrusoz, U., Gross, B.E., Sumer, S.O., Aksoy, B.A., Jacobsen, A., Byrne, C.J., Heuer, M.L., Larsson, E.*, et al.* (2012). The cBio cancer genomics portal: an open platform for exploring multidimensional cancer genomics data. Cancer discovery *2*, 401-404.

Chan, H.S., Gallie, B.L., DeBoer, G., Haddad, G., Ikegaki, N., Dimitroulakos, J., Yeger, H., and Ling, V. (1997). MYCN protein expression as a predictor of neuroblastoma prognosis. Clinical cancer research : an official journal of the American Association for Cancer Research *3*, 1699-1706.

Chen, X., Xu, H., Yuan, P., Fang, F., Huss, M., Vega, V.B., Wong, E., Orlov, Y.L., Zhang, W., Jiang, J.*, et al.* (2008). Integration of external signaling pathways with the core transcriptional network in embryonic stem cells. Cell *133*, 1106-1117.

Chiarugi, A., Dolle, C., Felici, R., and Ziegler, M. (2012). The NAD metabolome - a key determinant of cancer cell biology. Nature reviews Cancer *12*, 741-752.

Cho, H., Zhao, X., Hatori, M., Yu, R.T., Barish, G.D., Lam, M.T., Chong, L.W., DiTacchio, L., Atkins, A.R., Glass, C.K.*, et al.* (2012). Regulation of circadian behaviour and metabolism by REV-ERB-alpha and REV-ERB-beta. Nature *485*, 123-127.

Corcos, D., Vaulont, S., Denis, N., Lyonnet, S., Simon, M.P., Kitzis, A., Kahn, A., and Kruh, J. (1987). Expression of c-myc is under dietary control in rat liver. Oncogene research *1*, 193-199.
Dalla-Favera, R., Bregni, M., Erikson, J., Patterson, D., Gallo, R.C., and Croce, C.M. (1982). Human c-myc onc gene is located on the region of chromosome 8 that is translocated in Burkitt lymphoma cells. Proceedings of the National Academy of Sciences of the United States of America *79*, 7824-7827.

Dang, C.V. (2012). MYC on the path to cancer. Cell *149*, 22-35.

Dang, C.V. (2013). MYC, metabolism, cell growth, and tumorigenesis. Cold Spring Harbor perspectives in medicine *3*.

Dang, C.V. (2014). Gene regulation: fine-tuned amplification in cells. Nature *511*, 417-418.

David, C.J., Chen, M., Assanah, M., Canoll, P., and Manley, J.L. (2010). HnRNP proteins controlled by c-Myc deregulate pyruvate kinase mRNA splicing in cancer. Nature *463*, 364-368.

Delpuech, O., Griffiths, B., East, P., Essafi, A., Lam, E.W., Burgering, B., Downward, J., and Schulze, A. (2007). Induction of Mxi1-SR alpha by FOXO3a contributes to repression of Myc-dependent gene expression. Molecular and cellular biology *27*, 4917-4930.

Demontis, F., and Perrimon, N. (2009). Integration of Insulin receptor/Foxo signaling and dMyc activity during muscle growth regulates body size in Drosophila. Development *136*, 983-993.

Doherty, J.R., Yang, C., Scott, K.E., Cameron, M.D., Fallahi, M., Li, W., Hall, M.A., Amelio, A.L., Mishra, J.K., Li, F.*, et al.* (2014). Blocking lactate export by inhibiting the Myc target MCT1 Disables glycolysis and glutathione synthesis. Cancer research *74*, 908-920.

Duesberg, P.H., and Vogt, P.K. (1979). Avian acute leukemia viruses MC29 and MH2 share specific RNA sequences: evidence for a second class of transforming genes. Proceedings of the National Academy of Sciences of the United States of America *76*, 1633-1637.

Efeyan, A., Zoncu, R., and Sabatini, D.M. (2012). Amino acids and mTORC1: from lysosomes to disease. Trends in molecular medicine *18*, 524-533.

Eischen, C.M., Weber, J.D., Roussel, M.F., Sherr, C.J., and Cleveland, J.L. (1999). Disruption of the ARF-Mdm2-p53 tumor suppressor pathway in Myc-induced lymphomagenesis. Genes & development *13*, 2658-2669.

Fernandez, P.C., Frank, S.R., Wang, L., Schroeder, M., Liu, S., Greene, J., Cocito, A., and Amati, B. (2003). Genomic targets of the human c-Myc protein. Genes & development *17*, 1115-1129.

Fu, L., Pelicano, H., Liu, J., Huang, P., and Lee, C. (2002). The circadian gene Period2 plays an important role in tumor suppression and DNA damage response in vivo. Cell *111*, 41-50.

Gallant, P. (2013). Myc function in Drosophila. Cold Spring Harbor perspectives in medicine *3*, a014324.

Gao, J., Aksoy, B.A., Dogrusoz, U., Dresdner, G., Gross, B., Sumer, S.O., Sun, Y., Jacobsen, A., Sinha, R., Larsson, E.*, et al.* (2013). Integrative analysis of complex cancer genomics and clinical profiles using the cBioPortal. Science signaling *6*, pl1.

Gao, P., Tchernyshyov, I., Chang, T.C., Lee, Y.S., Kita, K., Ochi, T., Zeller, K.I., De Marzo, A.M., Van Eyk, J.E., Mendell, J.T.*, et al.* (2009). c-Myc suppression of miR-23a/b enhances mitochondrial glutaminase expression and glutamine metabolism. Nature *458*, 762-765.

Giangrande, P.H., Hallstrom, T.C., Tunyaplin, C., Calame, K., and Nevins, J.R. (2003). Identification of E-box factor TFE3 as a functional partner for the E2F3 transcription factor. Molecular and cellular biology *23*, 3707-3720.

Goldman, J., and McGuire, W.A. (1992). H-ras and c-myc RNA expression in human T-cell ALL and in normal human lymphocytes. Pediatric hematology and oncology *9*, 309-316.

Green, C.B., Takahashi, J.S., and Bass, J. (2008). The meter of metabolism. Cell *134*, 728-742.

Greer, C., Lee, M., Westerhof, M., Milholland, B., Spokony, R., Vijg, J., and Secombe, J. (2013). Myc-dependent genome instability and lifespan in Drosophila. PloS one *8*, e74641.

Grewal, S.S., Li, L., Orian, A., Eisenman, R.N., and Edgar, B.A. (2005). Myc-dependent regulation of ribosomal RNA synthesis during Drosophila development. Nature cell biology *7*, 295-302.

Hanoun, M., Eisele, L., Suzuki, M., Greally, J.M., Huttmann, A., Aydin, S., Scholtysik, R.,
Klein-Hitpass, L., Duhrsen, U., and Durig, J. (2012). Epigenetic silencing of the circadian clock gene CRY1 is associated with an indolent clinical course in chronic lymphocytic leukemia. PloS one *7*, e34347.

Hara, N., Yamada, K., Shibata, T., Osago, H., Hashimoto, T., and Tsuchiya, M. (2007). Elevation of cellular NAD levels by nicotinic acid and involvement of nicotinic acid phosphoribosyltransferase in human cells. The Journal of biological chemistry *282*, 24574-24582.

Hardie, D.G., and Alessi, D.R. (2013). LKB1 and AMPK and the cancer-metabolism link - ten years after. BMC biology *11*, 36.

He, T.C., Sparks, A.B., Rago, C., Hermeking, H., Zawel, L., da Costa, L.T., Morin, P.J., Vogelstein, B., and Kinzler, K.W. (1998). Identification of c-MYC as a target of the APC pathway. Science *281*, 1509-1512.

Hooker, C.W., and Hurlin, P.J. (2006). Of Myc and Mnt. Journal of cell science *119*, 208-216.

Hsieh, A.L., Walton, Z.E., Altman, B.J., Stine, Z.E., and Dang, C.V. (2015). MYC and metabolism on the path to cancer. Seminars in cell & developmental biology *43*, 11-21.

Hu, S., Balakrishnan, A., Bok, R.A., Anderton, B., Larson, P.E., Nelson, S.J., Kurhanewicz, J., Vigneron, D.B., and Goga, A. (2011). 13C-pyruvate imaging reveals

alterations in glycolysis that precede c-Myc-induced tumor formation and regression. Cell metabolism *14*, 131-142.

Hughes, M.E., Hogenesch, J.B., and Kornacker, K. (2010). JTK_CYCLE: an efficient nonparametric algorithm for detecting rhythmic components in genome-scale data sets. J Biol Rhythms *25*, 372-380.

Jiang, R., Xue, S., and Jin, Z. (2011). Stable knockdown of MYCN by lentivirus-based RNAi inhibits human neuroblastoma cells growth in vitro and in vivo. Biochemical and biophysical research communications *410*, 364-370.

Johnston, L.A., Prober, D.A., Edgar, B.A., Eisenman, R.N., and Gallant, P. (1999). Drosophila myc regulates cellular growth during development. Cell *98*, 779-790.

Kennaway, D.J., Varcoe, T.J., Voultsios, A., and Boden, M.J. (2013). Global loss of bmal1 expression alters adipose tissue hormones, gene expression and glucose metabolism. PloS one *8*, e65255.

Kent, W.J., Sugnet, C.W., Furey, T.S., Roskin, K.M., Pringle, T.H., Zahler, A.M., and Haussler, D. (2002). The human genome browser at UCSC. Genome research *12*, 996-1006.

Kohl, N.E., Gee, C.E., and Alt, F.W. (1984). Activated expression of the N-myc gene in human neuroblastomas and related tumors. Science *226*, 1335-1337.

Koike, N., Yoo, S.H., Huang, H.C., Kumar, V., Lee, C., Kim, T.K., and Takahashi, J.S. (2012). Transcriptional architecture and chromatin landscape of the core circadian clock in mammals. Science *338*, 349-354.

Konopka, R.J., and Benzer, S. (1971). Clock mutants of Drosophila melanogaster. Proceedings of the National Academy of Sciences of the United States of America *68*, 2112-2116.

Kornmann, B., Schaad, O., Bujard, H., Takahashi, J.S., and Schibler, U. (2007). System-driven and oscillator-dependent circadian transcription in mice with a conditionally active liver clock. PLoS biology *5*, e34.

Kourtidis, A., Jain, R., Carkner, R.D., Eifert, C., Brosnan, M.J., and Conklin, D.S. (2010). An RNA interference screen identifies metabolic regulators NR1D1 and PBP as novel survival factors for breast cancer cells with the ERBB2 signature. Cancer research *70*, 1783-1792.

Kumar, S., Chen, D., Jang, C., Nall, A., Zheng, X., and Sehgal, A. (2014). An ecdysone-responsive nuclear receptor regulates circadian rhythms in Drosophila. Nature communications *5*, 5697.

Kushner, B.H., Modak, S., Kramer, K., LaQuaglia, M.P., Yataghene, K., Basu, E.M., Roberts, S.S., and Cheung, N.K. (2014). Striking dichotomy in outcome of MYCN-amplified neuroblastoma in the contemporary era. Cancer *120*, 2050-2059.

La Starza, R., Borga, C., Barba, G., Pierini, V., Schwab, C., Matteucci, C., Lema Fernandez, A.G., Leszl, A., Cazzaniga, G., Chiaretti, S.*, et al.* (2014). Genetic profile of T-cell acute lymphoblastic leukemias with MYC translocations. Blood *124*, 3577-3582.

Lamia, K.A., Sachdeva, U.M., DiTacchio, L., Williams, E.C., Alvarez, J.G., Egan, D.F., Vasquez, D.S., Juguilon, H., Panda, S., Shaw, R.J.*, et al.* (2009). AMPK regulates the circadian clock by cryptochrome phosphorylation and degradation. Science *326*, 437-440.

Le, A., Cooper, C.R., Gouw, A.M., Dinavahi, R., Maitra, A., Deck, L.M., Royer, R.E., Vander Jagt, D.L., Semenza, G.L., and Dang, C.V. (2010). Inhibition of lactate dehydrogenase A induces oxidative stress and inhibits tumor progression. Proceedings of the National Academy of Sciences of the United States of America *107*, 2037-2042.

Le, A., Lane, A.N., Hamaker, M., Bose, S., Gouw, A., Barbi, J., Tsukamoto, T., Rojas, C.J., Slusher, B.S., Zhang, H.*, et al.* (2012). Glucose-independent glutamine metabolism via TCA cycling for proliferation and survival in B cells. Cell metabolism *15*, 110-121.

Lee, T., and Luo, L. (1999). Mosaic analysis with a repressible cell marker for studies of gene function in neuronal morphogenesis. Neuron *22*, 451-461.

Levi, F., Okyar, A., Dulong, S., Innominato, P.F., and Clairambault, J. (2010). Circadian timing in cancer treatments. Annual review of pharmacology and toxicology *50*, 377-421.

Lin, C.Y., Loven, J., Rahl, P.B., Paranal, R.M., Burge, C.B., Bradner, J.E., Lee, T.I., and Young, R.A. (2012). Transcriptional Amplification in Tumor Cells with Elevated c-Myc. Cell *151*, 56-67.

Lippman, S.I., and Broach, J.R. (2009). Protein kinase A and TORC1 activate genes for ribosomal biogenesis by inactivating repressors encoded by Dot6 and its homolog Tod6. Proceedings of the National Academy of Sciences of the United States of America *106*, 19928-19933.

Littlewood, T.D., Hancock, D.C., Danielian, P.S., Parker, M.G., and Evan, G.I. (1995). A modified oestrogen receptor ligand-binding domain as an improved switch for the regulation of heterologous proteins. Nucleic Acids Res *23*, 1686-1690.

Liu, W., Le, A., Hancock, C., Lane, A.N., Dang, C.V., Fan, T.W., and Phang, J.M. (2012). Reprogramming of proline and glutamine metabolism contributes to the proliferative and metabolic responses regulated by oncogenic transcription factor c-MYC. Proceedings of the National Academy of Sciences of the United States of America *109*, 8983-8988.

Malynn, B.A., de Alboran, I.M., O'Hagan, R.C., Bronson, R., Davidson, L., DePinho, R.A., and Alt, F.W. (2000). N-myc can functionally replace c-myc in murine development, cellular growth, and differentiation. Genes & development *14*, 1390-1399.

Menssen, A., Hydbring, P., Kapelle, K., Vervoorts, J., Diebold, J., Luscher, B., Larsson, L.G., and Hermeking, H. (2012). The c-MYC oncoprotein, the NAMPT enzyme, the SIRT1-inhibitor DBC1, and the SIRT1 deacetylase form a positive feedback loop. Proceedings of the National Academy of Sciences of the United States of America *109*, E187-196.

Morgenstern, J.P., and Land, H. (1990). Advanced mammalian gene transfer: high titre retroviral vectors with multiple drug selection markers and a complementary helper-free packaging cell line. Nucleic Acids Res *18*, 3587-3596.

Nakahata, Y., Sahar, S., Astarita, G., Kaluzova, M., and Sassone-Corsi, P. (2009). Circadian control of the NAD+ salvage pathway by CLOCK-SIRT1. Science *324*, 654-657.

Nau, M.M., Brooks, B.J., Battey, J., Sausville, E., Gazdar, A.F., Kirsch, I.R., McBride, O.W., Bertness, V., Hollis, G.F., and Minna, J.D. (1985). L-myc, a new myc-related gene amplified and expressed in human small cell lung cancer. Nature *318*, 69-73.

Nie, Z., Hu, G., Wei, G., Cui, K., Yamane, A., Resch, W., Wang, R., Green, D.R., Tessarollo, L., Casellas, R.*, et al.* (2012). c-Myc Is a Universal Amplifier of Expressed Genes in Lymphocytes and Embryonic Stem Cells. Cell *151*, 68-79.

Nilsson, J.A., Maclean, K.H., Keller, U.B., Pendeville, H., Baudino, T.A., and Cleveland, J.L. (2004). Mnt loss triggers Myc transcription targets, proliferation, apoptosis, and transformation. Molecular and cellular biology *24*, 1560-1569.

Osthus, R.C., Shim, H., Kim, S., Li, Q., Reddy, R., Mukherjee, M., Xu, Y., Wonsey, D., Lee, L.A., and Dang, C.V. (2000). Deregulation of glucose transporter 1 and glycolytic gene expression by c-Myc. The Journal of biological chemistry *275*, 21797-21800.

Park, J.H., Helfrich-Forster, C., Lee, G., Liu, L., Rosbash, M., and Hall, J.C. (2000). Differential regulation of circadian pacemaker output by separate clock genes in Drosophila. Proceedings of the National Academy of Sciences of the United States of America *97*, 3608-3613.

Paschos, G.K., Ibrahim, S., Song, W.L., Kunieda, T., Grant, G., Reyes, T.M., Bradfield, C.A., Vaughan, C.H., Eiden, M., Masoodi, M.*, et al.* (2012). Obesity in mice with adipocyte-specific deletion of clock component Arntl. Nature medicine *18*, 1768-1777.

Pierce, S.B., Yost, C., Anderson, S.A., Flynn, E.M., Delrow, J., and Eisenman, R.N. (2008). Drosophila growth and development in the absence of dMyc and dMnt. Developmental biology *315*, 303-316.

Preitner, N., Damiola, F., Lopez-Molina, L., Zakany, J., Duboule, D., Albrecht, U., and Schibler, U. (2002). The orphan nuclear receptor REV-ERBalpha controls circadian transcription within the positive limb of the mammalian circadian oscillator. Cell *110*, 251-260.

Pugh, T.J., Morozova, O., Attiyeh, E.F., Asgharzadeh, S., Wei, J.S., Auclair, D., Carter, S.L.,
Cibulskis, K., Hanna, M., Kiezun, A.*, et al.* (2013). The genetic landscape of high-risk neuroblastoma. Nature genetics *45*, 279-284.

Qi, Y., Gregory, M.A., Li, Z., Brousal, J.P., West, K., and Hann, S.R. (2004). p19ARF directly and differentially controls the functions of c-Myc independently of p53. Nature *431*, 712-717.

Rahl, P.B., Lin, C.Y., Seila, A.C., Flynn, R.A., McCuine, S., Burge, C.B., Sharp, P.A., and
Young, R.A. (2010). c-Myc regulates transcriptional pause release. Cell *141*, 432-445.

Ramsey, K.M., Yoshino, J., Brace, C.S., Abrassart, D., Kobayashi, Y., Marcheva, B., Hong, H.K., Chong, J.L., Buhr, E.D., Lee, C.*, et al.* (2009). Circadian clock feedback cycle through NAMPT-mediated NAD+ biosynthesis. Science *324*, 651-654.

Reitzer, L.J., Wice, B.M., and Kennell, D. (1979). Evidence that glutamine, not sugar, is the major energy source for cultured HeLa cells. The Journal of biological chemistry *254*, 2669-2676.

Relogio, A., Westermark, P.O., Wallach, T., Schellenberg, K., Kramer, A., and Herzel, H. (2011). Tuning the mammalian circadian clock: robust synergy of two loops. PLoS computational biology *7*, e1002309.

Repouskou, A., and Prombona, A. (2016). c-MYC targets the central oscillator gene Per1 and is regulated by the circadian clock at the post-transcriptional level. Biochimica et biophysica acta *1859*, 541-552.

Rutter, J., Reick, M., Wu, L.C., and McKnight, S.L. (2001). Regulation of clock and NPAS2 DNA binding by the redox state of NAD cofactors. Science *293*, 510-514.

Sabo, A., Kress, T.R., Pelizzola, M., de Pretis, S., Gorski, M.M., Tesi, A., Morelli, M.J., Bora, P., Doni, M., Verrecchia, A.*, et al.* (2014). Selective transcriptional regulation by Myc in cellular growth control and lymphomagenesis. Nature.

Sardiello, M., Palmieri, M., di Ronza, A., Medina, D.L., Valenza, M., Gennarino, V.A., Di Malta, C., Donaudy, F., Embrione, V., Polishchuk, R.S.*, et al.* (2009). A gene network regulating lysosomal biogenesis and function. Science *325*, 473-477.

Savvidis, C., and Koutsilieris, M. (2012). Circadian rhythm disruption in cancer biology. Mol Med.

Sehgal, A., Rothenfluh-Hilfiker, A., Hunter-Ensor, M., Chen, Y., Myers, M.P., and Young, M.W. (1995). Rhythmic expression of timeless: a basis for promoting circadian cycles in period gene autoregulation. Science *270*, 808-810.

Shachaf, C.M., Kopelman, A.M., Arvanitis, C., Karlsson, A., Beer, S., Mandl, S., Bachmann, M.H., Borowsky, A.D., Ruebner, B., Cardiff, R.D.*, et al.* (2004). MYC inactivation uncovers pluripotent differentiation and tumour dormancy in hepatocellular cancer. Nature *431*, 1112-1117.

Shi, S., Hida, A., McGuinness, O.P., Wasserman, D.H., Yamazaki, S., and Johnson, C.H. (2010). Circadian clock gene Bmal1 is not essential; functional replacement with its paralog, Bmal2. Current biology : CB *20*, 316-321.

Shimomura, K., Kumar, V., Koike, N., Kim, T.K., Chong, J., Buhr, E.D., Whiteley, A.R., Low, S.S., Omura, C., Fenner, D.*, et al.* (2013). Usf1, a suppressor of the circadian Clock mutant, reveals the nature of the DNA-binding of the CLOCK:BMAL1 complex in mice. eLife *2*, e00426.

Siepel, A., Bejerano, G., Pedersen, J.S., Hinrichs, A.S., Hou, M., Rosenbloom, K., Clawson, H., Spieth, J., Hillier, L.W., Richards, S.*, et al.* (2005). Evolutionarily conserved elements in vertebrate, insect, worm, and yeast genomes. Genome research *15*, 1034-1050.

Sin, Y.Y., Ballantyne, L.L., Mukherjee, K., St Amand, T., Kyriakopoulou, L., Schulze, A., and Funk, C.D. (2013). Inducible arginase 1 deficiency in mice leads to hyperargininemia and altered amino acid metabolism. PloS one *8*, e80001.

Slavc, I., Ellenbogen, R., Jung, W.H., Vawter, G.F., Kretschmar, C., Grier, H., and Korf, B.R. (1990). myc gene amplification and expression in primary human neuroblastoma. Cancer research *50*, 1459-1463.

Stewart, S.A., Dykxhoorn, D.M., Palliser, D., Mizuno, H., Yu, E.Y., An, D.S., Sabatini, D.M., Chen, I.S., Hahn, W.C., Sharp, P.A.*, et al.* (2003). Lentivirus-delivered stable gene silencing by RNAi in primary cells. RNA *9*, 493-501.

Stine, Z.E., Walton, Z.E., Altman, B.J., Hsieh, A.L., and Dang, C.V. (2015). MYC, Metabolism, and Cancer. Cancer discovery *5*, 1024-1039.

Tambellini, N.P., Zaremberg, V., Turner, R.J., and Weljie, A.M. (2013). Evaluation of extraction protocols for simultaneous polar and non-polar yeast metabolite analysis using multivariate projection methods. Metabolites *3*, 592-605.

Taniguchi, H., Fernandez, A.F., Setien, F., Ropero, S., Ballestar, E., Villanueva, A., Yamamoto, H., Imai, K., Shinomura, Y., and Esteller, M. (2009). Epigenetic inactivation of the circadian clock gene BMAL1 in hematologic malignancies. Cancer research *69*, 8447-8454.

Taub, R., Kirsch, I., Morton, C., Lenoir, G., Swan, D., Tronick, S., Aaronson, S., and Leder, P. (1982). Translocation of the c-myc gene into the immunoglobulin heavy chain locus in human Burkitt lymphoma and murine plasmacytoma cells. Proceedings of the National Academy of Sciences of the United States of America *79*, 7837-7841.

Team, R.C. (2015). R: A language and environment for statistical computing. http://www.R-project.org.

Teleman, A.A., Hietakangas, V., Sayadian, A.C., and Cohen, S.M. (2008). Nutritional control of protein biosynthetic capacity by insulin via Myc in Drosophila. Cell metabolism *7*, 21-32.

Tokunaga, H., Takebayashi, Y., Utsunomiya, H., Akahira, J., Higashimoto, M., Mashiko, M., Ito, K., Niikura, H., Takenoshita, S., and Yaegashi, N. (2008). Clinicopathological significance of circadian rhythm-related gene expression levels in patients with epithelial ovarian cancer. Acta obstetricia et gynecologica Scandinavica *87*, 1060-1070.

Umemura, Y., Koike, N., Matsumoto, T., Yoo, S.H., Chen, Z., Yasuhara, N., Takahashi, J.S., and Yagita, K. (2014). Transcriptional program of Kpna2/Importin-alpha2 regulates cellular differentiation-coupled circadian clock development in mammalian cells. Proceedings of the National Academy of Sciences of the United States of America *111*, E5039-5048.

Ushmorov, A., Hogarty, M.D., Liu, X., Knauss, H., Debatin, K.M., and Beltinger, C. (2008). N-myc augments death and attenuates protective effects of Bcl-2 in trophically stressed neuroblastoma cells. Oncogene *27*, 3424-3434.

Valentijn, L.J., Koppen, A., van Asperen, R., Root, H.A., Haneveld, F., and Versteeg, R. (2005). Inhibition of a new differentiation pathway in neuroblastoma by copy number defects of N-myc, Cdc42, and nm23 genes. Cancer research *65*, 3136-3145.

Vennstrom, B., Sheiness, D., Zabielski, J., and Bishop, J.M. (1982). Isolation and characterization of c-myc, a cellular homolog of the oncogene (v-myc) of avian myelocytomatosis virus strain 29. Journal of virology *42*, 773-779.

Walz, S., Lorenzin, F., Morton, J., Wiese, K.E., von Eyss, B., Herold, S., Rycak, L., Dumay-Odelot, H., Karim, S., Bartkuhn, M.*, et al.* (2014). Activation and repression by oncogenic MYC shape tumour-specific gene expression profiles. Nature.

Wang, J.B., Erickson, J.W., Fuji, R., Ramachandran, S., Gao, P., Dinavahi, R., Wilson, K.F., Ambrosio, A.L., Dias, S.M., Dang, C.V.*, et al.* (2010). Targeting mitochondrial glutaminase activity inhibits oncogenic transformation. Cancer cell *18*, 207-219.

Wang, Q., Diskin, S., Rappaport, E., Attiyeh, E., Mosse, Y., Shue, D., Seiser, E., Jagannathan, J., Shusterman, S., Bansal, M.*, et al.* (2006). Integrative genomics identifies distinct molecular classes of neuroblastoma and shows that multiple genes are targeted by regional alterations in DNA copy number. Cancer research *66*, 6050-6062.

Warburg, O., Wind, F., and Negelein, E. (1927). The Metabolism of Tumors in the Body. The Journal of general physiology *8*, 519-530.

Weljie, A.M., Newton, J., Mercier, P., Carlson, E., and Slupsky, C.M. (2006). Targeted profiling: quantitative analysis of 1H NMR metabolomics data. Anal Chem *78*, 4430-4442.

Wise, D.R., DeBerardinis, R.J., Mancuso, A., Sayed, N., Zhang, X.Y., Pfeiffer, H.K., Nissim, I., Daikhin, E., Yudkoff, M., McMahon, S.B.*, et al.* (2008). Myc regulates a transcriptional program that stimulates mitochondrial glutaminolysis and leads to glutamine addiction. Proceedings of the National Academy of Sciences of the United States of America *105*, 18782-18787.

Wolf, E., Lin, C.Y., Eilers, M., and Levens, D.L. (2014). Taming of the beast: shaping Myc-dependent amplification. Trends in cell biology.

Wong, J.V., Yao, G., Nevins, J.R., and You, L. (2011). Viral-mediated noisy gene expression
reveals biphasic E2f1 response to MYC. Molecular cell *41*, 275-285.

Wullschleger, S., Loewith, R., and Hall, M.N. (2006). TOR signaling in growth and metabolism. Cell *124*, 471-484.

Xiang, Y., Stine, Z.E., Xia, J., Lu, Y., O'Connor, R.S., Altman, B.J., Hsieh, A.L., Gouw, A.M., Thomas, A.G., Gao, P.*, et al.* (2015). Targeted inhibition of tumor-specific glutaminase diminishes cell-autonomous tumorigenesis. The Journal of clinical investigation.

Yasumoto, K., Yokoyama, K., Shibata, K., Tomita, Y., and Shibahara, S. (1994). Microphthalmia-associated transcription factor as a regulator for melanocyte-specific transcription of the human tyrosinase gene. Molecular and cellular biology *14*, 8058-8070.

Yeh, C.M., Shay, J., Zeng, T.C., Chou, J.L., Huang, T.H., Lai, H.C., and Chan, M.W. (2014). Epigenetic silencing of ARNTL, a circadian gene and potential tumor suppressor in ovarian cancer. International journal of oncology *45*, 2101-2107.

Yoo, S.H., Yamazaki, S., Lowrey, P.L., Shimomura, K., Ko, C.H., Buhr, E.D., Siepka, S.M., Hong, H.K., Oh, W.J., Yoo, O.J., *et al.* (2004). PERIOD2::LUCIFERASE real-time reporting of circadian dynamics reveals persistent circadian oscillations in mouse peripheral tissues. Proceedings of the National Academy of Sciences of the United States of America *101*, 5339-5346.

Yoshitane, H., Ozaki, H., Terajima, H., Du, N.H., Suzuki, Y., Fujimori, T., Kosaka, N., Shimba, S., Sugano, S., Takagi, T., *et al.* (2014). CLOCK-controlled polyphonic regulation of circadian rhythms through canonical and noncanonical E-boxes. Molecular and cellular biology *34*, 1776-1787.

Yuneva, M., Zamboni, N., Oefner, P., Sachidanandam, R., and Lazebnik, Y. (2007). Deficiency in glutamine but not glucose induces MYC-dependent apoptosis in human cells. The Journal of cell biology *178*, 93-105.

Yustein, J.T., Liu, Y.C., Gao, P., Jie, C., Le, A., Vuica-Ross, M., Chng, W.J., Eberhart, C.G., Bergsagel, P.L., and Dang, C.V. (2010). Induction of ectopic Myc target gene JAG2 augments hypoxic growth and tumorigenesis in a human B-cell model. Proceedings of the National Academy of Sciences of the United States of America *107*, 3534-3539.

Zhao, H., Zeng, Z.L., Yang, J., Jin, Y., Qiu, M.Z., Hu, X.Y., Han, J., Liu, K.Y., Liao, J.W., Xu, R.H., *et al.* (2014). Prognostic relevance of Period1 (Per1) and Period2 (Per2) expression in human gastric cancer. International journal of clinical and experimental pathology *7*, 619-630.

Annie L. Hsieh, MD

2400 Chestnut St. APT 1711, Philadelphia, PA 19103
(410) 812-3083 ahsieh@mail.med.upenn.edu
U.S. citizen
Place of Birth: Gaithersburg, MD

EDUCATION

Johns Hopkins University School of Medicine, Pathobiology, Ph.D. Candidate 8/2010-Present

Johns Hopkins Bloomberg School of Public Health, Certificate in Health Finance & Management 9/2010-5/2013

Tzu Chi University College of Medicine, Doctor of Medicine, GPA: 3.82, Rank in Class = 3/56 9/2003-6/2010

RESEARCH EXPERIENCE

University of Pennsylvania, Perelman School of Medicine, Abramson Cancer Center 8/2011-Present

Advisor: Chi V. Dang, M.D, Ph.D.

Study: Investigate the disruption of the circadian clock and metabolism caused by overexpressed oncogene *MYC* in cancer cells.

- Designed and performed experiments, acquired new techniques and wrote manuscript.
- Engineered mouse hepatocellular carcinoma cell lines with clock reporter to assess the recovery of circadian clock upon inactivation of MYC
- Developed colony suppression assay to clarify the role of a clock component (Bmal1) as a tumor suppressor
- Peer-reviewed Publication: Altman, BJ*, **Hsieh, AL*,** Sengupta, A, Krishnanaiah SY, Stine, ZE, Walton ZE, Gouw, AM, Venkataraman, A, Li, B, Goraksha-Hicks, P, Diskin, SJ, Dellovin, DI, Simon, MC, Rathmell, JC, Lazar, MA, Maris, JM, Felsher, DW, Hogenesch, JB, Weljie AM, Dang CV. MYC disrupts the circadian clock and metabolism in cancer cells *Cell Metabolism* **In press. *Co-first authors.**
- Oral presentation: Keystone Symposia: Molecular Clockworks and the Regulation of Cardio-Metabolic Function, 2013
- Poster presentation: Annual Society for Neuro-Oncology Scientific meeting, 2014; American Association of Cancer Research annual meeting, 2014, ASCI/AAP joint meeting, 2011

Howard Hughes Medical Institute, University of Pennsylvania, Department of Neuroscience 6/2014-Present

Advisor: Amita Sehgal, Ph.D. and Chi V. Dang, M.D., Ph.D.

Study: Investigate the role of Drosophila Myc in affecting circadian locomotor behavior in fruit flies.

- Initiated collaboration, designed and executed experiments.
- Developed method using mass spectrometry to analyze metabolomics of fly heads.
- Used drosophila activity monitors to assess circadian behavior of flies with overexpressed or hypomorphic Myc
- Poster presentation: Gordon Research Conference, Chronobiology, 2015; Johns Hopkins Pathobiology retreat, 2015

Johns Hopkins University, Department of Neuroscience, Department of Pathology 12/2010-2/2011

Advisor: Philip C. Wong, Ph.D.

Study: Examine transactive response DNA-binding protein 43 (TDP-43) gene function in myoblasts.

- Performed myoblast culture and developed glucose consumption measurement to assess metabolic alteration of myoblasts harboring TDP-43 mutation.

Johns Hopkins University, Department of Neuroscience, Department of Pathology 9/2010-12/2010

Advisor: Lee J. Martin, Ph.D.

Study: Investigate mitochondriopathy in superoxide dismutase 1(SOD1) mutated amyotrophic lateral sclerosis.

- Performed mitochondria isolation and immunohistochemistry staining of hind limb muscle from SOD1 mutated mice.

TEACHING EXPERIENCE

Basic Medical Mandarin, Johns Hopkins University School of Medicine, *Instructor* 2011

- Initiated and lectured Basic Medical Mandarin Course for medical and nursing students.
- Designed course material with interactive activities to familiarize students with symptomatic and diagnostic terms in Mandarin. Aimed to facilitate students' communication with Mandarin-speaking patients.

PUBLICATIONS

- Altman, BJ*, **Hsieh, AL*,** Sengupta, A, Krishnanaiah SY, Stine, ZE, Walton ZE, Gouw, AM, Venkataraman, A, Li, B, Goraksha-Hicks, P, Diskin, SJ, Dellovin, DI, Simon, MC, Rathmell, JC, Lazar, MA, Maris, JM, Felsher, DW, Hogenesch, JB, Weljie AM, Dang CV. MYC disrupts the circadian clock and metabolism in cancer cells *Cell Metab.* **In press.** *Co-first authors.
- **Hsieh, AL,** Walton, ZE, Altman, BJ, Stine, ZE, Dang, CV. MYC and metabolism on the path to cancer. *Semin Cell Dev Biol.* Aug 2015
- Xiang, Y, Stine, ZE, Xia, J, Lu, Y, O'connor, RS, Altman, BJ, **Hsieh, AL,** Gouw, AM, Thomas, AG, Gao, P, Sun, L, Song, L, Yan, B, Slusher, BS, Zhuo, J, Ooi, LL, Lee, CGL, Mancuso, A, Mccallion, AS, Le, A, Milone, M, Rayport, S, Felsher, D, Dang CV. Targeted inhibition of tumor-specific glutaminase diminishes cell-autonomous tumorigenesis. *J Clin Invest.* April 2015
- Stine, ZE, Walton, ZE, Altman, BJ, **Hsieh, AL,** Dang, CV. MYC, Metabolism and Cancer. *Cancer Discov.* **In press.**
- **Hsieh, AL,** Dang, CV. MYC, Metabolism and Cancer In *Metabolism in Cancer.* **In press.**
- Walton, ZE, **Hsieh, AL,** Dang, CV. Metabolism of hematologic neoplastic cells. In *Williams Hematology* 9th edition (Chapter 14). **In press.**
- Gouw, AM, **Hsieh, AL,** Stine, ZE, Dang, CV. (2015) MYC regulation of metabolism and cancer. In *Tumor cell metabolism* (pp. 101-122), S. Mazurek and M. Shoshan (Eds). Springer-Verlag Wien. 2015
- Stine, ZE, Altman, BJ, **Hsieh, AL,** Gouw, AM and Dang, CV. (2014) Deregulation of the cellular energetics of cancer cells. In *Pathobiology of Human Disease: A Dynamic Encyclopedia of Disease Mechanisms* (pp. 444-455), W. Coleman (Ed.). Elsevier. 2014

PRESENTATIONS

Oral Presentations

- **Hsieh, AL,** Altman, BJ, Venkataraman, A, Gouw, AM, Stine, ZE, Li, B, Goraksha-Hicks, P, Diskin, SJ, Bellovin, DI, Hogenesch, JB, Simon, MC, Rathmell, JC, Lazar, MA, Maris, JM, Felsher, DW, Dang, CV. Oncogenic c- and N-Myc Disrupt Circadian Rhythm. Keystone Symposia: Molecular Clockworks and the Regulation of Cardio-Metabolic Function, Snowbird, Utah, April 2013

Poster Presentations

- **Hsieh, AL**, Zheng X, Sehgal A, Dang CV. Drosophila Myc regulates circadian locomotor behavior in flies. Gordon Research Conference, Chronobiology, Girona, Spain, June, 2015
- Altman, BJ, **Hsieh, AL,** Stine, ZE, Gouw, AM, Venkataraman, A, Li, B, Goraksha-Hicks, P, Diskin, SJ, Bellovin, DI, Simon, MC, Rathmell, JC, Lazar, MA, Maris, JM, Felsher, DW, Hogenesch, JB, Dang, CV. MYC and MYCN disruption of the molecular clock in cancer cells. Annual Society for Neuro-Oncology (SNO) Scientific meeting, Miami, Florida, November, 2014
- Altman, BJ, **Hsieh, AL,** Gouw, AM, Stine, ZE, Venkataraman, A, Bellovin, DI, Diskin, SJ, Lu, W, Zhang, S, Felsher, DW, Maris, JM, Lazar, MA, Rabinowitz, JD, Hogenesch, JB, Dang, CV. Rev-erbα modulates Myc-driven cancer cell growth and altered metabolism. American Association of Cancer Research (AACR) annual meeting, San Diego, California, April, 2014
- **Hsieh, AL,** Altman, BJ, Venkataraman, A, Bellovin, DI, Felsher, DW, Hogenesch, JB, Dang, CV. Oncogenic Myc disrupts NAMPT circadian oscillation in mouse hepatocellular carcinoma cell line. American Association of Cancer Research (AACR) annual meeting, San Diego, California, April, 2014
- **Hsieh, AL,** Altman, BJ, Venkataraman, A, Gouw, AM, Stine, ZE, Li, B, Goraksha-Hicks, P, Diskin, SJ, Bellovin, DI, Hogenesch, JB, Simon, MC, Rathmell, JC, Lazar, MA, Maris, JM, Felsher, DW, Dang, CV. Oncogenic c-Myc Disrupts Circadian Rhythm. ASCI/AAP joint meeting, Chicago, Illinois, April, 2013

- Gouw, AM, **Hsieh, AL,** Zeller, K, Le, A, Higashi, R, Lane, A, Fan, TW, Wolfgang, M, Dang, CV. Myc suppresses fatty acid oxidation and directly stimulates lipogenesis in human P493 B cells. AACR Metabolism and Cancer meeting, Baltimore, Maryland, October, 2011

HONORS/AWARDS

- **ASCI/AAP Joint Meeting Travel Award** for excellent scientific abstract — 2013
- **Best Intern** in Tzu Chi University awarded to top 3 students in the class with outstanding performance during clinical rotations voted by attending physicians, residents and nurses. — 2010
- **GlaxoSmithKline Talent Scholarship** awarded to one student from each medical school for outstanding academic performance. — 2009
- **National Outstanding Youth of Taiwan** awarded by the president of the Republic of China for extraordinary academic and extracurricular performance — 2009
- **Best clinical history taking award** at the Objective Structured Clinical Examination international competition held by Shanghai Jiao Tong University, China. Chosen by the faculty as one of 4 medical students to represent school to participate this competition. — 2008
- **Outstanding Award in the Summer Research Program for Medical Students** awarded for significant research progress and excellent scientific presentation — 2007
- **Dean's List** awarded to top 5 students in the class per semester — 2003 – 2005

PROFESSIONAL ASSOCIATIONS

- American Academy of Neurology — 2014-Present
- American Association for Cancer Research — 2011-Present
- Society for Neuro-Oncology — 2014-2015
- American Physician Scientists Association — 2011-Present
- American Medical Association — 2014-Present

LEADERSHIP POSITIONS

American Physician Scientist Association (APSA) Membership Committee, *Vice-Chair* — 2014-Present
- Organized interactive sessions with prominent physician scientists to share experiences and career advice. Past speakers included Dr. Francis Collins, Dr. Alice Chen-Plotkin, Dr. Mukesh Jain and Dr. Ken Kaushansky.

JHMI Graduate Student Association, *Treasurer* — 2011-2012
- Encouraged students to submit applications, reviewed applications, set up selection committee and selected awardee for GSA travel award four times a year.

TCU Student Association of School of Medicine, *Executive secretary* — 2004-2006
- Coordinated one-week events including poster exhibition, introduction of historical medical devices and activities to practice suturing techniques using the pig skin
- Arranged speeches by prominent speakers including Senators of the Republic of China and industry executives

PUBLIC HEALTH EXPERIENCE

Let Love fly - Community medical mission project, Manila, Philippines — 2008
- Applied and received funding from Ministry of Education in Taiwan
- Initiated collaboration with local non-governmental organization Gawad Kalinga to help build houses for homeless families in the Philippines
- Organized summer camp to introduce hygiene concepts including hand washing and foot protection to children from low-income families
- Assisted in the free cataract surgery clinic through the Tzu Chi International Medical Association

Tzu Chi Earthquake relief program, Yogyakarta, Indonesia — 2007
- Provided emotional support to victims, delivered food aid and assisted wound care through the Tzu Chi International Medical Association

Elementary School Reading-Promotion Outreach Program 2006-2007

- Initiated project, organized educational outreach program for economically disadvantaged students and designed interactive activities to promote reading.

HOBBIES & INTERESTS

Ballroom dancing: *6th place in Bronze Foxtrot, Princeton Ballroom Competition*, 2013; Tzu Chi University Chorus Group: *Conductor*, 2004